PHYSICAL MODELING OF THE MOTIONS OF A CONTAINER SHIP MOORED TO A DOCK WITH COMPARISON TO NUMERICAL SIMULATION

A Thesis

by

YUANZHE ZHI

Submitted to the Office of Graduate Studies of
Texas A&M University
in partial fulfillment of the requirements for the degree of

MASTER OF SCIENCE

Chair of Committee,	Robert Randall
Committee Members,	Jun Zhang
	Joseph Pasciak
Head of Department,	Robin Authenrieth

August 2013

Major Subject: Ocean Engineering

ABSTRACT

Container vessel motions need to be small when loading and offloading cargo while moored to wharfs. Waves and their reflections from structures can induce ship motions. These motions are characterized by six degrees of freedom, including translations of surge, sway, and heave and rotations of pitch, roll, and yaw. Monitoring and quantifying these motions offer a reference for design and selection of the mooring system and wharf types. To measure the six degrees of freedom motions of a container ship moored to a dock, a 1:50 scale model is moored to two types of dock, solid wall dock and pile supported dock. Irregular waves of TMA spectrum with various periods, heights, and directions are generated in the wave basin to induce the motions of the model container ship. Optical motion capturing cameras are used to measure and quantify the six degree of freedom motions. Results of the effects of wave period, significant wave height, and wave direction on the motion characteristics of the model container ship moored at the solid dock and a pile supported dock are described in detail. A numerical simulation called aNySIM is applied to numerically predict the motion characteristics of the container ship moored to a solid wall dock only. The physical model experimental results of solid dock are also compared with the numerical simulation. These comparisons indicate that the motion characteristics of the model container ship represent similar trends for both rotations and translations. The experimental and numerical prediction values of motions of the ship moored to a solid wall dock display the same tendencies while differing in magnitude.

ACKNOWLEDGEMENTS

I would like to thank my parents for their caring and support for the last two years. Their consideration via telephone every weekend is my motivation and reminding me to keep on working on my research and thesis.

I would also like to thank my committee chair Dr. Robert Randall for his generosity and patience. He also supported me financially during the research. My two committee members Dr. Jun Zhang and Dr. Joseph Paciak also contributed a lot and keep on offering guidance in my research.

I also thank Dr. Nels Sultan from PND Engineers Inc. for funding the project. Many thanks to Arjan Voogt and Wei Xu from Marin Houston for providing the software license, training, and technical support for the aNySIM numerical software.

I would also like to thank the staff at the Haynes Coastal Engineering Laboratory. My thanks go to John Reed for his technical support and preparation of all the facilities for the experiment; my team member Andres Luai, for his designing of the mooring system; and the undergraduate student workers Ginny Whisenhunt, Shelby Clark, Cory Taylor, and Jacob Triska for their assistance during the experiments.

TABLE OF CONTENTS

Page

ABSTRACT ii

ACKNOWLEDGEMENTS iii

TABLE OF CONTENTS iv

LIST OF FIGURES vi

LIST OF TABLES viii

CHAPTER I INTRODUCTION AND LITERATURE REVIEW 1

Introduction 1
Objectives 4
Literature review 4

CHAPTER II EXPERIMENT PLAN 9

Case 1, solid dock 39 tests 11
Case 2, pile dock 39 tests 11
Case 3, numerical simulation 39 tests 11

CHAPTER III CONTAINER SHIP AND DOCK MODELS 12

Froude similarity 14
Container ship and dock scale 15
Wave basin and wave generator 17
Wave conditions in model and prototype 19

CHAPTER IV INSTRUMENTATION, SETTINGS, AND CALIBRATIONS 23

Wave generator and acquisition system 23
Wave generator 23
Wave gauges 24
Calibration of wave gauges 25
Motion capturing and acquisition system 26
Settings and calibration 27

CHAPTER V PROCEDURES 30

Phase 1, test preparation 30
Phase 2, physical model 30
Phase 3, numerical simulations 34
Phase 4, data acquisition and initial analysis 35
Wave data and reflection analysis 35
Motion data for experiments 37
Motion data for numerical simulations 39

CHAPTER VI DISCUSSIONS AND ANALYSIS OF RESULTS 43

Comparisons between solid wall and pile supported dock 43
Effect of wave height 44
Effect of wave period 46
Effect of wave direction 48
Repeatability 50
Comparisons between experiment and numerical simulation 51
Effect of wave height 52
Effect of wave period 54
Effect of wave direction 57
Repeatability 59
Effect of high frequency oscillations, accuracy, and data analysis on motion data .. 60
Discussion of differences between the experimental and numerical motion results 61

CHAPTER VII SUMMARY OF CONCLUSIONS AND RECOMMENDATIONS 63

REFERENCES 65

APPENDIX 67

LIST OF FIGURES

Page

Figure 1. Definitions of ship rotations and translations. 2

Figure 2. Model container ship moored to solid wall dock (top) and schematic of mooring line locations (bottom). 3

Figure 3. Plan view of the solid wall dock model. 13

Figure 4. Side view of solid wall dock model. 13

Figure 5. Plan view of pile supported dock model. 13

Figure 6. Side view of pile supported dock. 14

Figure 7. Shallow water (3D) basin arrangement and dimensions. 18

Figure 8. TMA and Jonswap spectrum comparisons 22

Figure 9. Multidirectional wave generator with 48 individual paddles. 24

Figure 10. Spacing and position of wave gauges. 24

Figure 11. Wave gauge calibration. 25

Figure 12. Instrument carriage with four cameras for motion tracking system 26

Figure 13. Location of reflective makers on model ship used by the motion tracking system. 27

Figure 14. L-shaped bar and wand on the model dock with moored ship prior to calibration 28

Figure 15. Roll damping test result 31

Figure 16. Translation result of static test of six degrees of freedom motion 32

Figure 17. Rotation result of static test of six degrees of freedom motion 33

Figure 18. Spectrum comparison between reflect (Upper) and incident (Lower) waves 36

Figure 19. Reflection (Upper) and translation (Lower) coefficients vs. time 36

Figure 20. Comparison of six degrees of motion for container ship moored in front of solid (Left) and pile (Right) docks 38

Figure 21. Translation elevation comparisons between experiment (Blue) and numerical simulation (Red) 40

Figure 22. Rotation elevation comparisons between experiment (Blue) and numerical simulation (Red) 41

Figure 23. Comparison of motions results under effect of wave height of container moored in front of solid wall and open pile dock 44

Figure 24. Comparison of motions results under effect of wave period of container moored in front of solid wall pile support docks 47

Figure 25. Comparison of motions results under effect of wave direction of container ship moored in front of solid wall and pile supported docks. 49

Figure 26. Comparison of motions results repeatability of container ship moored in front of solid wall and pile supported docks 51

Figure 27. Comparison of numerical and experimental results on the effect of wave height on moored ship motions. 52

Figure 28. Comparison of the effect of wave period on moored ship motions. 56

Figure 29. Comparison of the numerical and experimental results of the effect of wave direction on moored ship motions. 58

Figure 30. Comparison of numerical and experimental results for six degrees of freedom. 60

LIST OF TABLES

Page

Table 1. Test plan for solid and pile docks 9

Table 2. Direction equivalents for prototype, model and numerical model..... 10

Table 3. Model ship and dock for selected geometric scale and Froude scale (US) 15

Table 4. Wave basin condition for selected geometric scale and Froude scale (US)..... 16

Table 5 Model ship and dock for selected geometric scale and Froude scale (SI)..... 16

Table 6. Wave basin condition for selected geometric scale and Froude scale (SI) 16

Table 7. Shallow water (3-D) basin characteristics 17

Table 8. Wave length and classification..... 19

Table 9. Motion elevation information of test 13 39

Table 10. Mean value comparison of motions results under effect of wave height of container ship moored in front of quay wall and open quay wharf..... 45

Table 11. Mean value comparison of motions results under effect of wave period of the container ship moored in front of solid wall and pile supported docks 48

Table 12. Mean value comparison of motions results under effect of wave direction of container moored in front of solid wall and pile supported docks 49

Table 13. Standard deviation comparison of motions results repeatability of container ship moored in front of solid wall and pile supported docks..... 51

Table 14. Mean value comparison of numerical and experimental results on the effect of wave height on moored ship motions. 54

Table 15. Mean value comparison of numerical and experimental results on the effect of wave period on moored ship motions. 56

Table 16. Mean value comparison of numerical and experimental results on the effect of wave direction on moored ship motions. 59

Table 17. Standard deviation comparison of numerical and experimental results repeatability on moored ship motions. 60

Table 18. Mean value comparison of numerical and experimental results repeatability on moored ship motions. 60

CHAPTER I

INTRODUCTION AND LITERATURE REVIEW*

Introduction

Ocean shipping accounts for more than two thirds of international trade and the container ship accounts for the majority of the non-bulk freight cargo transportation. For example, a Panamax vessel has a length, width and draft of 294.13m (965ft), 32.31m (106ft) and 12.04m (39.5ft), respectively and is able to load 5000 TEUs. TEU is defined as a twenty-foot equivalent unit container, representing the cargo capacity of a standard intermodal container with 6.1m (20ft) length and 2.44m (8ft) width and height. The shipping price per each TEU from Shanghai, China to Los Angles, California, USA, is around US $ 2100/TEU, which has become an optimal option for both low and high value products. Canals, such as Panama and Suez, link seas and oceans. Harbors of United States are essential terminals for both international and domestic trade and are now requiring expansion and renovation to accommodate larger container ships.

Container ships require small motions to maintain a safe distance between the side of the ships and quays while loading or off-loading. Vertical-faced wharfs, including two types of docks i.e. quay wall (solid wall dock) and open quay (pile supported dock), are applicable for most seaports and river ports with fluctuating water levels less than 8m (26ft) and commonly used to moor container ships. The popularity of

* Part of the figures or tables reported in this chapter is reprinted with permission from "Comparison of Laboratory and Predicted Motions and Mooring Line Forces for a Container Ship Moored to a Dock" by Andres Luai and Yuanzhe Zhi, 2013. A conference report of the 18th Offshore Symposium Engineering the Future: The Arctic and Beyond. Houston Texas. Copyright [2013] by SNAME Texas Section.

this type of wharf is because of its simplified handling procedures, which decreases the terminal time and expenses and increases the handling efficiency. Correct selection of the types of dock terminals is based on the characteristics of these types of docks and the effects of waves and currents. The quay wall wharf or solid wall dock includes a gravity quay wall, a sheet-pile quay wall, and front sheet-pile platform and is defined as a dock of vertical solid wall resisting the earth pressure of the backfill behind it. Open quays are piers with a platform supported by piles, which allows waves and currents to pass through and penetrate underneath them and minimize the wave reflections. Waves are the major cause of ship motions, which has six degrees of freedom (Tupper, 1996), including surge, sway, and heave (translations) and roll, pitch and yaw (rotations), shown in Figure 1.

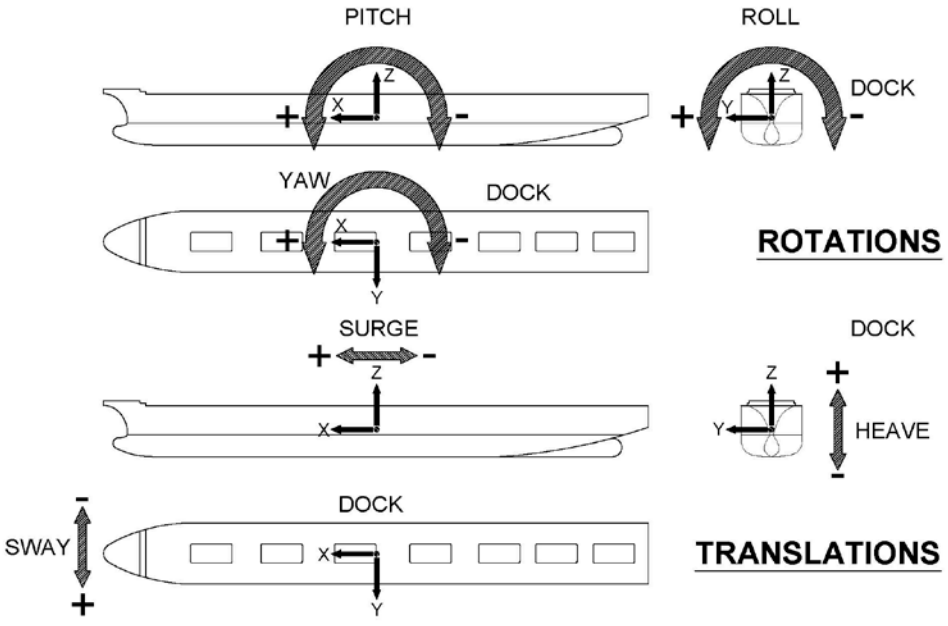

Figure 1. Definitions of ship rotations and translations.

For this thesis, the container ship is moored to a solid wall dock using 7 fenders and 14 synthetic mooring lines with three bow lines (1a, 1b, and 1c), two forward breast lines (2a and 2b), two after breast lines (5a and 5b), two forward spring lines (3a and 3b), two after spring lines (4a and 4b), and three stern lines (6a, 6b, and 6c), which are shown in Figure 2. The incoming waves that cause motions of the ship in front of these two types of piers were characterized by employing both model test, with the optical motion tracking system and numerical simulation with aNySIM (Marin 2012).

Figure 2. Model container ship moored to solid wall dock (top) and schematic of mooring line locations (bottom).

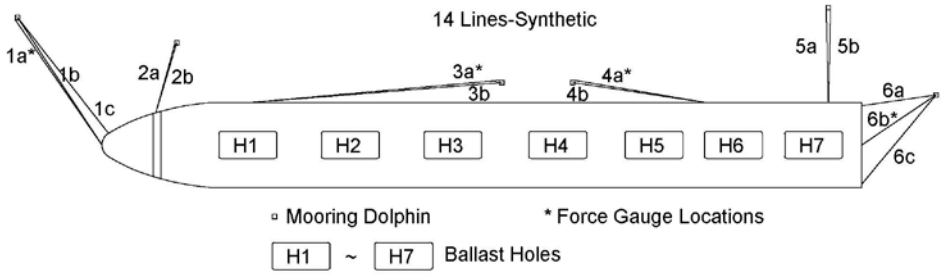

Figure 2. Continued.

Objectives

The first objective of this thesis is to describe the laboratory measurements of the translations (surge, sway, and heave) and rotations (roll, pitch, and yaw) motions of a model container ship that is moored to a solid wall dock and a pile supported dock and determine if one type of dock results in less motions than the other. For the second objective, a numerical simulation is used to compare the numerical model estimation of moored ship motions to the physical model test results of the model container ship moored to the solid dock.

Literature review

To capture and record the six degrees of freedom motions of floating structures, several efforts have been accomplished using either physical modeling or numerical modeling. Cobazas, Jagersand, and Sturm (2006) applied three dimensional sum-of-squared differences to track with three dimensional planes of six degrees of freedom motion. In their experiment, full 3D positions are calculated by calculation of the position of three dimensional planes of the three dimensional objective, rather than the

corresponding points. The motions of these planes are captured by tracking and matching each pixel intensity.

Clay (2011) applied the Qualisys optical motion tracking system, including four cameras, which are applied to detect the highly reflected markers placed on model, and Qualisys Track Manager Software, which records, transfers the 2D image to three dimensions, and calculates and exports the motion data of six degrees of freedom (6DOF), in the Haynes Laboratory to evaluate 6DOF motions of floating model barges. Two types of barges and a tower were tested and classified into three groups with different mooring methods and wave types, e.g. regular waves and irregular waves using JONSWAP spectrum. His report introduced the operation methods of Qualisys motion tracking system including hardware connection, calibration, rigid body definition, and motion tracking software. After exporting and format transformation, both translational and rotational response amplitude operators, which are defined as dividing displacements and rotations respectively by amplitude, were calculated and compared. These RAOs were compared with previous studies conducted by Pinkster (1980) and Domnisoru et al. (2008).

Several studies have been completed that contribute to the representation of moored ship behaviors. Santos, Gomes, Pinto and Dias (2010) applied an optical motion tracking system to characterize the motions of an oil tanker in a rough wave environment and two kinds of mooring layouts for the Leixões Oil Terminal. During this project a 1:100 scale model under two environmental conditions were tested. The first phase was a series of tests with a rough environmental model of uniform water depth. Four wave

gauges were used to record the water surface elevation, and these data were used for reflection analysis. An optical motion capturing system with three cameras was applied to capture and record the six degrees of freedom motion of the oil tanker using a capturing frequency of 24 Hz. The second phase has a much more detailed berth model with uniform water depth. The tanker in both phases was under the action of long crested irregular waves. Tschirky, Pinkster, Rolling's, Smith, and Cornett (2010) describe the 6-axis motions of moored ship behavior due to the influence of a passing ship by using two separate high-precision optical motion tracking systems.

Wave reflection is an important factor in generating the motion of floating vessels. Goda and Suzuki (1976) applied two measuring probes, named the Two-point Method, based on the assumption that the summation of two opposite directions while the same frequency sinusoids generate the wave elevation at each measuring probe, and they obtained the amplitude of the incident and reflected waves. Certain limitations, however, restrict the application of this Two-point Method. This method has a limited frequency range. That is to say, under the circumstance of large space between two probes, the ascending of frequency leads to descending of coherency factor and the reliability of reflection calculation. On contrary, when the space between two probes is short, a contrast loss exists in cross spectral analysis. Moreover, critical probe spacing is required. In addition, there is high sensitive error of wave measurement.

For irregular waves, Mansard and Funke (1980) applied a least squares method to separate the incident and reflected spectra from co-existing spectra based on the simultaneously measured wave data of the three probes. By applying a least square

method, the solution of Z_I and Z_R, are solved in (1) and (2). Then spectral densities S_I and S_R are computed, namely:

$$Z_{I,k} = C_{I,k} \cdot exp\left[i \cdot \frac{2\pi \cdot \left(X_1 + X_{1p}\right)}{L_k} + i \cdot \theta_k\right] \quad (1)$$

$$Z_{R,k} = C_{R,k} \cdot exp\left[i \cdot \frac{2\pi \cdot \left(X_1 + 2 \cdot X_{R1} - X_{1p}\right)}{L_k} + i \cdot (\theta_k + \phi_k)\right] \quad (2)$$

$$S_I(k \cdot \Delta f) = |Z_I(k \cdot \Delta f)|^2/(2 \cdot \Delta f) \quad (3)$$

$$S_R(k \cdot \Delta f) = |Z_R(k \cdot \Delta f)|^2/(2 \cdot \Delta f) \quad (4)$$

Among these above equations, $C_{I,k}$ and $C_{R,k}$ represent incident and reflect wave respectively. X_1, X_{1p}, and X_{R1} are distances between wave generator and wave gauge1, length between wave gauge1 and the rest of the wave gauges, distance from gauge 1 to the reflected object. L_k represent the wave length. Δf is the frequency of wave. θ_k and ϕ_k are arbitrary phase and phase change respectively. The reflection coefficient thus can be generated by dividing the incident and reflected spectral densities:

$$R(k \cdot \Delta f) = |Z_R(k \cdot \Delta f)|/|Z_I(k \cdot \Delta f)| \quad (5)$$

Their report also discussed the effect of probe spacing. The refection coefficient calculation becomes indeterminate when X_{12} equals to half or multiples of half a wave length and X_{13} is equal to multiples of X_{12}. The Mansard and Funke (1980) wave probe spacing suggestions are:

$$X_{12} = \frac{L_p}{10} \quad (6)$$

$$\frac{L_p}{6} < X_{13} < \frac{L_p}{3} \quad (7)$$

$$X_{13} \neq \frac{L_p}{5} \tag{8}$$

$$X_{13} \neq \frac{3L_p}{10} \tag{9}$$

where $L_p$is wave length. Compared with the two probes method, the three gauge method has a wider frequency range and reduces the noise deviation and critical probe spacing sensitivities.

CHAPTER II

EXPERIMENT PLAN

Plans for the experimental tests contain two cases of physical modeling, which are a model container ship moored to a solid dock and a piled dock. Only the model ship moored to the solid dock is simulated numerically by applying aNySIM. The experimental plan cases are illustrated in Table 1. The conversion of wave direction between the proto type and model are stated in Table 2.

Table 1. Test plan for solid and pile docks.

Test	Model			Proto Type		
	Hs_m (m)	Tp_m (s)	Dir_m (◦)	Hs_p(m)	Tp_p (s)	Dir_p (◦)
1	0.012	1.13	0	0.6	7.99	143
2	0.024	1.41	0	1.2	9.97	143
3	0.037	1.7	0	1.85	12.02	143
4	0.049	1.98	0	2.45	14.00	143
5	0.037	1.7	0	1.85	12.02	143
6	0.037	0.566	0	1.85	4.00	143
7	0.037	0.85	0	1.85	6.01	143
8	0.037	1.13	0	1.85	7.99	143
9	0.037	1.41	0	1.85	9.97	143
10	0.037	1.98	0	1.85	14.00	143
11	0.037	2.26	0	1.85	15.98	143
12	0.037	2.55	0	1.85	18.03	143
13	0.037	2.83	0	1.85	20.01	143
14	0.012	1.7	0	0.6	12.02	143
15	0.024	1.7	0	1.2	12.02	143
16	0.049	1.7	0	2.45	12.02	143
17	0.037	1.7	-30	1.85	12.02	113
18	0.037	1.7	-15	1.85	12.02	128
19	0.037	1.7	15	1.85	12.02	158
20	0.037	1.7	30	1.85	12.02	173

Table 1. Continued.

Test	Model			Proto Type		
	Hs_m (m)	Tp_m (s)	Dir_m (◦)	Hs_p(m)	Tp_p (s)	Dir_p (◦)
21	0.037	1.7	0	1.85	12.02	143
22	0.037	1.7	0	1.85	12.02	143
23	0.037	1.7	0	1.85	12.02	143
24	0.037	1.7	0	1.85	12.02	143
25	0.037	1.7	0	1.85	12.02	143
26	0.037	1.7	0	1.85	12.02	143
27	0.037	1.7	0	1.85	12.02	143
28	0.037	1.7	0	1.85	12.02	143
29	0.012	1.13	0	0.6	7.99	143
30	0.024	1.41	0	1.2	9.97	143
31	0.024	1.41	-15	1.2	9.97	128
32	0.024	1.41	15	1.2	9.97	158
33	0.024	1.41	0	1.2	9.97	143
34	0.037	1.7	0	1.85	12.02	143
35	0.037	1.7	-30	1.85	12.02	173
36	0.037	1.7	0	1.85	12.02	143
37	0.037	1.7	0	1.83	12.02	143
38	0.037	1.7	0	1.83	12.02	143
39	0.037	1.7	0	1.85	12.02	143

Table 2. Direction equivalents for prototype, model and numerical model.

Test	Proto Type (◦)	Model (◦)	aNySIM (◦)
17	113	-30	240
18	128	-15	255
19	158	15	285
20	173	30	300
31	128	-15	255
32	158	15	285
35	173	-30	240

Case 1, solid dock 39 tests

For the solid wall dock, Case 1, the TMA spectra with four variations of significant wave heights of 0.6m (2ft), 1.2m (4ft), 1.85m (6ft), and 2.45m (8ft) for proto type and 0.012m (0.04ft), 0.024m (0.08ft), 0.037m (0.12ft), and 0.049m (0.16ft) for the model are tested. Nine different wave periods from 4s to 20s for the proto type and 0.57s to 2.83s for model are tested, and 5 wave directions, i.e. 30, 15, 0,-15, -30 degrees in the model and 113, 128, 143, 158, 173 degrees in the prototype are simulated.

Case 2, pile dock 39 tests

In Case 2, the same tests are repeated for the piled dock.

Case 3, numerical simulation 39 tests

The translations of sway, surge, and heave and the rotations of roll, yaw, and pitch for the container ship moored to a solid dock, which are the same 39 tests as in Case 1with typical draft of 8.53m (28ft), are numerically simulated by using the numerical software aNySIM.

CHAPTER III

CONTAINER SHIP AND DOCK MODELS*

The model system contains one model ship, one solid wall dock, and one piled dock. Figure 3 and Figure 4 represent drawings of the plan and side views of the model solid wall dock, respectively. This dock is composed by many 30 degree sections of PVC cylindrical caissons to form the vertical solid wall (quay wall) with a supporting platform on top of it. Model fenders are mounted between the container ship and dock. The toe of the dock is protected by rock and gravel in proto type and model respectively. Figure 5 and Figure 6 illustrate the plan view and side view of pile supported dock respectively, in which the platform is supported by vertical and inclined piles with small rock simulating a rock beach slope. Fenders are attached and hung on the edge of the platform between the model container ship and the dock. The water depths in front of these two types of docks are 15.24m (50ft) and 0.30m (1ft) for proto type and model type respectively.

* Part of the figures or tables reported in this chapter is reprinted with permission from "Comparison of Laboratory and Predicted Motions and Mooring Line Forces for a Container Ship Moored to a Dock" by Andres Luai and Yuanzhe Zhi, 2013. A conference report of the 18th Offshore Symposium Engineering the Future: The Arctic and Beyond. Houston Texas. Copyright [2013] by SNAME Texas Section.

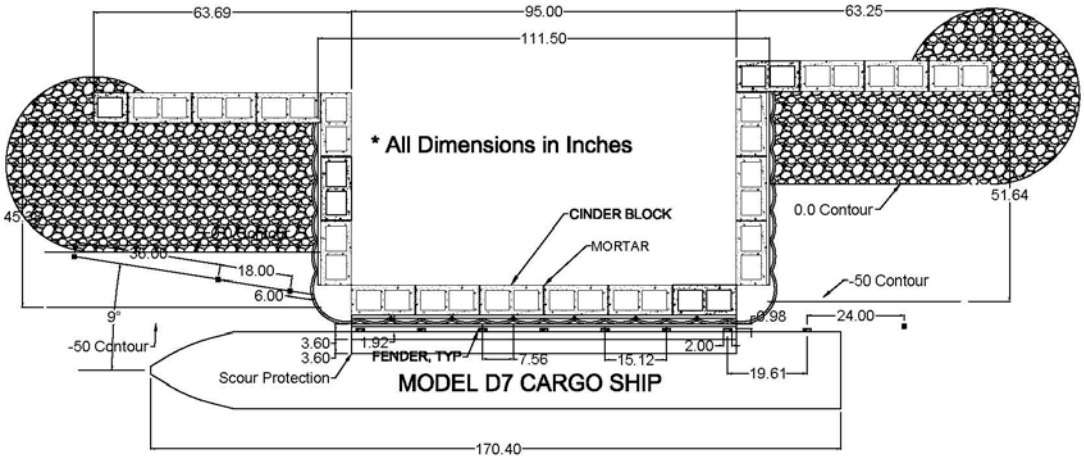

Figure 3. Plan view of the solid wall dock model.

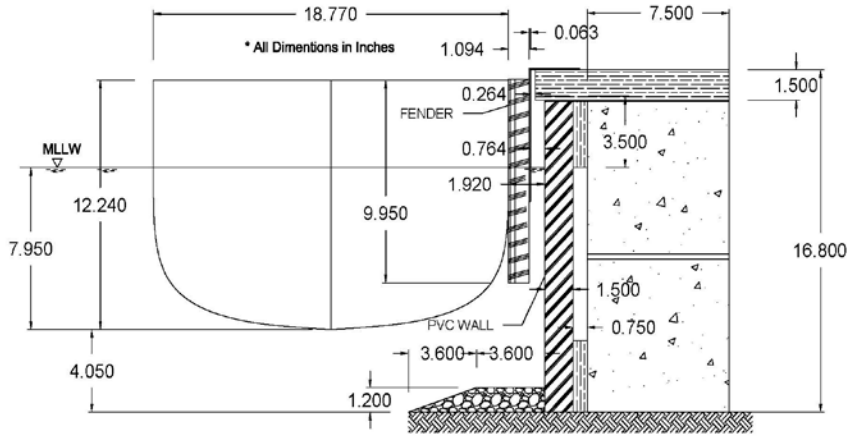

Figure 4. Side view of solid wall dock model.

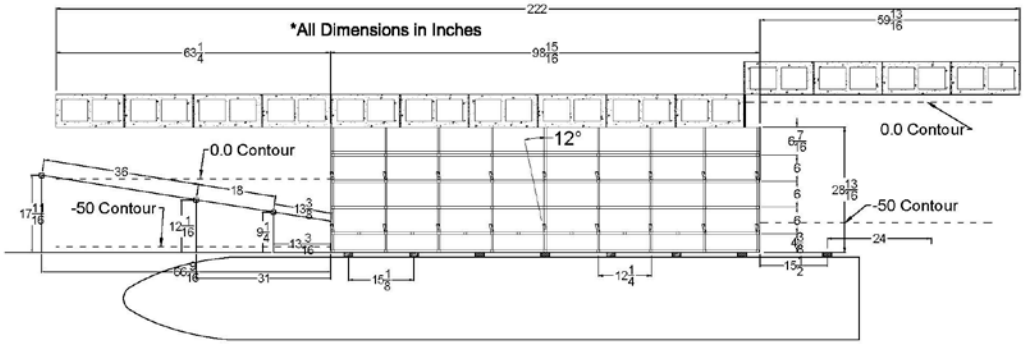

Figure 5. Plan view of pile supported dock model.

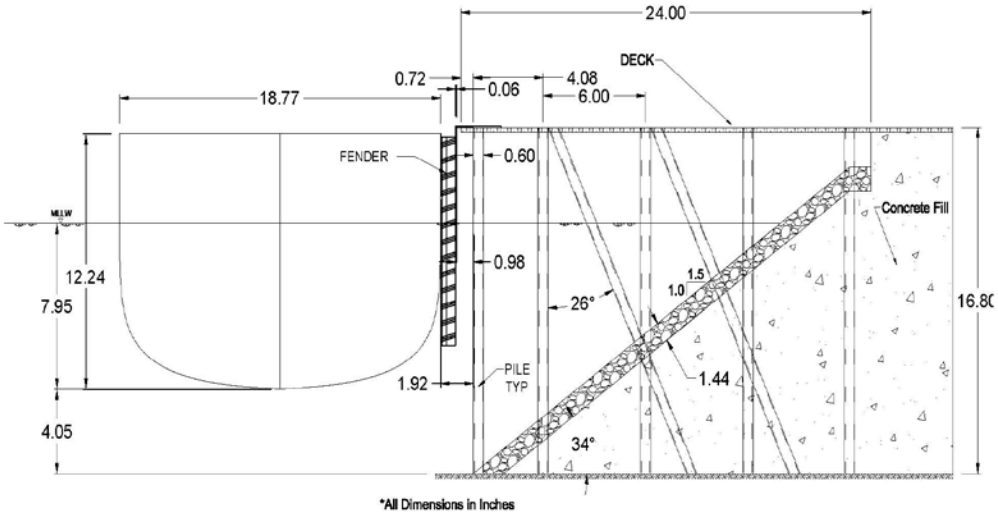

Figure 6. Side view of pile supported dock.

Froude similarity

The Froude similarity (Kundu & Cohen, 2008) is applied, which is defined as

$$Fr = \frac{V}{\sqrt{gL}} \tag{10}$$

where V is the velocity, g is gravitational acceleration, and L is the length. Accordingly the geometry scale, time scale, and speed scale are illustrated in equation (11), (12), and (13) respectively (Hughes, 1993).

$$\lambda_l = l_p / l_m \tag{11}$$

$$\lambda_t = \sqrt{\lambda_l} \tag{12}$$

$$\lambda_v = \sqrt{\lambda_l} \tag{13}$$

Container ship and dock scale

Since the time scale is the square root of the geometric model scale, 50:1, then the time in the model is 7.07 times slower in the wave basin than in the prototype. Accordingly, the model ship has a length, width, and typical draft of 4.328 m (170.4 inches), 0.477m (18.77 inches), and 0.171m (6.72 inches) respectively. The environmental conditions in the wave basin are a water depth of 0.305 m (12 inches) at mean low water and 0.366 m (14.4 inches) at mean high tide in the wave basin. A comparison between the prototype container ship, environmental conditions, and the scale model in US units are illustrated in Table 3 and Table 4 respectively, of which the SI units are illustrated in Table 5 and Table 6 respectively.

Table 3. Model ship and dock for selected geometric scale and Froude scale (US).

Ship Characteristics	**Prototype**	**Prototype Units**	**Model Ship**	**Model Units**
Displacement	37474	tons (US)	599.58	lbs
Length	710	ft	170.40	inches
Beam	78.21	ft	18.77	inches
Depth	51	ft	12.24	inches
Draft (typical), (light)	28, 13	ft	6.72, 3.12	inches

Table 4. Wave basin condition for selected geometric scale and Froude scale (US).

Environment Conditions	Prototype	Prototype Units	Model Ship	Model Units
Water depth	50	ft	12.0	inches
Water depth +high tide	58.8	ft	14.4	inches
Quayside distance	8	ft	1.92	inches
Significant wave heights	2,4,6,8,10	ft	0.48, 0.96, 1.44, 1.92, 2.40	inches
Wave periods	4,6,8,10,12, 14,16,18,20	s	0.57,0.85, 1.13, 1.41, 1.70, 1.98, 2.26,2.56,2.83	s

Table 5. Model ship and dock for selected geometric scale and Froude scale (SI).

Ship Characteristics	Prototype	Prototype Units	Model Ship	Model Units
Displacement	33996	tons (SI)	271.97	Kg
Length	216.41	m	4328	mm
Beam	23.84	m	477	mm
Depth	15.54	m	311	mm
Draft (typical), (light)	8.53, 3.96	m	171, 79	mm

Table 6. Wave basin condition for selected geometric scale and Froude scale (SI).

Environment Conditions	Prototype	Prototype Units	Model Ship	Model Units
Water depth	15.24	m	305	mm
Water depth +high tide	17.92	m	366	mm
Quayside distance	2.44	m	49	mm
Significant wave heights	0.61, 1.22, 1.83, 2.44, 3.05	m	12, 24, 37, 49, 61	mm
Wave periods	4,6,8,10,12, 14,16,18,20	s	0.57,0.85, 1.13, 1.41, 1.70, 1.98, 2.26,2.56,2.83	s

Wave basin and wave generator

The wave basin in the Haynes Coastal Engineering Laboratory is illustrated in Figure 7. This figure illustrates the model container ship, moored in front of the solid dock, three wave gauges with specific distances according to three probe methods (Mansard and Funke 1980), and data acquisition carriage, including the wave data acquisition system and optical motion tracking system. Waves are generated by the laboratory multidirectional wave generator. The wave heights, periods, and water depth are measured with wave gauges and recorded by the data acquisition system. The shallow water basin is 36.6m (120ft), 21.9m (75ft), and 1.2m (4ft) in length, width, and depth respectively, which is shown in Table 7 along with the general characteristics of the wave generation system.

Table 7. Shallow water (3-D) basin characteristics.

Geometry size	Length	36.6m	120ft
	Width	22.9m	75ft
	Depth	1.2m	4ft
Wave generator	Wave generator type	Segmented piston type directional capabilities	48 paddles
	Wave Periods	0.5 to 5 sec	
	Irregular Wave heights	Up to 0.36m in 1.0m water depth at 2.3s wave period	Up to 1.20ft in 3.28ft water depth at 2.3s wave period
	Wave Types	harmonic, irregular, or any type of wave spectra (linear and nonlinear); short-crested and broad-crested	

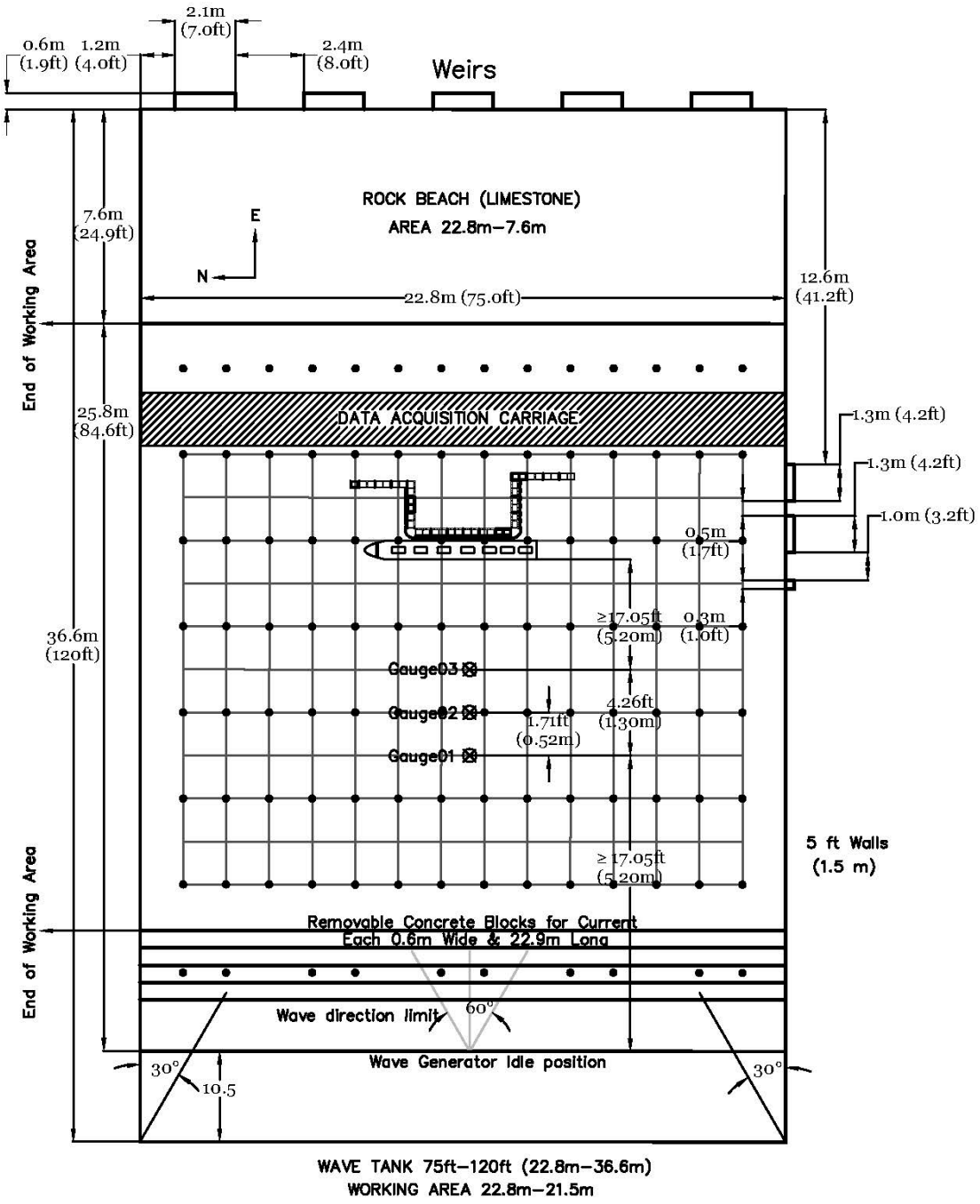

Figure 7. Shallow water (3D) basin arrangement and dimensions.

Wave conditions in model and prototype

The prototype project site is located in a coastal area with a water depth of 15.24m (50ft). The dispersion relationship to generate the relationship between wave period and wavelength is

$$L = \frac{g}{2\pi} T^2 \, tanh \frac{2\pi h}{L} \tag{14}$$

where L is wavelength, g is gravity, T is wave period, and h is water depth. A shallow water wave occurs when the water depth over the wavelength (h/L) is less than 0.05, and for deep water waves the h/L is larger than 0.5. Otherwise the waves are classified as intermediate water waves, and this is the case for the waves for this thesis, represented in Table 8. In this table, wavelengths are computed by iteration in Equation (14) and the water depth divided by wavelength is tabulated.

Table 8. Wave length and classification.

Hs (m)	Ts (s)	f (Hz)	Spectra Peak Factor	Dir (°)	h (m)	L (m)	h/L
0.012	1.13	0.885	3.3	0	0.36576	1.7316	0.2112
0.024	1.41	0.709	3.3	0	0.36576	2.3402	0.1563
0.037	1.7	0.588	3.3	0	0.36576	2.9456	0.1242
0.049	1.98	0.505	3.3	0	0.36576	3.5149	0.1041
0.037	1.7	0.588	3.3	0	0.36576	2.9456	0.1242
0.037	0.566	1.767	3.3	0	0.36576	0.5001	0.7314
0.037	0.85	1.178	3.3	0	0.36576	1.0947	0.3341
0.037	1.13	0.885	3.3	0	0.36576	1.7316	0.2112
0.037	1.41	0.709	3.3	0	0.36576	2.3402	0.1563
0.037	1.98	0.505	3.3	0	0.36576	3.5149	0.1041
0.037	2.26	0.442	3.3	0	0.36576	4.0746	0.0898
0.037	2.55	0.392	3.3	0	0.36576	4.6475	0.0787
0.037	2.83	0.353	3.3	0	0.36576	5.196	0.0704
0.012	1.7	0.588	3.3	0	0.36576	2.9456	0.1242

Table 8. Continued.

Hs (m)	Ts (s)	f (Hz)	Spectra Peak Factor	Dir (°)	h (m)	L (m)	h/L
0.024	1.7	0.588	3.3	0	0.36576	2.9456	0.1242
0.049	1.7	0.588	3.3	0	0.36576	2.9456	0.1242

The modeling concentrates on a short term storm wave analysis that means the waves occur within one storm that is approximately 1 hour for prototype and 8 min for model. The TMA spectrum is a modified Jonswap spectrum under the circumstance of shallow water the spectral density of Jonswap is multiplied byΦ_d, which is introduced by Bouws et al. in 1983, 1984 (Kamphuis, 2002). Φ_d is equivalent to 1 in deep water, because under condition of deep water, kh is large, and sinh 2kh of n from equation (19) is extremely large compared with 2kh which derive that n equals to 0.5 under deep water. On the other hand, $\tanh\frac{2\pi h}{L}$ is approximate to 1 (Dean & Dalrymple, 1991). For that matter the equation (16) equals to 1 for deep water conditions. The TMA spectral density function is stated as follows:

$$S_{TMA}(f,d) = S_J(f)\Phi_d \tag{15}$$

$$\Phi_d = \frac{1}{2n}tanh^2\frac{2\pi h}{L} \tag{16}$$

where S_J is Phillips function, h is water depth, and L is wave length.

Since the Jonswap spectrum is

$$S_J(f) = \frac{\alpha H_{1/3}^2 \gamma^{e^a}}{T^4 f^5} e^{-\frac{5}{4}\left(\frac{f}{f_p}\right)^{-4}} \tag{17}$$

where $H_{1/3}$ is significant wave height, T is wave period, f is frequency, and f_p is peak frequency. Recall that the peak enhancement factor

$$\gamma = 3.3 \tag{18}$$

$$n = \frac{1}{2}\left(1 + \frac{2kh}{sinh\ 2kh}\right) \tag{19}$$

$$\alpha \approx 0.2044 \tag{20}$$

and peak frequency f_p, are used to generate the density function of TMA spectrum,

$$S_{TMA}(f) = 0.2044 \frac{H_{1/3}^2}{T^4 f^5} e^{-\frac{5}{4}\left(\frac{f}{f_p}\right)^{-4}} 3.3^{exp\left[\frac{-(f-f_p)^2}{2\delta^2 f_p^2}\right]} \frac{1}{\left(1 + \frac{2kh}{sinh\ 2kh}\right)} tanh^2 \frac{2\pi h}{L} \tag{21}$$

This expression of density function is used for generating the wave file for the numerical simulation of aNySIM. However, the plot of the TMA spectrum is coincident to the Jonswap spectrum, and under the circumstance of intermediate water depth for numerical simulation using aNySIM, the Jonswap is applied. An example comparison of TMA spectrum (WAFO, WAFO. Description of tmaspec, 2005) and Jonswap (WAFO, WAFO. Description of jonswap, 2005) is generated by the MatLab tool WAFO for Test 3 with significant wave height, period, peak frequency, and wave length which are shown in equation (22), (23), (24), and (25) respectively. This is illustrated in Figure 8., indicating that under the experimental wave conditions both TMA and Jonswap spectrum can be applied.

$$H_{1/3} = 0.037m \tag{22}$$

$$T = 1.7s \tag{23}$$

$$f_p = 0.588Hz \tag{24}$$

$$L = 2.9456m \tag{25}$$

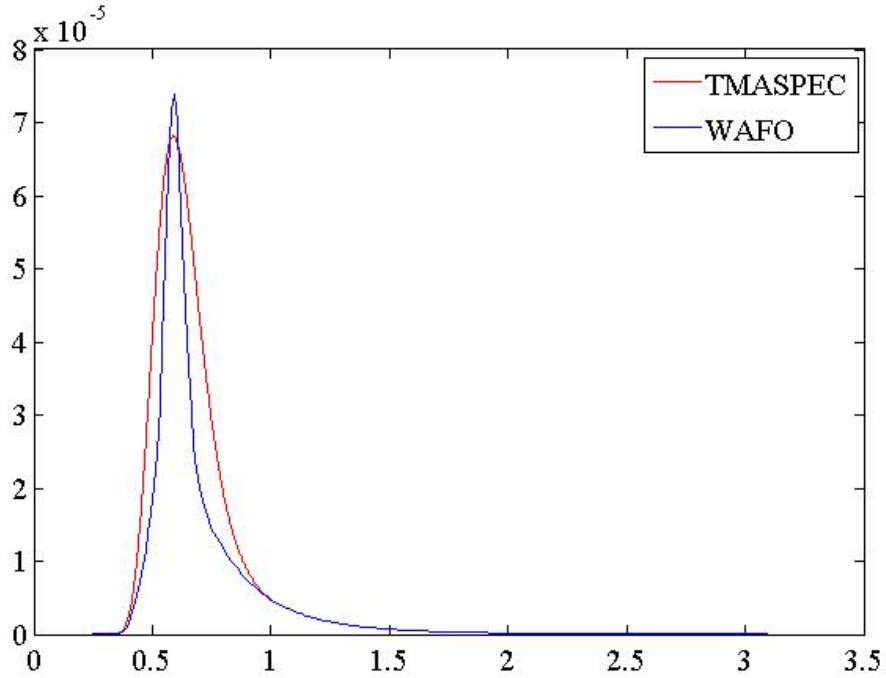

Figure 8. TMA and Jonswap spectrum comparisons (Red solid lineTMA (red), by applying equation (21) and blue solid line TMAspec & Jonswap, generated by WAFO)

CHAPTER IV

INSTRUMENTATION, SETTINGS, AND CALIBRATIONS*

Wave generator and acquisition system

Waves for experiments are generated by the Rexroth multidirectional wave generator. The water elevations are acquired by wired wave gauges connected to the Labview data acquisition (DAQ), and controlled by the Labview based wave data acquisition software.

Wave generator

Waves are generated by the multidirectional wave generator, and 48 paddled are individually controlled at the operator station. The 48 paddles allow the wave generator to generate regular waves up to 0.61m (2ft) wave height for period of 2.3s and at a period range of 0.5 - 5s at the maximum water depth of 1m (3.3ft). Multiple directions of propagation waves, ranging from 0 to 30 degrees on either side of the basin centerline, can be generated for both regular and spectral waves. To reduce the effect of reflections, active reflection absorption (ARA) system is available. In addition, a rock beach that has a slope of approximately 1V:6H absorbs the waves. The wave generator is shown in Figure 9.

* Part of the figures or tables reported in this chapter is reprinted with permission from "Comparison of Laboratory and Predicted Motions and Mooring Line Forces for a Container Ship Moored to a Dock" by Andres Luai and Yuanzhe Zhi, 2013. A conference report of the 18th Offshore Symposium Engineering the Future: The Arctic and Beyond. Houston Texas. Copyright [2013] by SNAME Texas Section.

Figure 9. Multidirectional wave generator with 48 individual paddles.

Wave gauges

Wave data including significant wave height, period and reflection coefficients are measured and recorded using the data acquisition system. This system contains three wave probes. In order to determine the reflection coefficient, the three wave gauges are arranged in a line perpendicular to the ship with the spacing suggested by Mansard and Funke (1980). Spacing among these three wave gauges is illustrated in Figure 10. The space between gauge 1 (p1) and gauge 2 (p2) is 0.52m (1.71ft), which is 1/10 of the maximum wave length in test plan, and the space between gauge 1 (p1) and gauge 3 (p3) is 1.30m (4.26ft), which is ¼ of the maximum wave length in test plan.

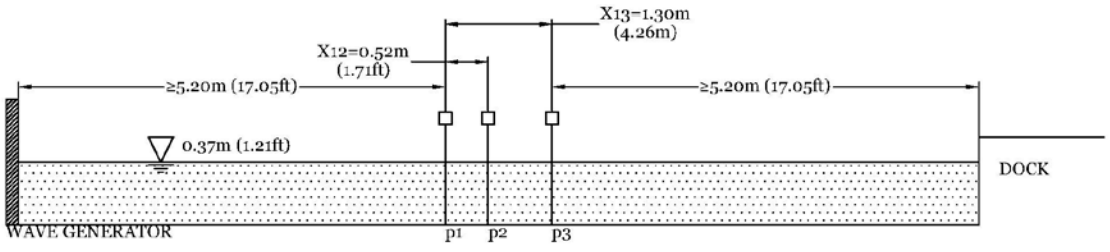

Figure 10. Spacing and position of wave gauges.

Calibration of wave gauges

Wave gauges transfer the wave elevations or water surface to voltages. These voltages are amplified before connected to the data acquisition computer via National Instrument DAQ. Accordingly, calibrations are needed to define the specific water levels to the relative voltages for each wave gauge. For calibration of each wave gauge, five points with equal distance between each other are selected and are individually placed at the water surface. Then, the voltages are recorded for each point. After that, slope and intercept are calculated represented in voltage vs. distance format. The relationship of voltage and distance should be linear, which can be plotted and represented in Figure 11 below, which contains distance for X axle and voltage for Y axle. The accuracy of the wave gauge is ±2mm.

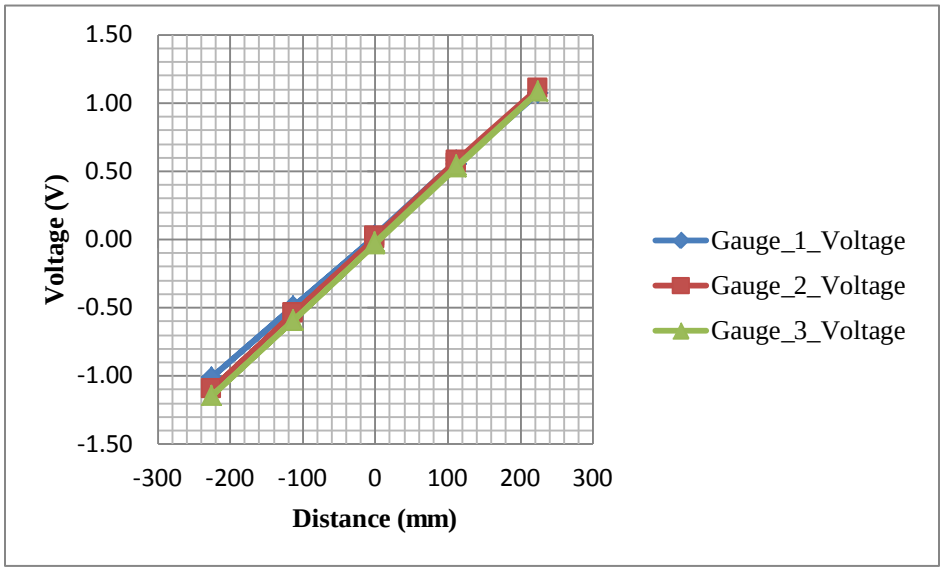

Figure 11. Wave gauge calibration.

Motion capturing and acquisition system

The six degree of freedom motions of the model container ship are captured using the optical motion tracking system, which consists of 4 cameras, shown in Figure 12, a calibration kit, and highly reflected markers adhered to the model container ship. A data acquisition computer installed with Qualisys Track Manager (QTM) is also used for recording and analyzing the motion data. This software allows the user to realize 2D and 3D motion capture that provides both real time 2D, 3D, and 6D data while motion capturing, and the data are output in several formats acceptable for Excel and MatLab.

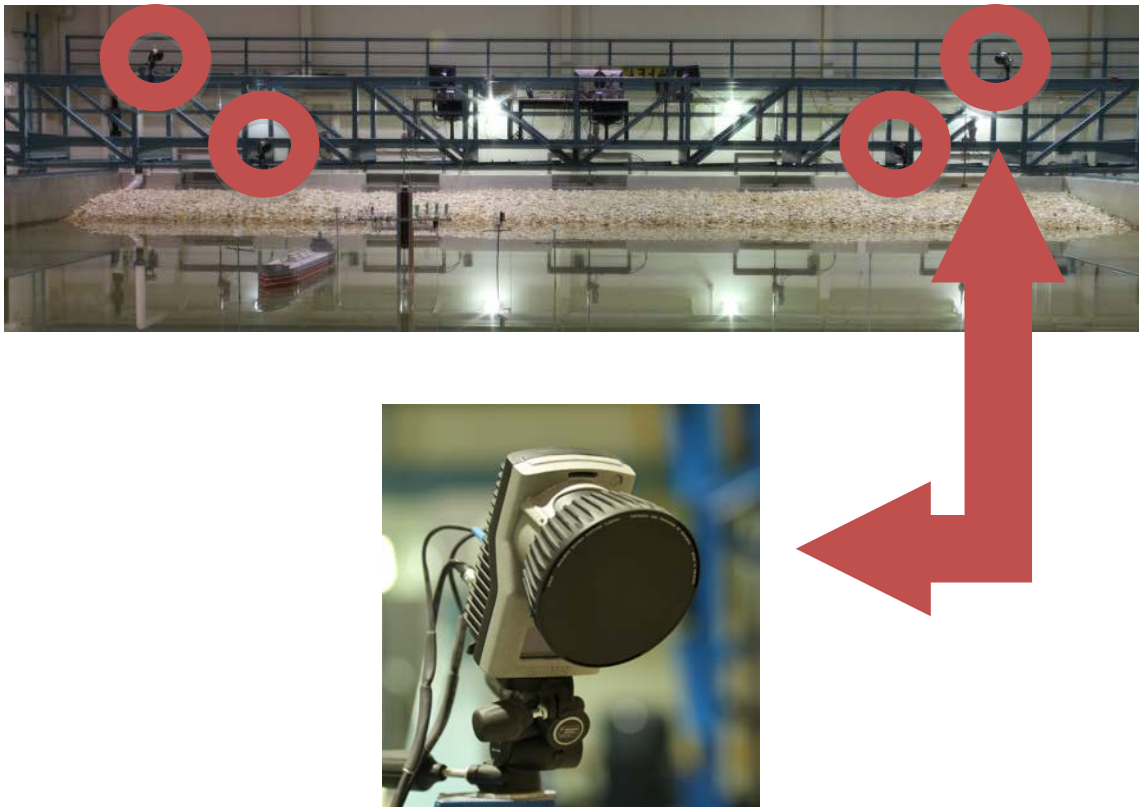

Figure 12. Instrument carriage with four cameras for motion tracking system

Settings and calibration

Highly reflected markers, shown in Figure 13, are adhered to the model container ship to be captured and define the model. To avoid covering each other, these markers are at different heights. Since the model is regarded as a rigid body, the connection between each marker and container should be fixed, in order to guarantee that the relative distances between each marker are constant during the calibration and testing.

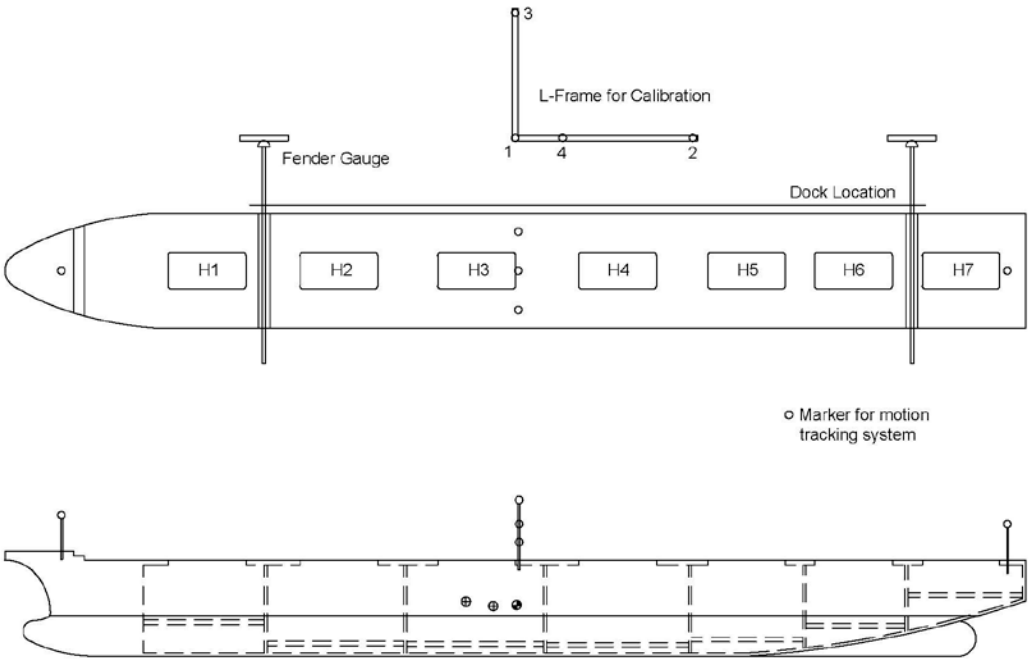

Figure 13. Location of reflective makers on model ship used by the motion tracking system.

The global coordinate system and the size of the capture volume are determined by calibration. The motion tracking system is calibrated using an L-shaped frame with

four passive reflective markers that are placed on the dock as illustrated in Figure 14. The L-shaped frame has its long axis parallel to the model ship centerline axis and the short axis perpendicular to the model ship. The origin of global coordinate system is located at the intersection of the X and Y axes that are parallel to the long and short axes of the L-frame, respectively. The wand device has two reflective markers on each end of a rod and the markers are located at a known distance of 748.3 mm. The wand is employed to measure the size of the capturing volume. This wand is connected to a long extension rod in order to reach the measurement area. A person rotates the wand in the area of the L-shaped frame and the area of the model ship to calibrate the four cameras in the motion tracking system. Once the calibration is completed, the L-shaped frame and wand are removed, and the calibration file is used by the software for capturing the motion data.

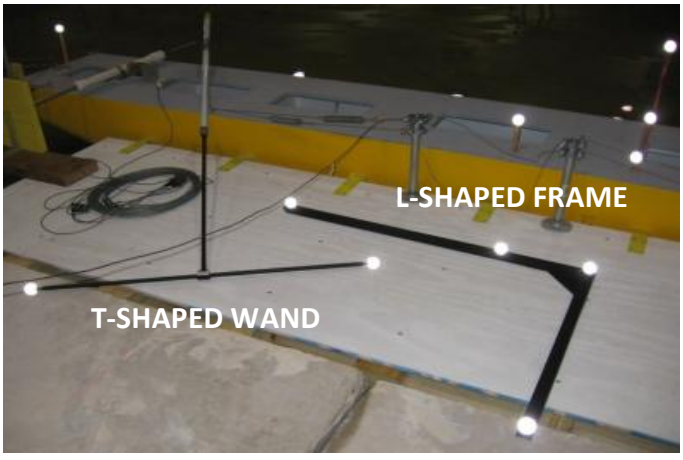

Figure 14. L-shaped bar and wand on the model dock with moored ship prior to calibration

The accuracy of instrument is needed, which attributed to these different results between numerical simulation and physical models. According to the operation methods applied on motion capture settings, the gap tolerances are set as 3 to 5mm. This setting defines the upper restriction of tiny vibrations of highly reflected markers, which defines the rigid body to be captured. The larger the gap tolerance define the lower accuracy are represented from the results. The accuracy of the motion tracking system is ± 2mm and ± 0.04°.

CHAPTER V

PROCEDURES

In order to achieve the purpose of the experiment, test preparations, physical modeling test, numerical simulation, and data analysis are conducted.

Phase 1, test preparation

During the test preparation, the necessary equipment and instrumentation is set-up and connected. The solid wall dock is built and installed in the wave basin. The basin is filled with water to a depth of 0.305m (1ft). Accordingly, prospective input wave files listed previously in Table 1 and Table 4 are loaded into the wave generator computer. After that, the model ship is moored to the dock, and the five reflective markers are adhered to solid wooden dowels at bow, stern, port side, starboard side and center of the model ship at various heights to define the rigid body of the model container ship.

Phase 2, physical model

For the physical model there are two processes to be accomplished, i.e. the solid dock and the piled dock. The model container ship motions are simulated under the effect of different significant wave heights, wave periods, and wave directions. Calibration of wave gauges and the motion tracking system is under taken at the beginning of each day. Data analysis occurs right after the test. After the completion of solid dock test, the dock is removed to make room for pile dock construction. Each test lasts 8 min and another 3-5 min is needed for the water surface to calm down between tests.

Before motion capturing of model container ship, roll damping tests are under taken, by pushing the model container on port side and applying the optical motion capturing system to record the rolling motion of the model container ship. After that, the time and motion data are applied to plot the roll vs. time, shown in Figure 15, and to calculate the natural frequency of roll. The calculation results indicate that the natural frequency of roll is around 1.5s for the model.

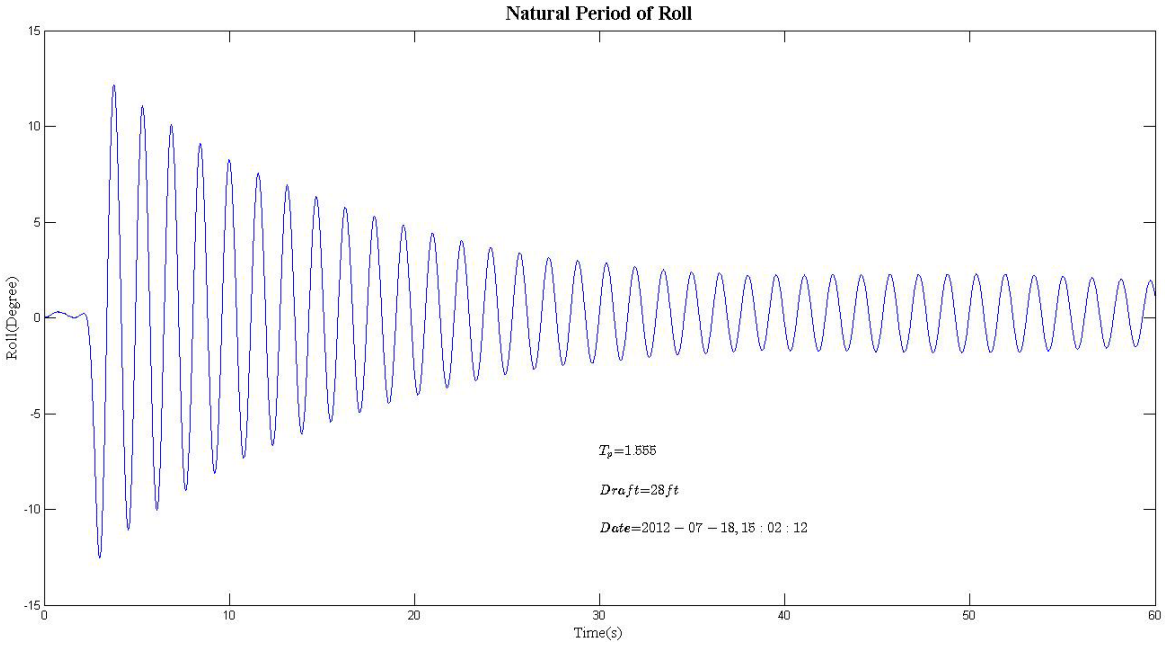

Figure 15. Roll damping test result

Static tests were also conducted with the model container ship moored in front of pile support dock to test the mooring system. The reason for choosing the pile support dock is due to the fact that the reflected waves generated by the ship motion are expected

to pass through the piles under wharf and cause relatively less wave reflections from the piled dock than the solid wall dock. Results indicate that, as shown in

Figure 16 and Figure 17, the mooring system can reduce and calm down the motion efficiently within one minute for model type.

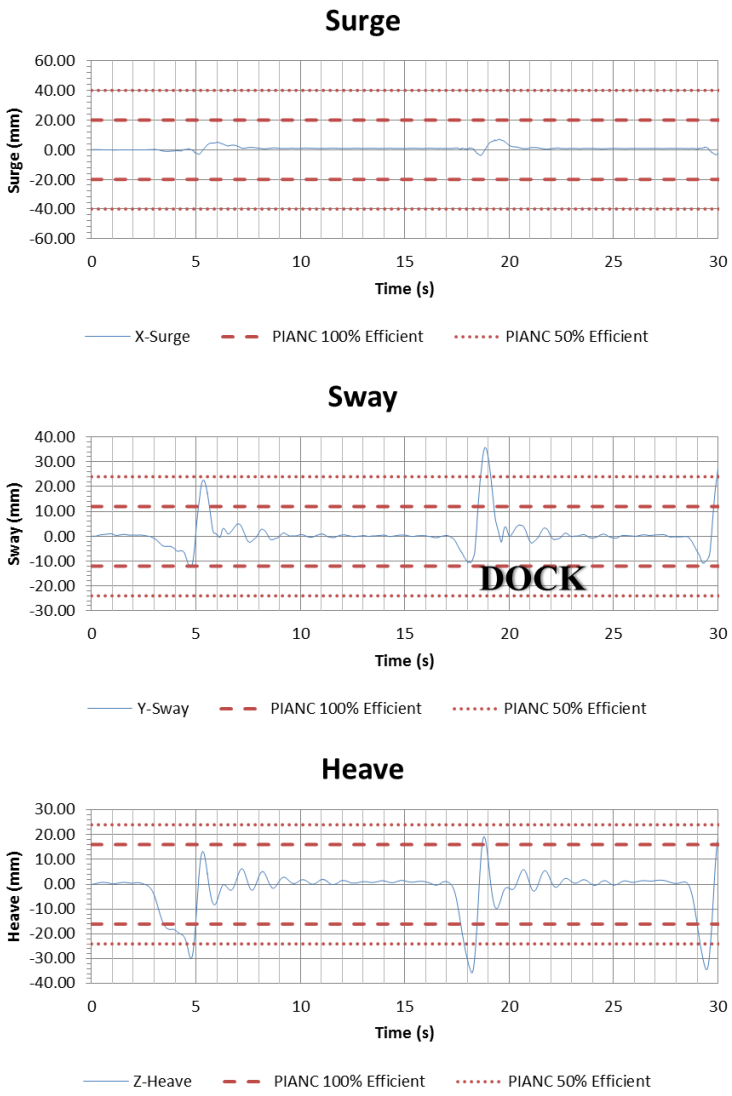

Figure 16. Translation result of static test of six degrees of freedom motion

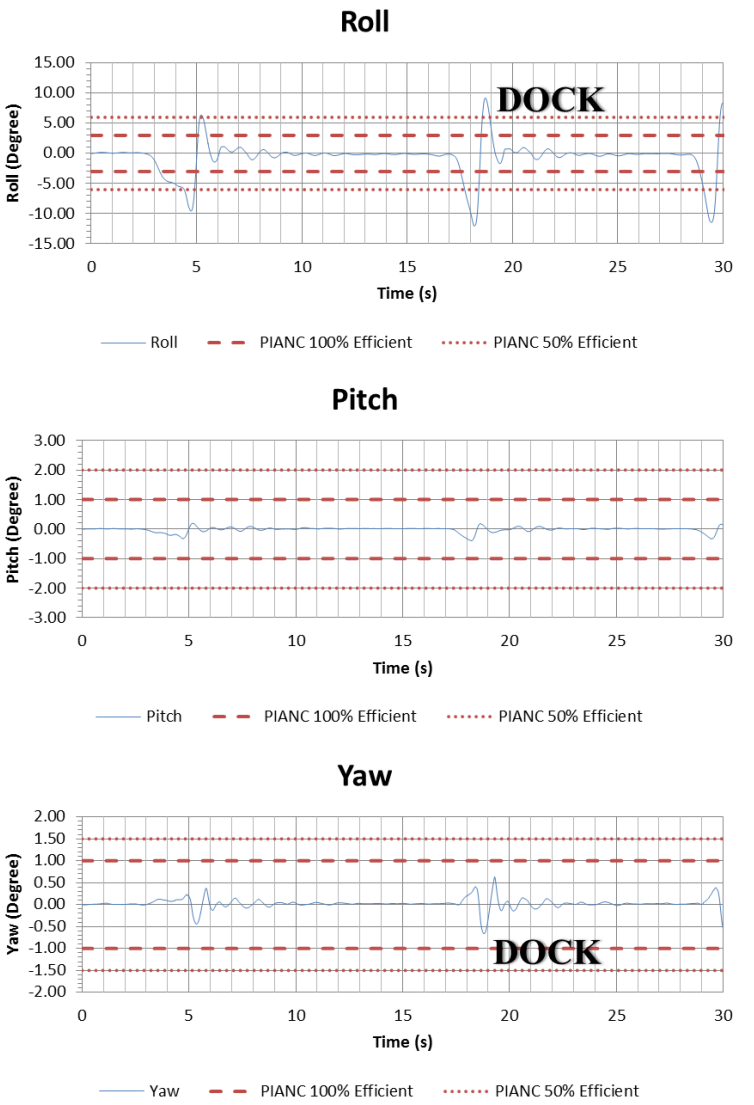

Figure 17. Rotation result of static test of six degrees of freedom motion

These statistic tests are represented as the same format as that of test results, of which the elevation of motions of six degrees of freedom vs. time are demonstrated and compared with PIANC limitations of upper and lower 100% and 50% efficiencies, which are denoted as red dashed lines and dot lines respectively. The definition and

values of PIANC limitations will be demonstrated in later Phase 4, data acquisition and initial analysis, section Motion data for experiments and Appendix.

Phase 3, numerical simulations

The numerical model aNySIM is applied for numerical simulation of the model container ship motions while moored to the solid dock. The aNySIM software is time domain software (Marin, 2012), predicting the motions of moored floating bodies. The motions contain both stochastic and deterministic components in the open sea area. Rather than applying traditional simple mass-damper-spring analysis, the fluid reactive forces are characterized by impulse response theory. To describe the 6 degrees of freedom motions of a floating structure with fluid reactive forces characterized by potential theory under time varying external loads is stated in equation (26)

$$\sum_{j=1}^{6}\left(M_{kj}+m_{kj}\right)\ddot{x}_k+\int_{-\infty}^{t}R_{kj}(t-\tau)\dot{x}(\tau)\,d\tau+C_{kj}x_k=F_k(t)\qquad k=1,2,\dots 6 \quad (26)$$

where M_{kj} is inertial matrix, $m_{kj}$is added inertial matrix, R_{kj} is matrix of retardation functions, C_{kj} is matrix of hydrostatic functions, x_k is motion in j-direction, $F_k(t)$ is time varying arbitrarily external force in the k-model of motion, and k, j are models of motion.

To simulate the motion of the container ship moored in front of solid dock, both input and output settings need to be generated. Input data, which is realized by generating a txt. format file, consists of general information including test durations, number of rigid bodies to be tested, total line and fender number, etc. Body information contains the type of body, body center of gravity and center of global coordinate system,

length between perpendiculars, beam, draft, depth, mass vector, 6×6 linear damping matrix, and displacement. Wave information consists of wave type, either regular or irregular, significant wave height, wave period, wave speed, and direction. Line and fender information define the mooring and fender locations and pretensions. Output settings restrict the format of the column number in the output file, type of output results, and units of the output data.

Phase 4, data acquisition and initial analysis

Wave data and reflection analysis

Wave and motion data were collected using the data acquisition and motion capturing systems. Wave elevation data were acquired from three wave gauges, distributed according to the three wave gauge method, especially dealing with the irregular wave and splitting the incident and reflection wave as described by Mansard and Funke (1980). After collecting wave data for each test, the spectrum of both the incident and the reflected wave are plotted and compared with theoretical spectrum curve, illustrated in Figure 18, using the GEDAP software (Miles & Funk, 1989). The reflection coefficients are also generated, and varying of reflection coefficient vs. time is also plotted as shown in Figure 19, to correlate with the motion fluctuations.

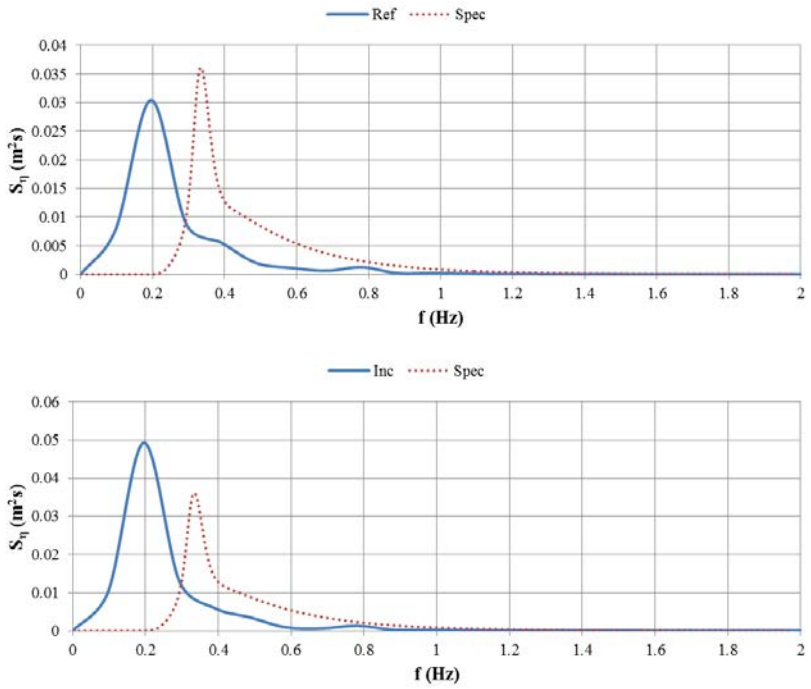

Figure 18. Spectrum comparison between reflect (Upper) and incident (Lower) waves

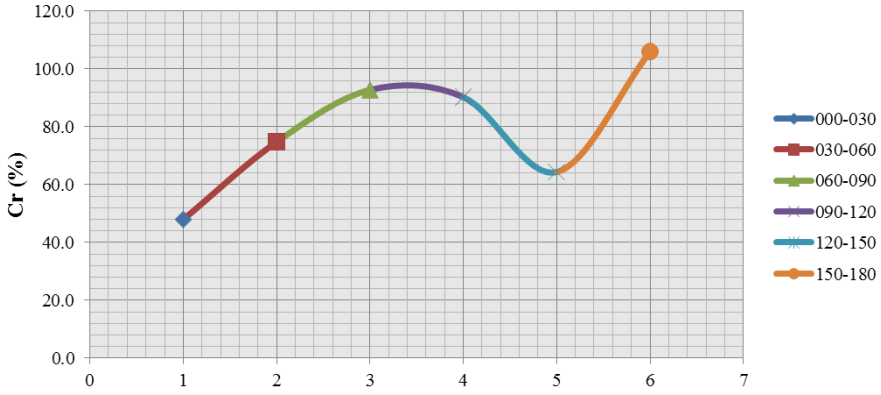

Figure 19. Reflection (Upper) and translation (Lower) coefficients vs. time

Figure 18 demonstrates the density spectrum comparison of incident and reflection wave to theoretical spectrum. The spectrum of the incident and reflected

waves are represented as the blue solid line, and the red dash line illustrates the theoretical spectrum. Figure 19 represents the varying of reflection coefficient vs. time. There are only three wave probes used in front of the model container ship and dock and no wave gauges behind the model thus there are only coefficients of reflection for this experiment. Since it is dry land behind the dock in real case, for that matter, there is no need to place any wave gauge behind the dock for computing the transmission coefficients.

Motion data for experiments

Motion data for translations and rotations are represented separately and compared between solid and pile supported dock under the format of motion elevation vs. time, represented in Figure 20. Motion elevations are also compared with the PIANC limitations, and numbers of elevation surpassing the limitation are also calculated as illustrated in Table 9.

Limitations of PIANC are the criteria of ship motions in front of the dock while installation, which cannot be surpassed to increase the efficiency of handling. The 100% and 50% efficient represent the loading and unloading efficiency under specific values of motion criteria (PIANC, 1995). For proto type scale, the PIANC of upper and lower 100% efficient are ±1.00m (±3.28ft), ±0.60m (±1.97ft), and ±0.80m (±2.62ft) for surge, sway, and heave respectively, and ±3°, ±1°, and ±1° for roll, pitch, and yaw respectively; the PIANC of upper and lower 50% efficient are ±2.00m (±6.56ft), ±1.20m (±3.94ft), and ±1.20m (±3.94ft) for surge, sway, and heave respectively, and ±6°, ±2°, and ±1.5° for roll, pitch, and yaw respectively.

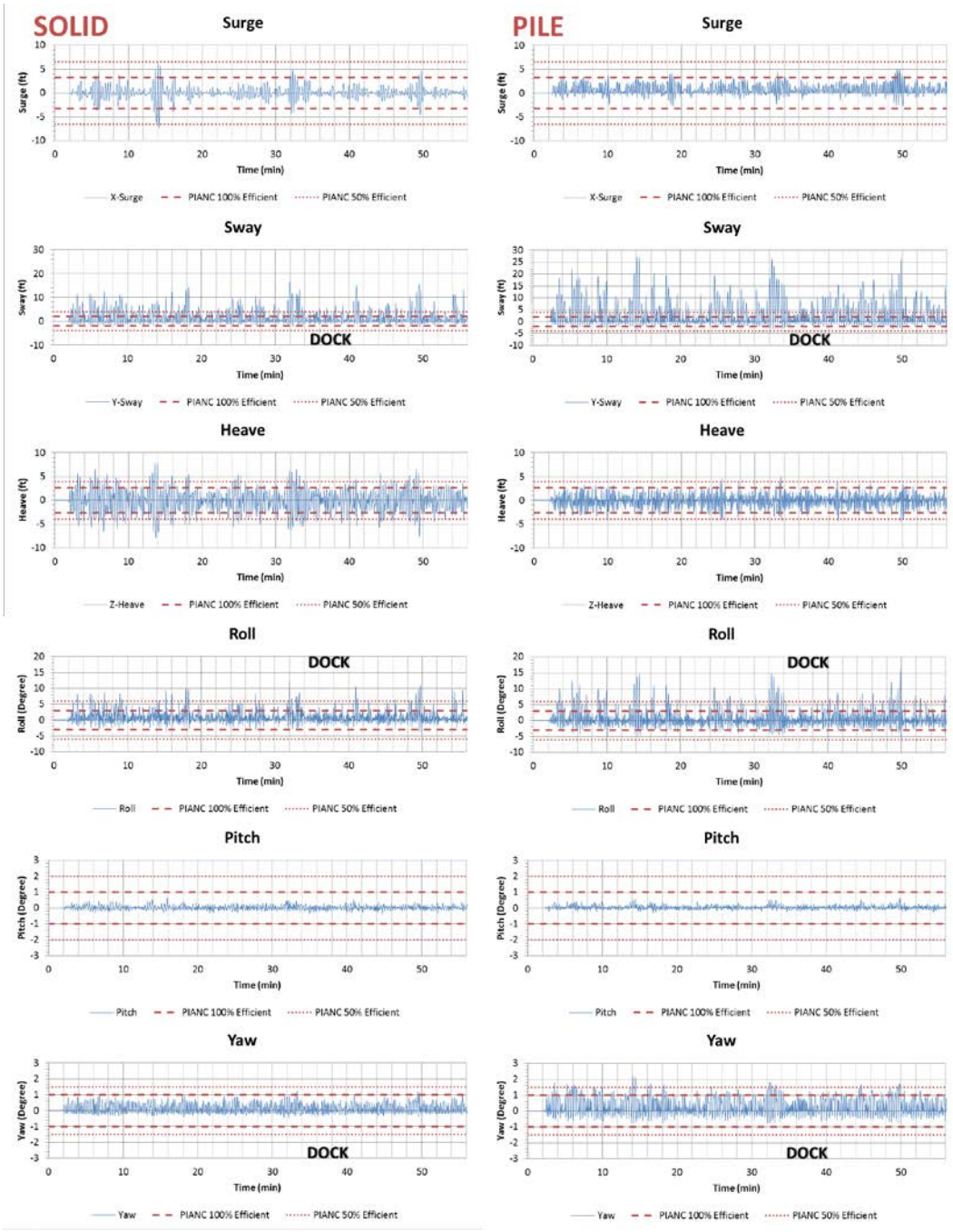

Figure 20. Comparison of six degrees of motion for container ship moored in front of solid (Left) and pile (Right) docks

Table 9. Motion elevation information of test 13

Test13	X-Surge	Y-Sway	Z-Heave	Roll	Pitch	Yaw	Test13p	X-Surge	Y-Sway	Z-Heave	Roll	Pitch	Yaw
Maximum	6.47	16.48	7.89	12.23	0.65	1.27	Maximum	5.02	27.23	4.91	15.98	0.61	2.22
Minimum	-7.34	-2.42	-7.88	-3.87	-0.39	-0.46	Minimum	-2.85	-3.59	-4.73	-6.64	-0.31	-0.84
Significant	4.09	6.75	7.05	5.11	0.44	0.94	Significant	2.79	7.51	3.75	5.78	0.29	1.01
Total Num	219	563	425	625	417	357	Total Num	692	922	633	823	765	837
Upper %	0.00%	20.07%	7.46%	4.79%	0.00%	0.00%	Upper%	0.00%	21.37%	0.43%	5.83%	0.00%	2.27%
Lower%	45.66%	0.00%	10.12%	0.00%	0.00%	0.00%	Lower%	0.00%	0.00%	0.65%	0.12%	0.00%	0.00%

Figure 20 employs two columns of data, for each of which, motions of six degrees of freedom of test 13 for both solid wall dock (left) and pile dock (right) are listed. This figure illustrates directly the comparison of range of motions between solid and pile docks. It is also a straightforward method to indicate the number of motions surpass the PIANC limitations. Motion characteristics, including maximum, minimum, and significant motion values, total number of motion elevation for each degree of freedom, number of motion limitation surpass the upper and lower limitation of PIANC restriction, then are quantitatively represented in Table 9.

The results of experiments, from Test 1 to Test 39 under the same format as Test 13, mentioned above, are stated later in the Appendix

Motion data for numerical simulations

For numerical simulations, data of both motions of the container ship moored in front of solid dock for both experiments and numerical simulations are plotted and compared. The motion elevation data, take test 13 with significant wave height (Hs), wave period (Tp), and direction of 1.85m (6ft), 20s, and 143° respectively as an example, is also superposed with experimental data to qualitatively compare with the experiment results, which is shown in Figure 21for translations and Figure 22 for rotations.

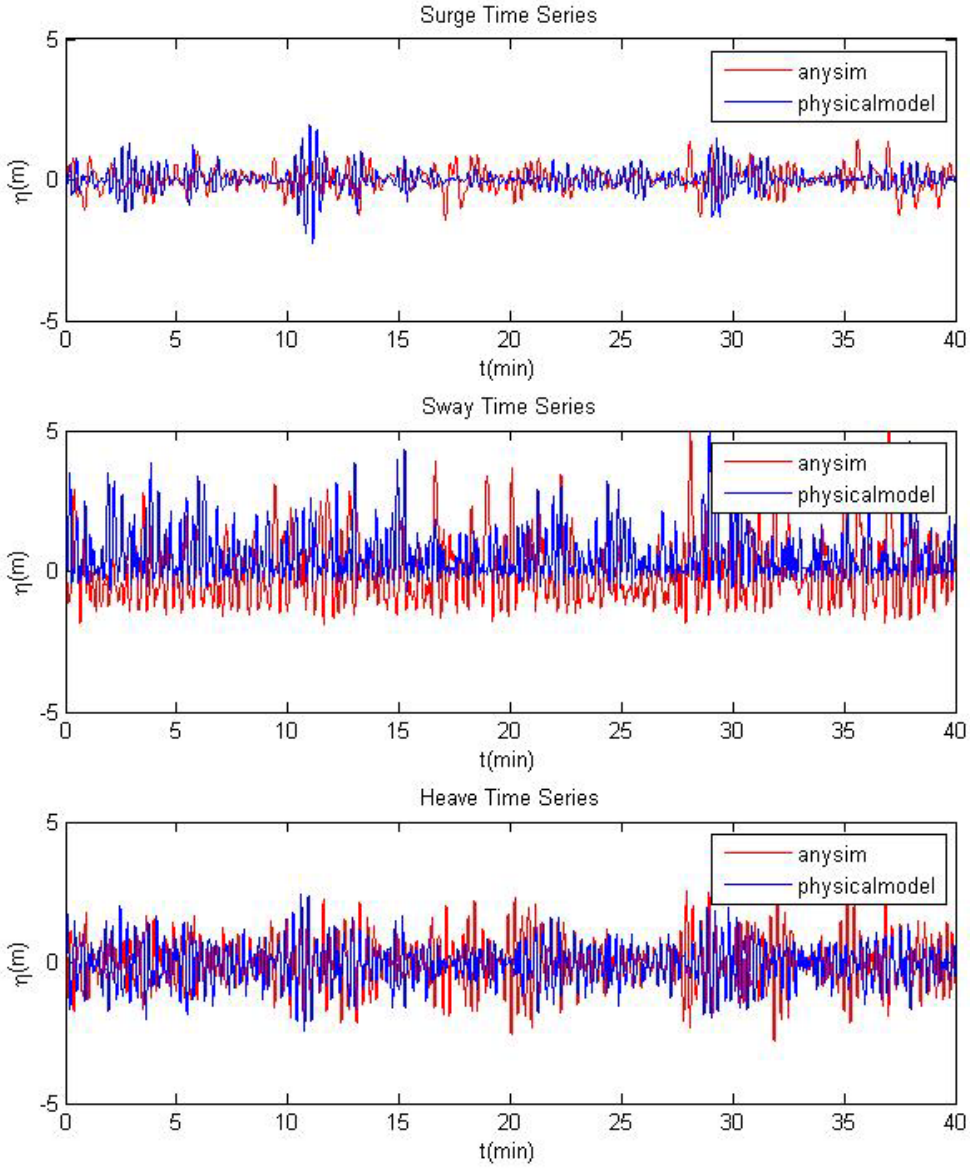

Figure 21. Translation elevation comparisons between experiment (Blue) and numerical simulation (Red)

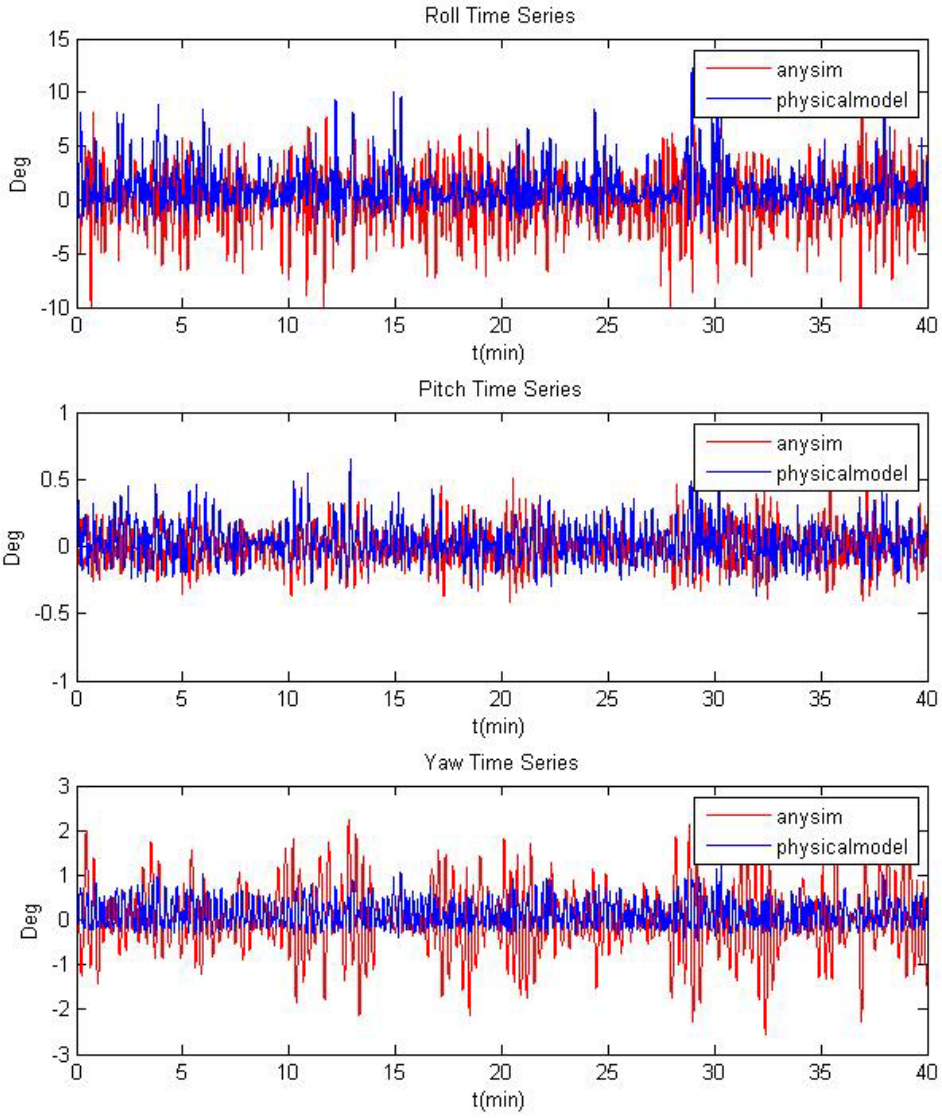

Figure 22. Rotation elevation comparisons between experiment (Blue) and numerical simulation (Red)

The red and blue line in these six plots above represent the motion data of the container ship moored in front of solid dock for numerical simulation and experiment of

test 13 respectively. These plots represent the differences and correlations relationship of both translations and rotations between the experimental and predicted values. Accordingly, experimental and predicted data are generally correlated with each other, especially reflected on surge and heave for translation and pitch for roll. Even though, the lower range of sway from aNySIM is approximately 0.5m lower than that of physical model; the lower range of roll from aNySIM is approximately 2.0° lower than that of physical model; both upper and lower range of yaw is approximately 1.0° higher and lower respectively than that of physical model. These plots also reflects that, for translations, the waves affect more on sway and heave than that of surge, because the value of sway and heave is larger than that of surge. Moreover, for rotations, that the value of roll is larger than that of pitch and yaw represents that wave effect affects more significantly on roll than pitch and yaw. Most of the comparison between numerical simulations and physical model tests represent the similar quantitative relationships, which are displayed and discussed later in the next chapter, Discussion and Analysis of Results. These correlations verify that numerical simulations are able to characterize the motions of the container ship in physical model experiments.

CHAPTER VI

DISCUSSIONS AND ANALYSIS OF RESULTS*

Comparisons of moored ship motion, including translations (surge, sway, and heave) and rotations (roll, pitch, and yaw), as a result of different wave periods, significant heights, and wave directions for the vessel moored in front of solid wall dock and open piled dock are discussed to illustrate the effect of wave height, wave period, and wave direction on the moored ship motions due to these two kinds of docks. There are comparisons with the same wave height but different wave periods, same wave period with various heights, and the same wave height and period for different wave directions. Moreover, experimental results for the solid wall dock were simulated numerically. The motion data comparisons of both experiment and numerical simulation under the different wave conditions discussed previously for experiment results are also illustrated. In addition, tests under the condition of the same wave period, significant height, and wave direction are discussed to verify validation of data for both numerical simulation and experiment.

Comparisons between solid wall and pile supported dock

Motions of the ship model moored to the solid wall dock and open piled dock under circumstances of different wave environments are discussed and compared to demonstrate the effect of wave height, wave period and wave direction, respectively.

* Part of the data reported in this chapter is reprinted with permission from "Comparison of Laboratory and Predicted Motions and Mooring Line Forces for a Container Ship Moored to a Dock" by Andres Luai and Yuanzhe Zhi, 2013. A conference report of the 18th Offshore Symposium Engineering the Future: The Arctic and Beyond. Houston Texas. Copyright [2013] by SNAME Texas Section.

Effect of wave height

The effect of wave height on the motions of a ship moored to solid dock and a piled dock were measured in test 14, 15, 16, and 21, and the results are shown in Figure 23. These tests have the same prototype wave period and direction of 12s and 143° (1.7s and 0° for model) respectively, while the significant prototype wave heights are 0.6m (2ft), 1.2m (4ft), 2.45m (8ft), and 1.85m (6ft) for each of these four tests respectively The experimental results displayed below are scaled up and represented in proto scale.

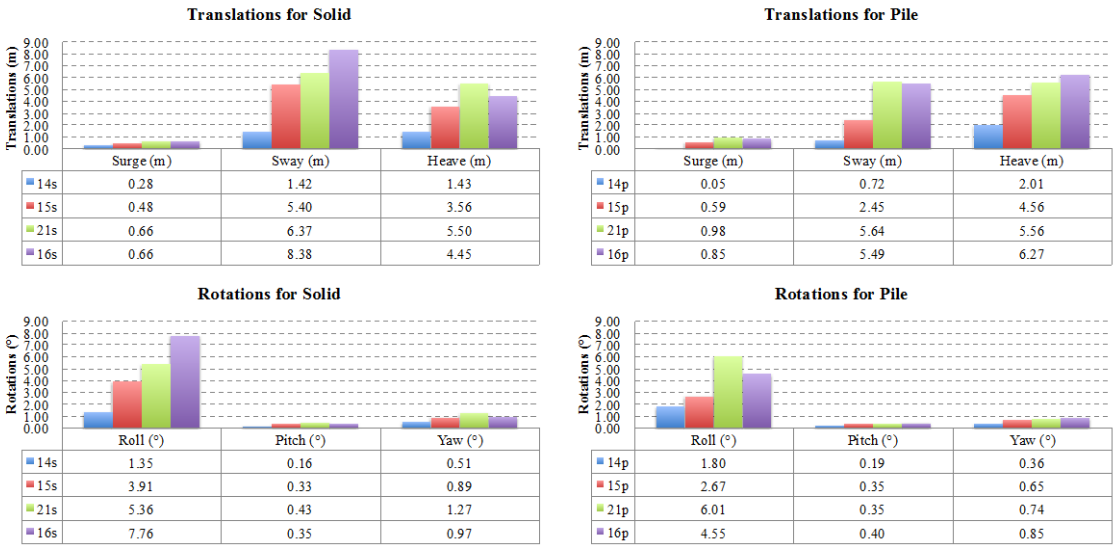

Figure 23. Comparison of motions results under effect of wave height of container moored in front of solid wall and open pile dock

The amount of both translations and rotations of the moored container ship in front of both the solid dock and pile supported dock are proportional to the significant wave height. Though, heave, pitch, and yaw for test 16s and, surge sway and roll for test

16p, illustrate reverse trends, where the lowercase s and p represent the solid wall dock pile dock respectively. According to Table 10 below, the mean value of surge, sway, heave, roll, pitch, and yaw for solid dock are 0.84, 1.51, 0.81, 1.22, 1.00, and 1.4 times of that of pile respectively, which indicate that the amount of differences between motions for solid and pile docks are slight. Table 10 also illustrates that significant wave heights affect the sway and heave more than that of surge for translations. Roll is likewise influenced more by the wave height than that of pitch and yaw. For translations, the mean values of sway and heave are 10 and 7 times more than that of surge for ship in front of quay wall wharf; 6 and 7 times more than that of surge for container in front of pile supported dock. Among rotations, mean values of roll are 14 and 5 times larger than that of pitch and yaw respectively for the vessel in front of solid dock; 12 and 6 times than that of pitch and yaw respectively when the container is moored in front of piled dock.

Accordingly, both translations and rotations generally increase proportionally to the increase of wave height. Wave height affects more on sway, heave, and roll than surge, pitch, and yaw for both solid and pile docks. Differences of each motion values between solid and pile docks are slight.

Table 10. Mean value comparison of motions results under effect of wave height of container ship moored in front of quay wall and open quay wharf

	Surge (m)	Sway (m)	Heave (m)	Roll (°)	Pitch (°)	Yaw (°)
Solid	0.52	5.39	3.74	4.59	0.32	0.91
Pile	0.62	3.58	4.60	3.76	0.32	0.65

Effect of wave period

The effects of wave period on motions of the ship moored in front of solid wall and pile supported docks, which are illustrated in Figure 24, are characterized by test numbers from 6 to 13 with various wave periods of 4s, 6s, 8s, 10s, 14s, 16s, 18s, and 20s respectively, same significant wave height of 1.85m (6ft), and same wave direction of 143° (0° for model).

Accordingly, from test 6 to test 10, for both solid wall and pile support docks, translations increase proportionally with increasing wave period, and decrease with the increasing periods from test 11 to test 13. In addition, increasing period shows more of an effect on sway and heave than on surge. That is to say, sway and heave increase rapidly with the increasing periods while the increase in surge is relatively moderate. It is also observed that the increase of period has more of an effect on roll than on pitch and yaw. Roll shows a rapid climb with the increasing wave period, while the increase of pitch and yaw tend to level off.

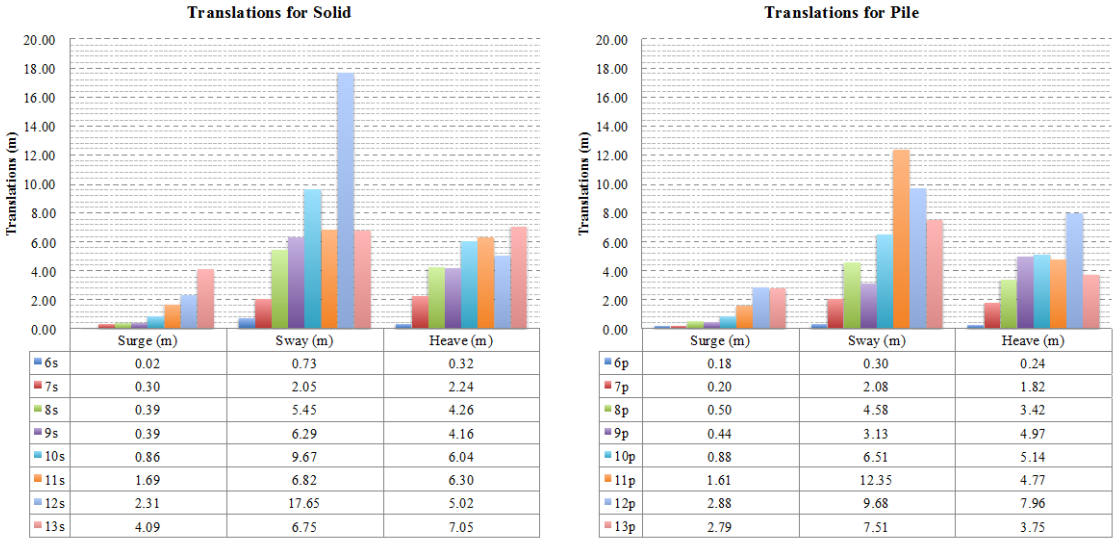

	Surge (m)	Sway (m)	Heave (m)
6s	0.02	0.73	0.32
7s	0.30	2.05	2.24
8s	0.39	5.45	4.26
9s	0.39	6.29	4.16
10s	0.86	9.67	6.04
11s	1.69	6.82	6.30
12s	2.31	17.65	5.02
13s	4.09	6.75	7.05

	Surge (m)	Sway (m)	Heave (m)
6p	0.18	0.30	0.24
7p	0.20	2.08	1.82
8p	0.50	4.58	3.42
9p	0.44	3.13	4.97
10p	0.88	6.51	5.14
11p	1.61	12.35	4.77
12p	2.88	9.68	7.96
13p	2.79	7.51	3.75

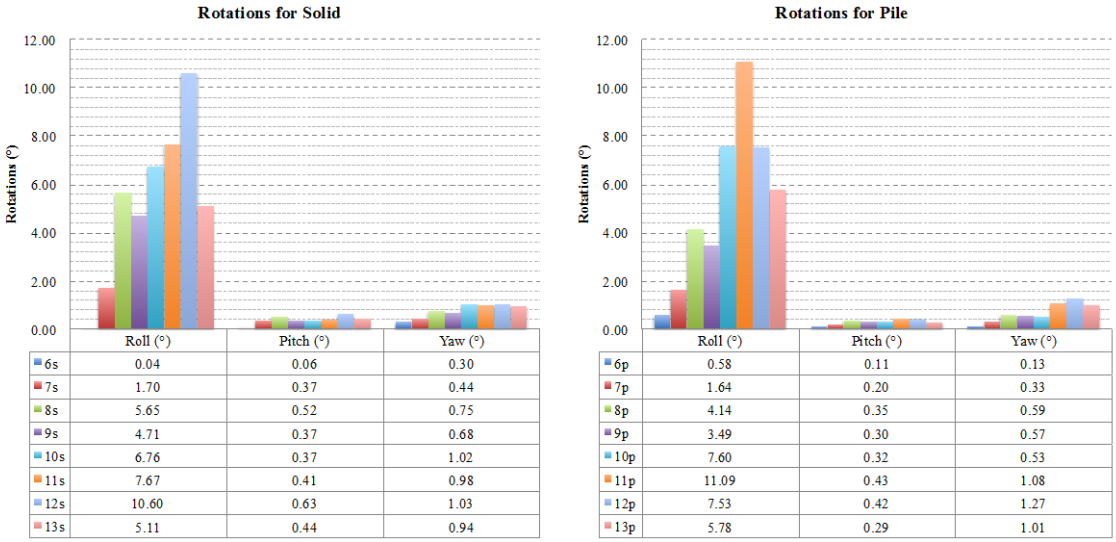

	Roll (°)	Pitch (°)	Yaw (°)
6s	0.04	0.06	0.30
7s	1.70	0.37	0.44
8s	5.65	0.52	0.75
9s	4.71	0.37	0.68
10s	6.76	0.37	1.02
11s	7.67	0.41	0.98
12s	10.60	0.63	1.03
13s	5.11	0.44	0.94

	Roll (°)	Pitch (°)	Yaw (°)
6p	0.58	0.11	0.13
7p	1.64	0.20	0.33
8p	4.14	0.35	0.59
9p	3.49	0.30	0.57
10p	7.60	0.32	0.53
11p	11.09	0.43	1.08
12p	7.53	0.42	1.27
13p	5.78	0.29	1.01

Figure 24. Comparison of motions results under effect of wave period of container moored in front of solid wall pile support docks

Table 11 shows the mean values of the motions for both solid wall and pile docks. Accordingly, for the solid dock, the mean values of sway and heave are 5.5 and 3.5 times more than that of surge respectively; the mean value of roll is 13.2 and 6.9 times than that of pitch and yaw respectively. For the pile supported dock, mean values

of sway and heave are 4.8 and 3.4 times than that of surge respectively; mean value of roll is 17.4 and 7.6 times than that of pitch. The Table 11 below also indicates that the mean value of translations and rotations of solid dock are similar to that of pile support dock.

Motions for both solid and pile docks represent the same trend with the increasing wave period. Like the effect of wave heights, these wave periods affect more on sway, heave and roll, than surge, pitch, and yaw for both solid and pile docks. Each motion between solid and pile dock indicates minor difference.

Table 11. Mean value comparison of motions results under effect of wave period of the container ship moored in front of solid wall and pile supported docks

	Surge (m)	Sway (m)	Heave (m)	Roll (°)	Pitch (°)	Yaw (°)
Solid	1.26	6.93	4.42	5.28	0.40	0.77
Pile	1.19	5.77	4.01	5.23	0.30	0.69

Effect of wave direction

Test numbers 17, 18, 19, and 52 have the same wave height and period of 1.83m (6ft) and 12 s respectively, while the wave directions are 113°, 128°, 158°, and 173° (-30°, -15°, 15°, and 30° for model) respectively. For convenience of discussion, directions for model, that is to say directions for model -30°, -15°, 15°, and 30° are applied to represent directions for that of prototypes 113°, 128°, 158°, and 173°. According to Figure 25, the translations of the vessel in front of solid dock show that sway is larger than that of surge and heave, but when container ship is moored in front of pile dock

heave is larger than that of surge and sway. For rotations, under conditions of both in front of solid and pile docks, the amount of roll is larger than that of pitch and yaw. Generally, the wave effects are larger for the direction of -15° than any other direction. Table 12 illustrates that the mean value of each degree of freedom motion is approximately the same value between conditions of the container moored in front of solid and pile docks, under the effects of the varying wave directions. Both Figure 23and Table 12 illustrate that the wave direction affects sway, heave, and roll more than surge, pitch, and yaw.

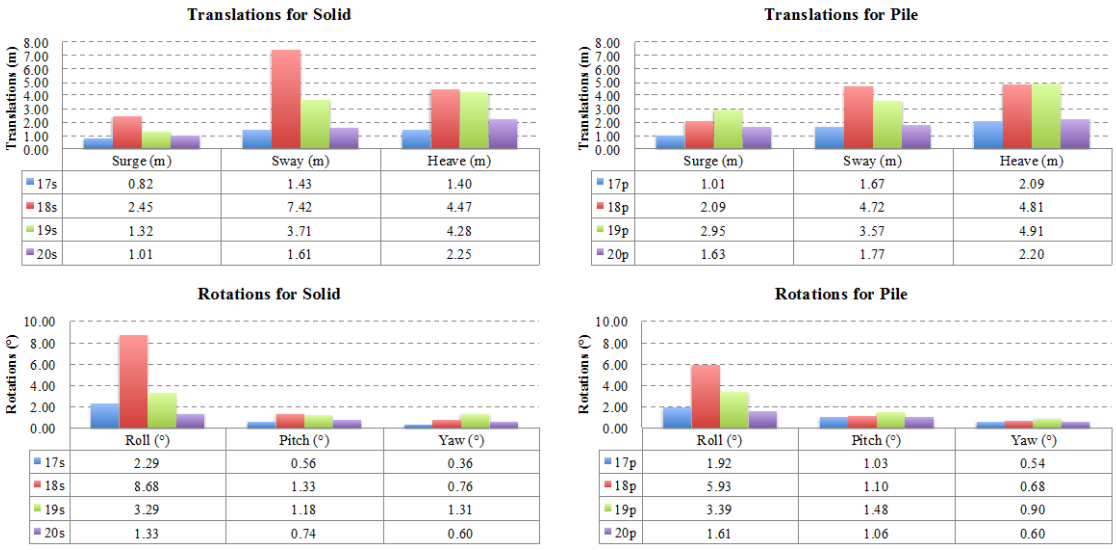

Figure 25. Comparison of motions results under effect of wave direction of container ship moored in front of solid wall and pile supported docks.

Table 12. Mean value comparison of motions results under effect of wave direction of container moored in front of solid wall and pile supported docks

	Surge (m)	Sway (m)	Heave (m)	Roll (°)	Pitch (°)	Yaw (°)
Solid	1.40	3.54	3.10	3.90	0.95	0.76
Pile	1.92	2.93	3.50	3.21	1.17	0.68

The effects of wave directions indicate that translations and rotations represents the same trend and motion amount for each degree of freedom for both solid and pile docks. For both of these two types of dock, wave directions affect more on sway, heave, and roll than that of surge, pitch, and yaw.

Repeatability

The surge, sway, heave, roll, pitch, and yaw for three repeated tests 3, 21, and 36 with the same significant wave height of 1.86m (Hs=6ft) and period of 12 s are displayed in Figure 26 under conditions when the vessel was moored in front of the solid wall dock and a pile supported dock to illustrate the repeatability. The deviations of translations and rotations are shown to further verify the repeatability of the tests. According to Figure 26, the fluctuation of both translations and rotations are stable, and the standard deviations are all under 1, shown in Table 13. That is to say both the solid and pile docks show good repeatability. The amount of sway and heave are 16.8 and 12.1 times the amount of surge. For rotations, the magnitude of roll is 13.0 and 5.1 larger than that of pitch and yaw respectively, which further proves that waves effect sway, heave, and roll more than surge, pitch, and yaw.

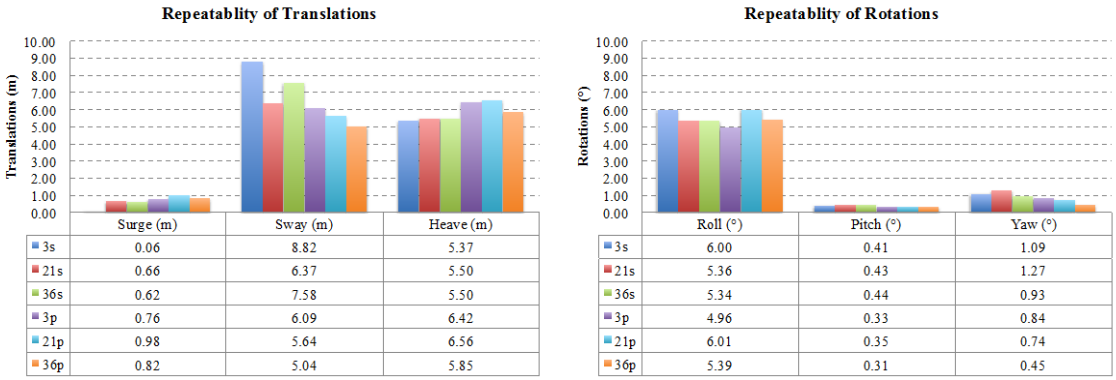

	Surge (m)	Sway (m)	Heave (m)
3s	0.06	8.82	5.37
21s	0.66	6.37	5.50
36s	0.62	7.58	5.50
3p	0.76	6.09	6.42
21p	0.98	5.64	6.56
36p	0.82	5.04	5.85

	Roll (°)	Pitch (°)	Yaw (°)
3s	6.00	0.41	1.09
21s	5.36	0.43	1.27
36s	5.34	0.44	0.93
3p	4.96	0.33	0.84
21p	6.01	0.35	0.74
36p	5.39	0.31	0.45

Figure 26. Comparison of motions results repeatability of container ship moored in front of solid wall and pile supported docks

Table 13. Standard deviation comparison of motions results repeatability of container ship moored in front of solid wall and pile supported docks

	Surge	Sway	Heave	Roll	Pitch	Yaw
Solid	0.27	1.00	0.06	0.31	0.01	0.14
Pile	0.09	0.43	0.31	0.43	0.02	0.17

Comparisons between experiment and numerical simulation

Translations and rotations of the container ship for both experiment and numerical simulation under condition when the vessel is moored in front of solid wall dock are discussed and compared. Both numerical simulation and experiment are under prototype scale. Comparisons are represented under conditions of various wave heights while at the same wave period and direction to demonstrate the effect of wave heights. Moreover, for the case of different wave periods but same wave height and wave direction are used to illustrate the effect of wave period. In addition, effects of wave direction are illustrated by comparing motion characters under varying wave directions while fixed in wave height and period. The comparisons of motions of 6 degrees of freedom under the condition of same significant wave height, wave period, wave

direction, and mooring conditions are also illustrated to demonstrate the repeatability. For each test number displayed on either figures or tables, the lowercase s represent the container ship moored in front of solid dock, while the symbol aNy represent the results from the software aNySIM, which is the software applied for numerical simulation.

Effect of wave height

Test 14, 15, 16 and 21 are tests with various wave heights of 0.6m (2ft), 1.2m (4ft), 2.45m (8ft), and 1.85m (6ft), while the uniformed wave period of 12s and direction of 143° (0° for proto type), which demonstrate the effect of wave height on the moored ship in front of solid wall dock for both experiments and numerical simulations. Comparison results are shown in Figure 27.

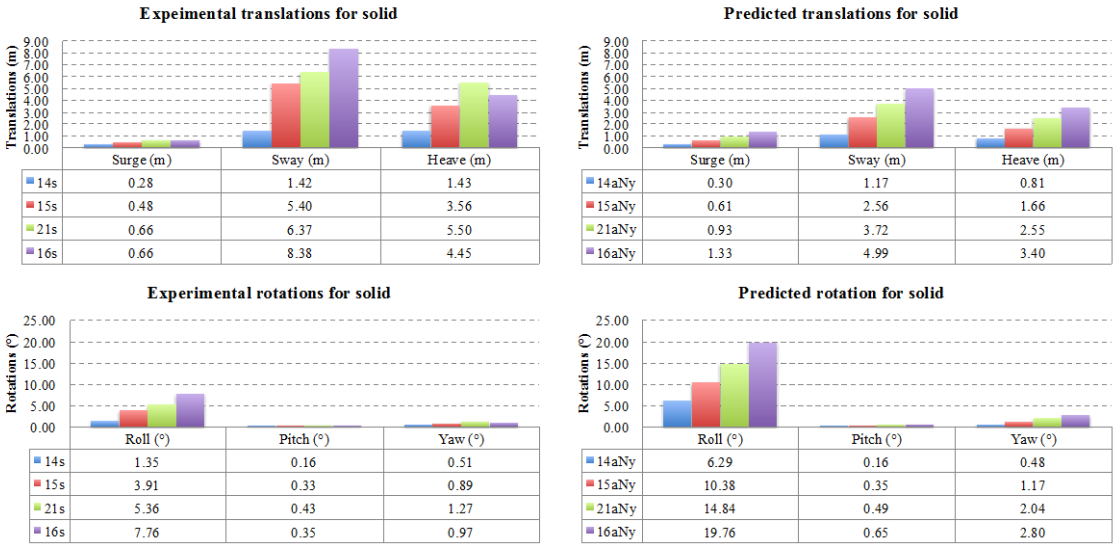

	Surge (m)	Sway (m)	Heave (m)
14s	0.28	1.42	1.43
15s	0.48	5.40	3.56
21s	0.66	6.37	5.50
16s	0.66	8.38	4.45

	Surge (m)	Sway (m)	Heave (m)
14aNy	0.30	1.17	0.81
15aNy	0.61	2.56	1.66
21aNy	0.93	3.72	2.55
16aNy	1.33	4.99	3.40

	Roll (°)	Pitch (°)	Yaw (°)
14s	1.35	0.16	0.51
15s	3.91	0.33	0.89
21s	5.36	0.43	1.27
16s	7.76	0.35	0.97

	Roll (°)	Pitch (°)	Yaw (°)
14aNy	6.29	0.16	0.48
15aNy	10.38	0.35	1.17
21aNy	14.84	0.49	2.04
16aNy	19.76	0.65	2.80

Figure 27. Comparison of numerical and experimental results on the effect of wave height on moored ship motions.

The translations and rotations are generally proportional to the significant wave height, though heave, pitch, and yaw of test 16 for experiment represent a slightly different trend. Moreover, sway and heave of the experiment are larger than that of the physical model, while the amount of surge is approximately equivalent to surge of numerical prediction. According to Table 14, mean values of sway and heave of experiment is 1.73 and 1.78 times that that of numerical simulations respectively. For rotations the prediction of the roll, pitch, and yaw are 2.79, 1.28, and 1.78 times larger than that of physical model test, indicating that wave height has a greater effect on the rotational motions predicted with the numerical simulation than that measured in the physical model experiments.

Accordingly, Figure 27 indicates that the translations and rotations represent the same trend with the increasing wave height for both experimental and predicted results. This figure also illustrates that, for experiments and numerical simulations, the changing wave heights affect sway, heave and roll more, which is also reflected among the mean values in Table 14. However, the table indicates that the value of each motion of degree of freedom between experiments and prediction represent differently. The rotations of predicted data are larger than that of experiment. The translations, besides surge, one the other hand, represent reversely. These differences are significant on rotations while slight on translations.

Table 14. Mean value comparison of numerical and experimental results on the effect of wave height on moored ship motions.

	Surge (m)	Sway (m)	Heave (m)	Roll (°)	Pitch (°)	Yaw (°)
Experiment	0.52	5.39	3.74	4.59	0.32	0.91
aNySIM	0.80	3.11	2.10	12.82	0.41	1.62

Effect of wave period

In order to represent the motion comparisons of experiments and numerical model predictions of the moored container in front of solid dock, the magnitude of the translations and rotations were obtained for the same significant wave height of 1.85m (6ft) and wave direction of 143° (0° for proto type) at different significant periods of 4s, 6s, 8s, 10s, 14s, 16s, 18s, and 20 s.

According to Figure 28, translations generally increase with the increasing wave period. Though, for experiments, sway of test 11 and 13, heave of test 12, and roll of test 12 illustrate a reverse trend; for numerical simulations, surge of test 10 and 13, sway of test 11 and 12, and heave of test 13 are negatively correlated to the increasing wave period. These reversed trends, compared with the generally increasing tendency, are very small. On the other hand, for rotations the amount of pitch and yaw do not illustrate a regular pattern with the increase of period. However for most rotations, the magnitude of the rotations is generally larger than that under relatively larger periods than those under smaller periods. For example, the value of roll for the experiment increase with period up to 10 s and then decrease, yaw angles increase gradually, while the pitch angles are nearly constant with increasing period.

Translations and rotation under effect of period represent almost the same tendency for numerical simulation as that of experiment, but the magnitude of pitch angle fluctuates with the increase of periods. According to Table 15, the length of wave period exerts more of an effect on translations for the experiment than that of the numerically predicted values. That is to say, surge, sway, and heave for the physical model is 1.24, 2.48, and 1.96 times larger than that of numerical simulations, respectively. However, rotations illustrate an opposite trend, and the numerical predictions of roll, pitch, and yaw angles are 1.93, 1.2, and 2.55 times larger than that measured in the experiments. Moreover, among rotations for both experiment and numerical simulation of roll tends to be more sensitive to the effect of wave period than pitch and yaw.

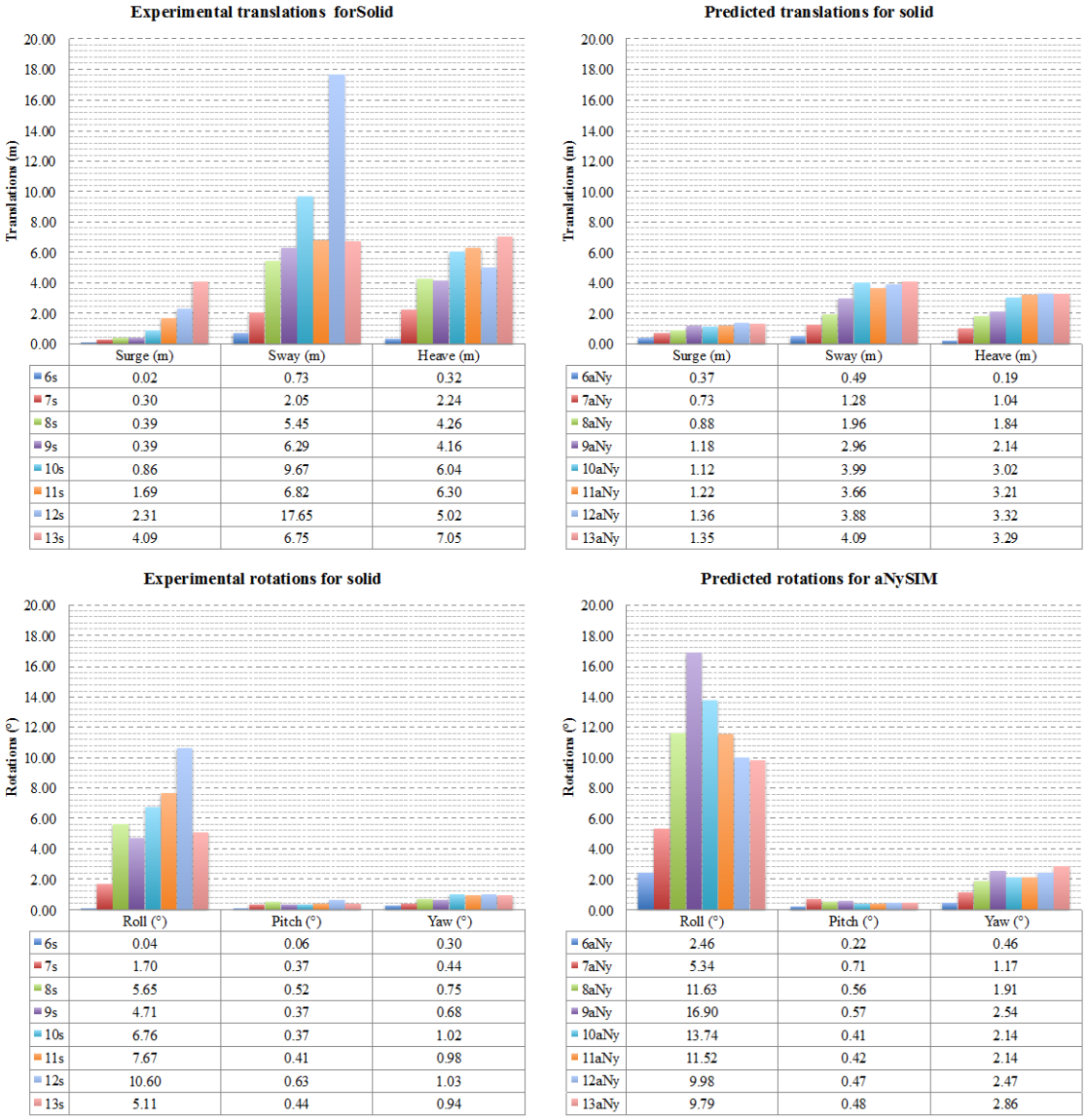

Figure 28. Comparison of the effect of wave period on moored ship motions.

Table 15. Mean value comparison of numerical and experimental results on the effect of wave period on moored ship motions.

	Surge (m)	Sway (m)	Heave (m)	Roll (°)	Pitch (°)	Yaw (°)
Experiment	1.26	6.93	4.42	5.28	0.40	0.77
aNySIM	1.02	2.79	2.26	10.17	0.48	1.96

According to both Figure 28 and Table 15, translations and rotations represent the same tendency under the effects of wave periods between both experiments and predictions. The varying wave periods effects more on sway, heave, and roll while less on surge, pitch, and yaw for both experimental and predicted values. Mean values listed in Table 15 also reveal that the rotation values predicted by aNySIM are larger than that of experiments. Translations, however, represent the opposite tendency.

Effect of wave direction

The effect of wave directions on motions of containers in front of solid wall dock is represented by comparing both physical model and numerical simulation, including test numbers 17, 18, 19, and 20 with the same wave height and period of 1.86m (6 ft) and 12s respectively, but their wave directions are 113°, 128°, 158°, and 173°, which are -30°, -15°, 15°, and 30° for model respectively.

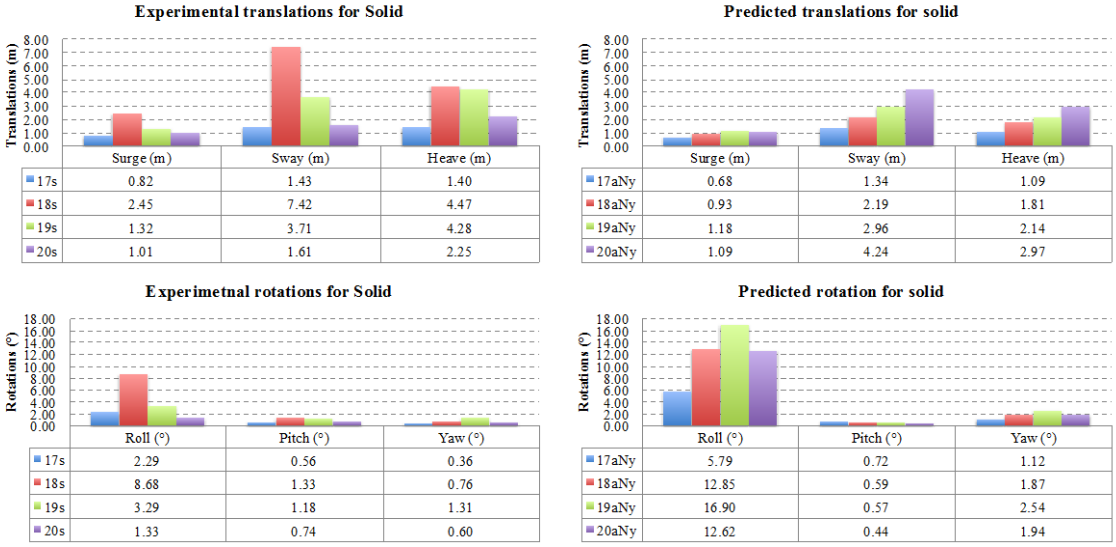

Figure 29. Comparison of the numerical and experimental results of the effect of wave direction on moored ship motions.

Figure 29 shows experimental results the test 18, which is for the wave direction is -15°. Both rotations and translations reach their peak, with the exception for yaw where the peak is located at 15° for test 19. For numerical simulations, translations generally increase with the varying wave directions. Predicted rotations reach their peak in test 19 with the direction of 15° for both roll and yaw, and test 17 with direction of 30° for pitch. According to Table 16, the wave direction change results in larger roll and yaw for numerical over that measured in the physical experiments. For example, the roll and yaw for numerical simulation test 18aNy are 3.09 times and 2.46 times larger than that of experiment. On the contrary, the numerical model prediction illustrates the translations, including surge, sway and heave are 69%, 76%, and 65% larger than that measured in the physical model. The mean value of pitch for the numerical simulation is 61% of that of the experiment. For both numerical simulation and experiment, varying of

wave direction effects roll more significantly than the rest of the rotations, which for numerical simulation the mean value of roll for these four tests is 20.76 and 6.44 times of pitch and yaw respectively. For the experiment the mean value of roll is 4.11 and 5.13 times of pitch and yaw respectively. However, among the translations of experiment and numerical simulation, sway and heave are approximate 100% larger than that of surge.

Table 16. Mean value comparison of numerical and experimental results on the effect of wave direction on moored ship motions.

	Surge (m)	Sway (m)	Heave (m)	Roll (°)	Pitch (°)	Yaw (°)
Experiment	1.40	3.54	3.10	3.90	0.95	0.76
aNySIM	0.97	2.68	2.00	12.04	0.58	1.87

Repeatability

Repeatability of ship motions of surge, sway, heave, roll, pitch, and yaw are illustrated in Figure 30 for experiment and numerical simulation, by illustrating repeated test 3, 21, and 36 with the same significant wave height of 1.86m (6ft), period of 12s, and direction of 143° (0° for model). Repeatability is reflected among translations and rotations for both experiment and numerical simulation. According to Table 17, none of the standard deviations of motions for both predicted value and experiment results are larger than one. Moreover, the wave effect is larger for translations than for experiment, and the effect on sway and heave is more significant than surge. Table 18 indicates that the surge, sway, and heave of experiment are 1.28, 2.79, and 2.07 times of that of predictions. The magnitude relation is reversed, that is to say, the prediction of roll is

2.57 times of that of experiment. In addition, for both numerical simulation and experiment, the wave effect is more on roll than the rest of the rotations.

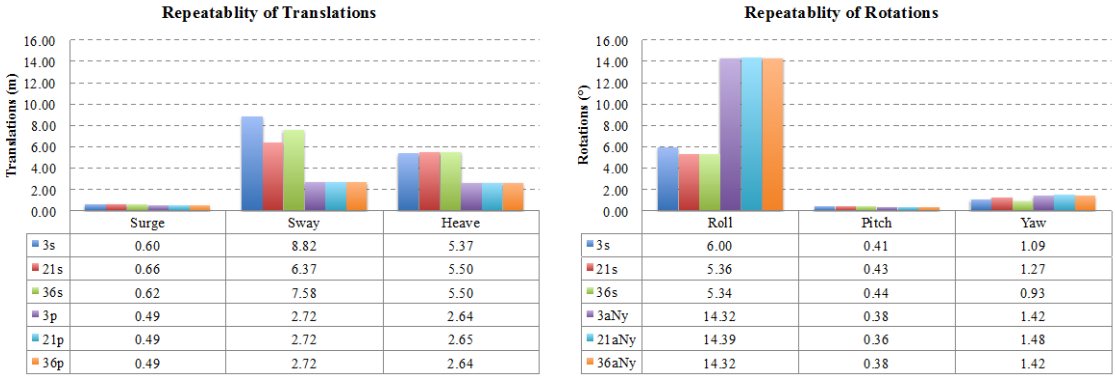

	Surge	Sway	Heave
3s	0.60	8.82	5.37
21s	0.66	6.37	5.50
36s	0.62	7.58	5.50
3p	0.49	2.72	2.64
21p	0.49	2.72	2.65
36p	0.49	2.72	2.64

	Roll	Pitch	Yaw
3s	6.00	0.41	1.09
21s	5.36	0.43	1.27
36s	5.34	0.44	0.93
3aNy	14.32	0.38	1.42
21aNy	14.39	0.36	1.48
36aNy	14.32	0.38	1.42

Figure 30. Comparison of numerical and experimental results for six degrees of freedom.

Table 17. Standard deviation comparison of numerical and experimental results repeatability on moored ship motions.

	Surge	Sway	Heave	Roll	Pitch	Yaw
Experiment	0.27	1.00	0.06	0.31	0.01	0.14
aNySIM	0.00	0.00	0.00	0.03	0.01	0.03

Table 18. Mean value comparison of numerical and experimental results repeatability on moored ship motions.

	Surge (m)	Sway (m)	Heave (m)	Roll (°)	Pitch (°)	Yaw (°)
Experiment	0.63	7.59	5.46	5.57	0.43	1.10
aNySIM	0.49	2.72	2.64	14.34	0.37	1.44

Effect of high frequency oscillations, accuracy, and data analysis on motion data

Number of motion data points of test 06, 17, 38, and 39 are relatively larger than others. However, compared with the majority number of tests, these tests are only minority exceptions. This phenomenon occurs because of high frequency oscillations,

accuracy of instrument, and the methods of data analysis. High frequency oscillations, generated by either high frequency waves or oscillations of mooring system, might be attributed to these large data points. Accuracy of instrument is based on the definition of rigid body. A rigid body is defined by markers positioned on the object to be captured and slight changes of position or occasional blockage of those markers leads to missing data, which is defined as a gap. Increasing the gap tolerance of model in program will decrease the sensitivity of motion capture device on position change of a marker and lower the number of gaps. The method of data analysis is another reason leading to relatively larger number of data points. Outputs of these gaps are represented as zeros, which lead to the appearance of several spikes when the motion vs. time is plotted. To fill the gaps, rather than being connected linearly, initial data, or first non-zero data, is inserted to replace those zero positions. This method creates more crests and toughs. After zero crossing, by subtraction of mean value from each original data point, those crests and toughs, which originally suspend above or below zero, will cross the zero and contribute to the calculation of number of motion data points.

Discussion of differences between the experimental and numerical motion results

Ship motions are characterized by six degrees of freedom, including translations, i.e. surge, sway, and heave, defining as the position in Cartesian Coordinates; rotations, i.e. roll, pitch, and yaw, illustrated as rigid body or mass point rotating around the axes of Cartesian Coordinates. The rotations are computed by moment of inertia, which is determined by both mass distribution and shape. Geometry shape of a vessel can be relatively accurately scale down, so do the draft of vessel by ballasting. While, due to the

material applied for constructing the model, the mass distributions cannot be easily scaled down. Moreover, some of the components on proto type ship are too small to simulate. In addition, the budget issue lowering the accurate of a ship, for example the container ship used in these experiments doesn't have superstructure and no containers, while in the real case of typical draft, defining fully loaded, to the container ship would have a superstructure and containers above the deck. The numerical simulation dealing with the containers moored in front of quays, of which the setting of moment of inertia for calculating the damping matrix is based on the numerical model of ship. This numerical model can simulate both the geometry scale and mass distributions.

CHAPTER VII

SUMMARY OF CONCLUSIONS AND RECOMMENDATIONS

The container ship moored in front of solid wall and pile supported docks shows approximately the same trend and magnitude of translations and rotations under the actions of wave period and significant wave height. The translations (surge, sway, and heave) and rotations (roll, pitch, and yaw) of a ship moored to a dock are proportional to significant wave height. Translations are generally proportional to wave period, but rotations increase first and then decrease. For waves perpendicular to the beam of a container ship moored to a dock, the wave periods and significant heights have relatively more effects on sway, heave, and roll and less effect on surge, pitch and yaw. These tendencies are also reflected on the repeatability for both the solid wall and pile supported dock, namely that wave effect is greater for sway and heave than that of surge, and the wave effects are larger for roll than that for pitch and yaw. Changing the wave direction between +/- 15º and +/- 30º show that the moored container ship motions are greater for the +/-15 degree direction.

Numerical simulations generally illustrate the same trend as that of the experiments. That is to say, the translations and rotations increase proportionally with the increase of significant wave heights. Motions reflect a variable tendency under the effect of wave periods. Sway, heave, and roll are affected more than that of surge, pitch, and yaw by the effects of significant wave height and periods. Motions also show the same trend, which reacts more between +/- 15º than other directions, under effect of

varying wave direction. The amount of motion under wave effects between results of experiments and numerical prediction are different. That is to say, under the effect of significant wave period, the sway and heave in the experimental measurements are larger than that of numerical predictions. The numerical prediction of roll simulation is larger than that of physical model measurements.

It is recommended that mass properties of model container ship and those used in the numerical model be further investigated to determine if any of the mass property differences can be attributed to the differences in the measured and numerical results.

REFERENCES

Clay, S. (2011). *Application of the Qualisys optical motion tracking system evaluate six degree of freedom motion for floating model barges and a tower in the Haynes Laboratory wave basin.* College Station, Texas: Unpublished experiment report, Haynes Coastal Engineering Laboratory, Texas A&M University.

Cobazas, D., Jagersand, M., & Sturm, P. (2009). 3D SSD tracking with estimate 3D planes. *Image and Vision Computing, 27*, 69-97.

Dean, R. G., & Dalrymple, R. A. (1991). Energy flux. In R. G. Dean, & R. A. Dalrymple, *Water wave mechanics for engineers and scientists* (pp. 97-100). Singapore: World Scientific Publishing Co. Pte. Ltd.

Domnisoru, L., Stoicescu, L., & Domnisoru, D. (2008). The linear numerical analysis of displacement response amplitude operator, based on the hydroelasticity theory, for a barge test ship. *Romanian Journal of Physics, 53.1-2*, 121-127.

Goda, Y., & Suzuki, Y. (1976). Estimation of incident and reflected waves in random wave experiments. *Coastal Engineering, I*, 828-845.

Hughes, S. A. (1993). Froude criterion. In S. A. Hughes, *Physical models and laboratory techniques in coastal engineering* (pp. 64-65). Singapore: World Scientific Publishing Co. Pte. Ltd.

Kamphuis, J. W. (2002). Common parametric expressions for wave spectra. In J. W. Kamphuis, *Introduction to coastal engineering and management* (pp. 75-78). Singapore: World Scientific Publishing Co. Pte. Ltd.

Kundu, P. K., & Cohen, I. M. (2008). Dynamic similarity. In P. K. Kundu, & I. M. Cohen, *Fluid mechanics* (pp. 279-295). Kidlington, Oxford: Elservier Inc.

Mansard, E. P., & Funke, E. R. (1980). The measurement of inxidnet and reflected spectra using a least squares method. *Coastal Engineering*, 154-172.

Marin. (2012). *General*. Retrieved from http://wiki.marin.nl/images/1/16/-GENERAL-.pdf

Miles, M. D., & Funk, E. R. (1989, August). The GEDAP software for hydraulics laboratory data analysis. *Proceedings: IAHR Workshop on Instrumentation for Hydraulics Laboratories*. Burlington, Ontario.

PIANC. (1995). *Criteria for movements of moored ships in harbours - a practical guide, Report of Working Group No. 24, PTC II Supplement to Bulletin no. 88.* Permanent International Association of Navigation Congress (PIANC).

Pinkster, J. A. (1980). *Low frequency second order wave exciting forces on floating structures*. Retrieved from Delft University of Technilogy: http://repository.tudelft.nl/assets/uuid:d6d42e9c-c349-47e5-8d63-5c6454196b04/180719.pdf

Santos, P. R., Gomes, F. V., & Dias, E. B. (2010). *Physical Modelling of Leixões Oil Terminal - Portugal*. Retrieved from Port Infrastructure Seminar 2010: http://www.portseminar2010.tudelft.nl

Tschirky, P., Pinkster, J. A., Rollings, S., Smith, E., & Cornett, A. (2010). Modelling moored ship response to a passing ship. *Ports 2010: Building on the Past, Respecting the Future* (pp. 669-678). Jacksonville, FL: ASCE.

Tupper, E. C. (1996). Flotation and stability. In E. Tupper, *Introduction to Naval Architecture* (pp. 30-31). Jersey City, New Jersey: Reed Educational and Professional Publishing Ltd.

WAFO. (2005, October 6). *WAFO. Description of jonswap*. Retrieved from WAFO. Wave Analysis for Fatigue and Oceanography: http://www.maths.lth.se/matstat/wafo/documentation/wafodoc/wafo/spec/jonswap.html

WAFO. (2005, October 6). *WAFO. Description of tmaspec*. Retrieved from WAFO. Wave Analysis for Fatigue and Oceanography: http://www.maths.lth.se/matstat/wafo/documentation/wafodoc/wafo/spec/tmaspec.html

APPENDIX

This section listed all of the motion data from test 01 to 39. Motion data for both solid and open pile docks, captured by qualisys motion tracking system, are represented as a format of motion elevation data vs. time. There are two columns, the left one represents the data for the solid dock and the right one illustrates the data for pile supported dock. For each column, there are six rows, representing each motion degree of freedom, i.e. surge, sway, heave, roll, pitch, and yaw. These data are also compared with PIANC 100% efficiency and 50% efficiency, denoted by maroon dash and dot lines respectively. The upper and lower limitation, which are denoted by + and – respectively, are ±1m (±3.28ft), ±0.6m (±1.97ft), ±0.8m (±2.62ft), ±3°, ±1°, and ±1° for surge, sway, heave, roll, pitch, and yaw respectively for PIANC 100% efficiency; ±2m (±6.56ft), ±1.2m (±3.94ft), ±1.2m (±3.94ft), ±6°, ±2°, and ±1.5° for surge, sway, heave, roll, pitch, and yaw respectively for PIANC 50% efficiency.

Maximum, minimum, significant, and total numbers of motion data for each degree of freedom are also listed. The maximum and the minimum represents the positive maximum and negtive minimum data of motion respectively. The method to derive the significant value and total number for motions is the same as wave data analysis. Data is initially zero crossed by substraction between each degree of freedom and its mean value. Then, upper corssing points are found and total numbers of space between each neibor zero crossing point are regared as total number of motions. After that, by substraction of maximum and minimum value between each neibor zero crossing point, amount of motions are derived. These motion amounts are sorted from

large to small and the first one thirds largest amounts are averaged, namely the significant.

The number of positive and negetive motion, which surpass PIANC 100% and 50%, denoted as upper % and lower % respectively, are also calculated respectively.

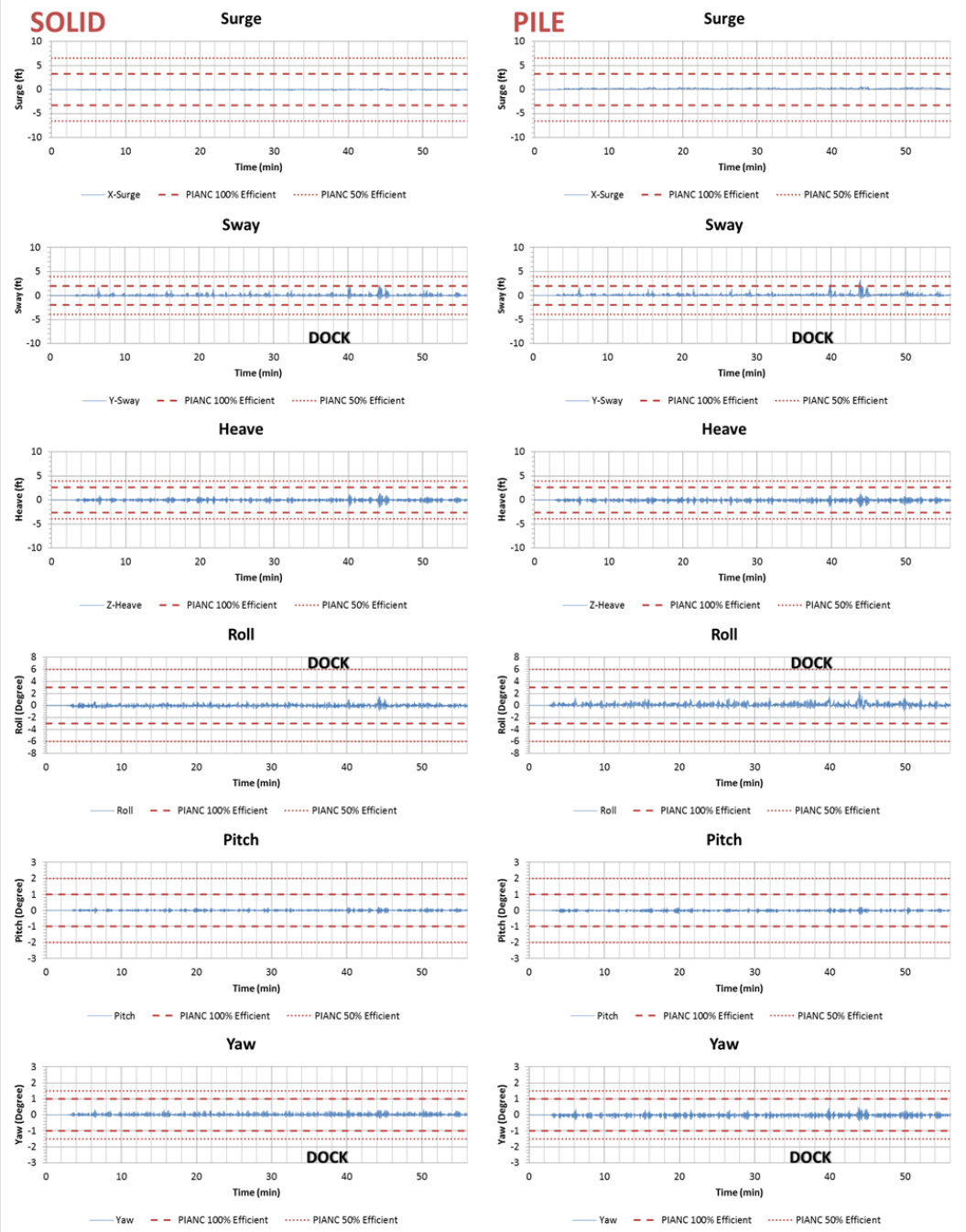

Test01	X-Surge	Y-Sway	Z-Heave	Roll	Pitch	Yaw
Maximum	0.28	2.23	1.45	1.56	0.22	0.35
Minimum	-0.26	-0.84	-1.63	-0.96	-0.25	-0.22
Significant	0.16	0.83	1.03	0.86	0.19	0.33
Total Num	956	566	521	487	674	455
Upper %	0.00%	0.00%	0.00%	0.00%	0.00%	0.00%
Lower%	0.00%	0.00%	0.00%	0.00%	0.00%	0.00%

Test01p	X-Surge	Y-Sway	Z-Heave	Roll	Pitch	Yaw
Maximum	0.67	3.28	1.36	2.36	0.23	0.51
Minimum	-0.16	-0.66	-1.56	-0.99	-0.28	-0.39
Significant	0.06	0.65	1.06	1.01	0.17	0.32
Total Num	448	890	666	653	968	852
Upper%	0.00%	0.00%	0.00%	0.00%	0.00%	0.00%
Lower%	0.00%	0.00%	0.00%	0.00%	0.00%	0.00%

Appendix Figure 1. Motion comparison of test 01 Hs=0.6m, Tp=7.99s, Dir=143˚

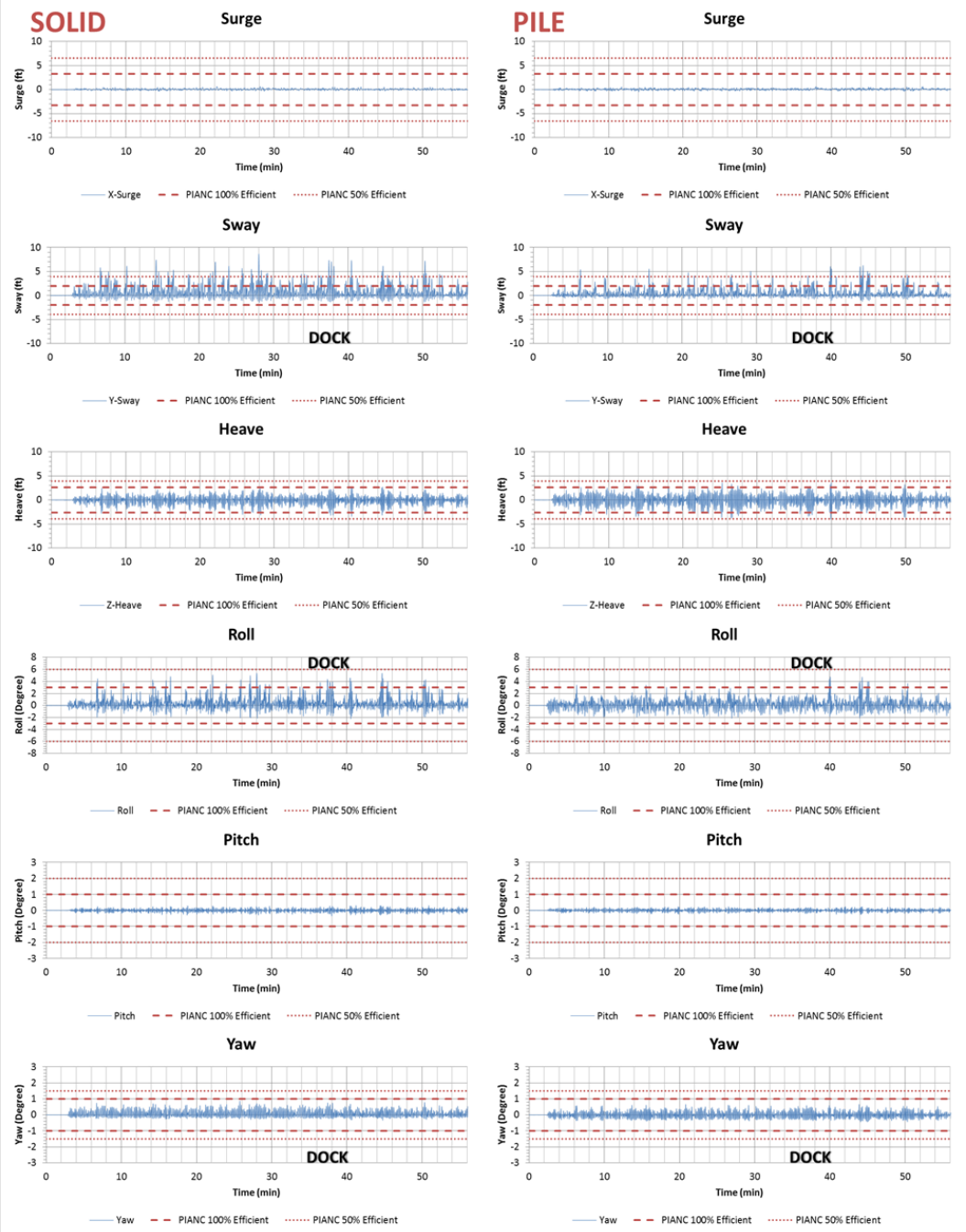

Test02	X-Surge	Y-Sway	Z-Heave	Roll	Pitch	Yaw
Maximum	0.65	8.65	2.72	5.38	0.31	0.87
Minimum	-0.37	-1.45	-3.44	-2.26	-0.36	-0.35
Significant	0.28	3.66	2.54	2.94	0.30	0.58
Total Num	884	658	756	625	787	890
Upper %	0.00%	7.47%	0.00%	0.00%	0.00%	0.00%
Lower%	0.00%	0.00%	0.00%	0.00%	0.00%	0.00%

Test02p	X-Surge	Y-Sway	Z-Heave	Roll	Pitch	Yaw
Maximum	0.64	6.27	3.63	4.77	0.24	0.67
Minimum	-0.46	-1.30	-4.06	-2.18	-0.26	-0.44
Significant	0.38	2.27	3.94	2.48	0.26	0.67
Total Num	701	701	470	703	717	593
Upper%	0.00%	2.57%	0.00%	0.00%	0.00%	0.00%
Lower%	0.00%	0.00%	0.14%	0.00%	0.00%	0.00%

Appendix Figure 2. Motion comparison of test 02 Hs=1.2m, Tp=9.97s, Dir=143˚

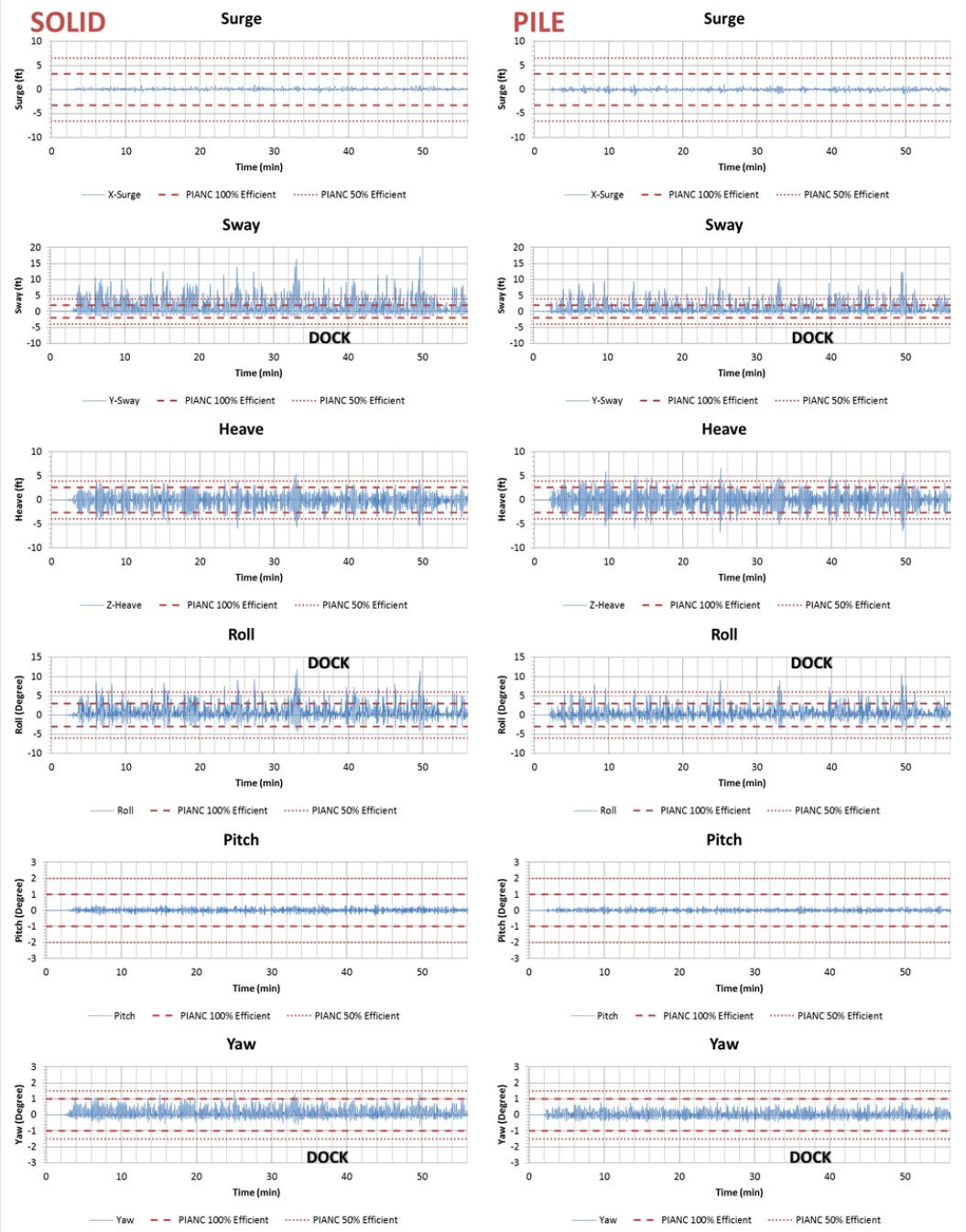

Test03	X-Surge	Y-Sway	Z-Heave	Roll	Pitch	Yaw
Maximum	0.97	17.21	5.41	11.95	0.38	1.47
Minimum	-0.70	-2.13	-5.92	-4.35	-0.43	-0.68
Significant	0.60	8.82	5.37	6.00	0.41	1.09
Total Num	485	355	425	608	607	395
Upper %	0.00%	45.07%	1.41%	5.10%	0.00%	0.00%
Lower%	0.00%	0.00%	3.94%	0.00%	0.00%	0.00%

Test03p	X-Surge	Y-Sway	Z-Heave	Roll	Pitch	Yaw
Maximum	1.12	12.39	6.64	10.55	0.36	0.83
Minimum	-1.39	-1.76	-6.76	-4.33	-0.28	-0.47
Significant	0.76	6.09	6.42	4.96	0.33	0.84
Total Num	595	407	425	546	529	356
Upper%	0.00%	22.85%	7.13%	3.11%	0.00%	0.00%
Lower%	0.00%	0.00%	5.90%	0.00%	0.00%	0.00%

Appendix Figure 3. Motion comparison of test 03 Hs=1.85m, Tp=12.02s, Dir=143˚

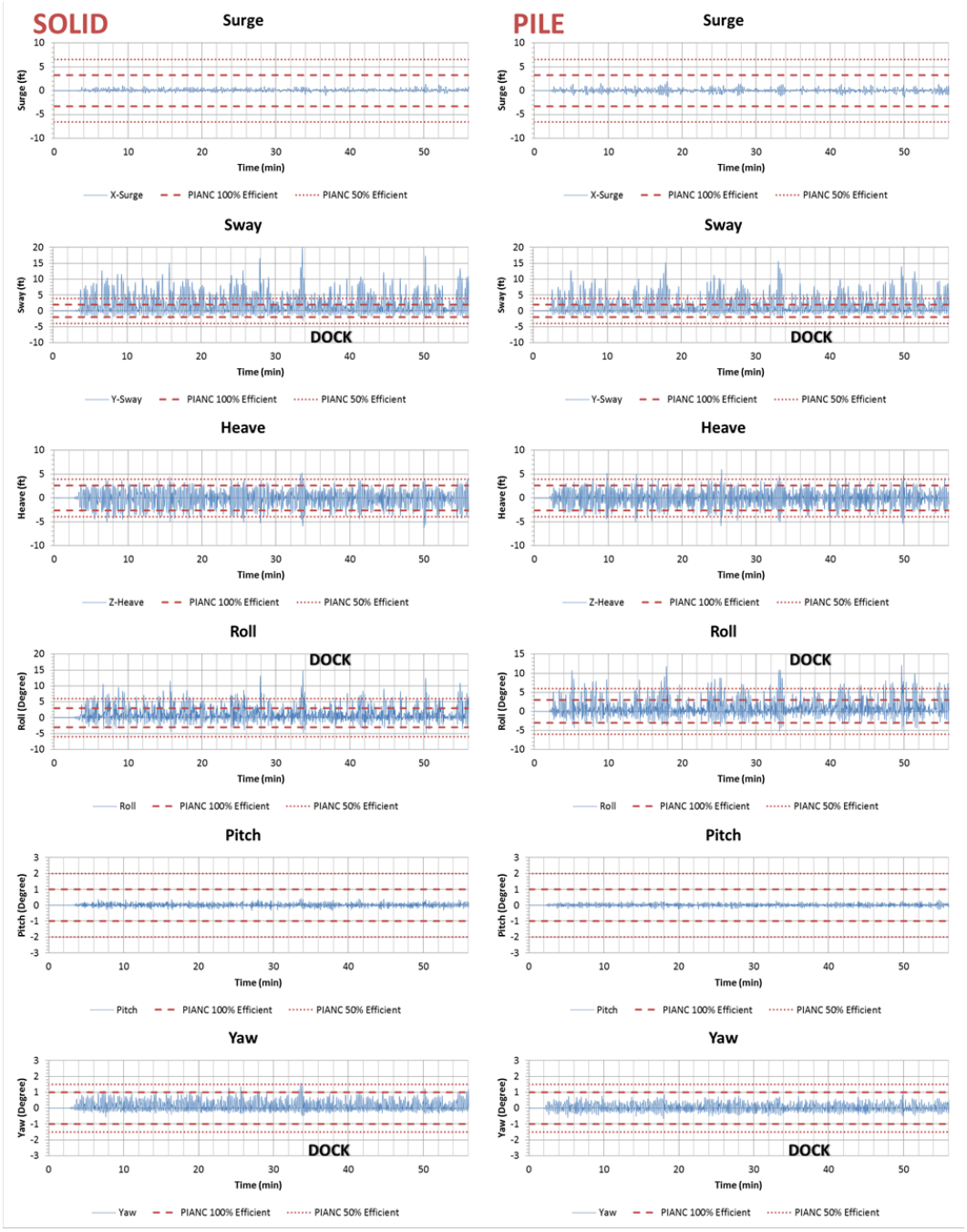

Test04	X-Surge	Y-Sway	Z-Heave	Roll	Pitch	Yaw	Test04p	X-Surge	Y-Sway	Z-Heave	Roll	Pitch	Yaw
Maximum	1.40	20.15	5.31	14.85	0.44	1.59	Maximum	1.93	15.70	6.03	12.09	0.35	0.87
Minimum	-1.11	-3.12	-6.28	-4.89	-0.34	-0.57	Minimum	-1.40	-2.25	-5.88	-5.26	-0.30	-0.66
Significant	0.70	7.35	5.70	6.70	0.30	0.96	Significant	1.17	7.95	5.87	7.88	0.31	0.88
Total Num	554	686	469	626	939	545	Total Num	467	457	336	419	448	353
Upper %	0.00%	22.74%	0.87%	10.22%	0.00%	0.18%	Upper%	0.00%	27.79%	1.97%	12.65%	0.00%	0.00%
Lower%	0.00%	0.00%	4.23%	0.00%	0.00%	0.00%	Lower%	0.00%	0.00%	3.06%	0.00%	0.00%	0.00%

Appendix Figure 4. Motion comparison of test 04 Hs=2.45m, Tp=14s, Dir=143°

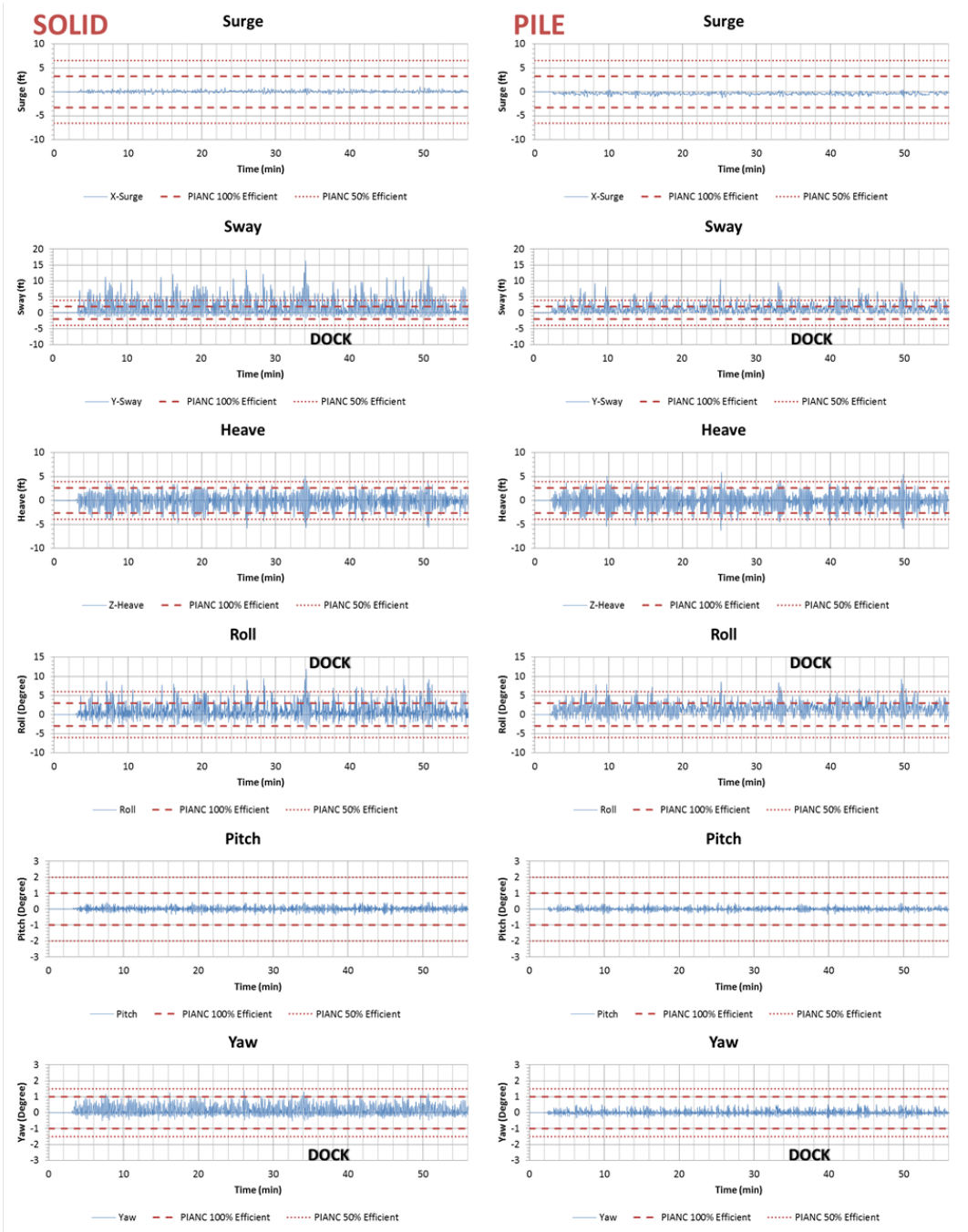

Test05	X-Surge	Y-Sway	Z-Heave	Roll	Pitch	Yaw
Maximum	1.08	16.33	5.19	11.95	0.45	1.43
Minimum	-0.70	-2.09	-5.85	-3.88	-0.39	-0.54
Significant	0.42	7.57	4.77	5.27	0.36	0.85
Total Num	842	518	586	755	1024	833
Upper %	0.00%	31.85%	0.77%	4.50%	0.00%	0.00%
Lower%	0.00%	0.00%	2.90%	0.00%	0.00%	0.00%

Test05p	X-Surge	Y-Sway	Z-Heave	Roll	Pitch	Yaw
Maximum	0.56	10.59	5.93	9.37	0.41	0.57
Minimum	-1.37	-1.39	-6.33	-3.90	-0.35	-0.43
Significant	0.40	5.03	5.61	5.36	0.31	0.46
Total Num	509	323	458	416	859	752
Upper%	0.00%	20.12%	2.48%	4.09%	0.00%	0.00%
Lower%	0.00%	0.00%	7.12%	0.00%	0.00%	0.00%

Appendix Figure 5. Motion comparison of test 05 Hs=1.85m, Tp=12.02s, Dir=143˚

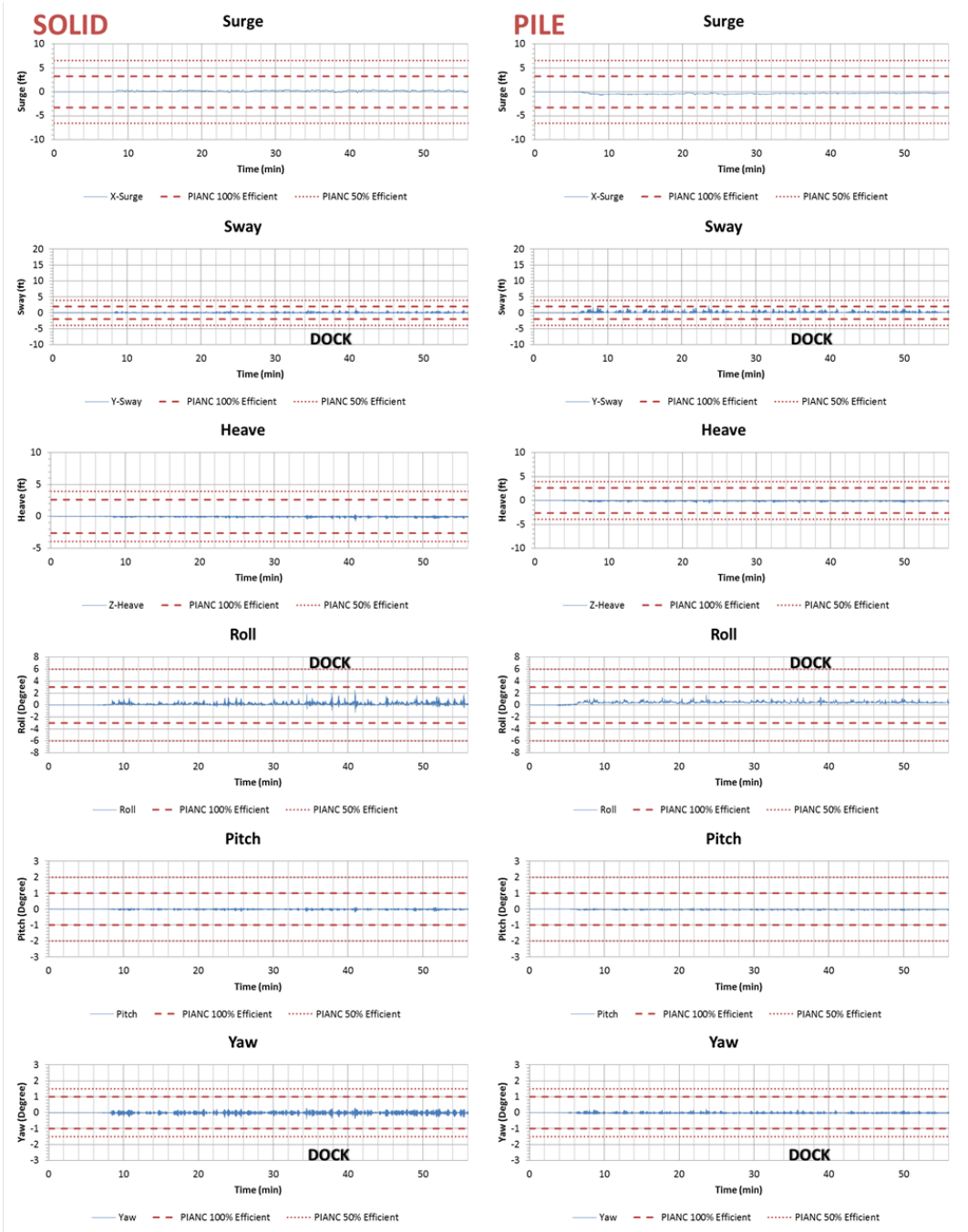

Test06	X-Surge	Y-Sway	Z-Heave	Roll	Pitch	Yaw
Maximum	0.53	1.54	0.31	2.51	0.13	0.29
Minimum	-0.22	-0.38	-0.79	-1.25	-0.21	-0.41
Significant	0.02	0.73	0.32	0.04	0.06	0.30
Total Num	362	1202	553	689	665	1059
Upper %	0.00%	0.00%	0.00%	0.00%	0.00%	0.00%
Lower%	0.00%	0.00%	0.00%	0.00%	0.00%	0.00%

Test06p	X-Surge	Y-Sway	Z-Heave	Roll	Pitch	Yaw
Maximum	0.03	2.32	0.26	1.71	0.09	0.23
Minimum	-0.72	-0.36	-0.67	-0.18	-0.13	-0.11
Significant	0.18	0.30	0.24	0.58	0.11	0.13
Total Num	155	2079	1116	755	944	1204
Upper%	0.00%	0.00%	0.00%	0.00%	0.00%	0.00%
Lower%	0.00%	0.00%	0.00%	0.00%	0.00%	0.00%

Appendix Figure 6. Motion comparison of test 06 Hs=1.85m, Tp=4s, Dir=143°

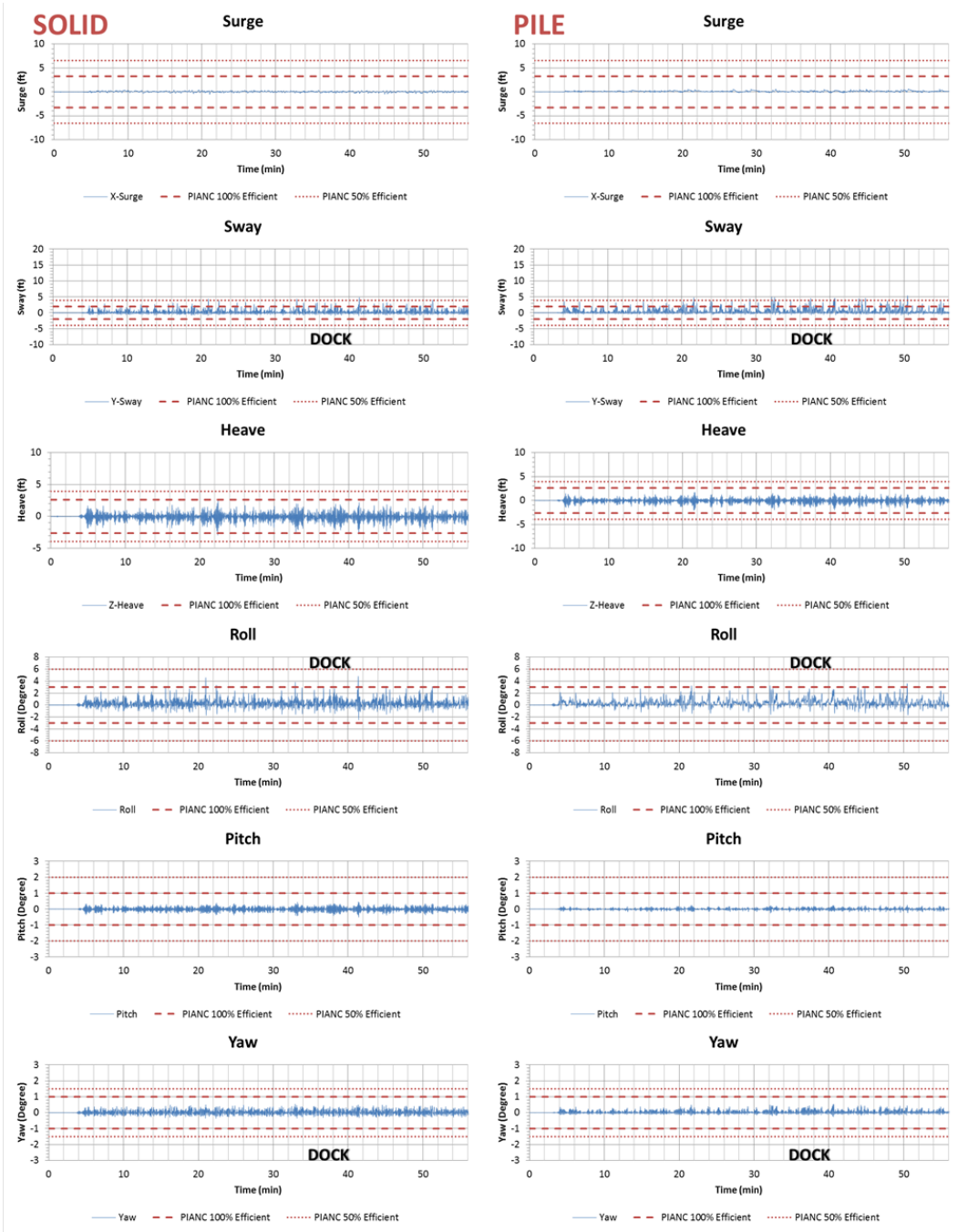

Test07	X-Surge	Y-Sway	Z-Heave	Roll	Pitch	Yaw
Maximum	0.44	4.83	2.51	4.82	0.45	0.54
Minimum	-0.50	-0.97	-2.96	-2.48	-0.52	-0.36
Significant	0.30	2.05	2.24	1.70	0.37	0.44
Total Num	576	697	690	1095	1223	1022
Upper %	0.00%	0.00%	0.00%	0.00%	0.00%	0.00%
Lower%	0.00%	0.00%	0.00%	0.00%	0.00%	0.00%

Test07p	X-Surge	Y-Sway	Z-Heave	Roll	Pitch	Yaw
Maximum	0.63	5.42	1.73	3.62	0.25	0.54
Minimum	-0.22	-0.72	-2.11	-1.71	-0.26	-0.26
Significant	0.20	2.08	1.82	1.64	0.20	0.33
Total Num	744	823	641	550	880	835
Upper%	0.00%	0.00%	0.00%	0.00%	0.00%	0.00%
Lower%	0.00%	0.00%	0.00%	0.00%	0.00%	0.00%

Appendix Figure 7. Motion comparison of test 07 Hs=1.85m, Tp=6.01s, Dir=143˚

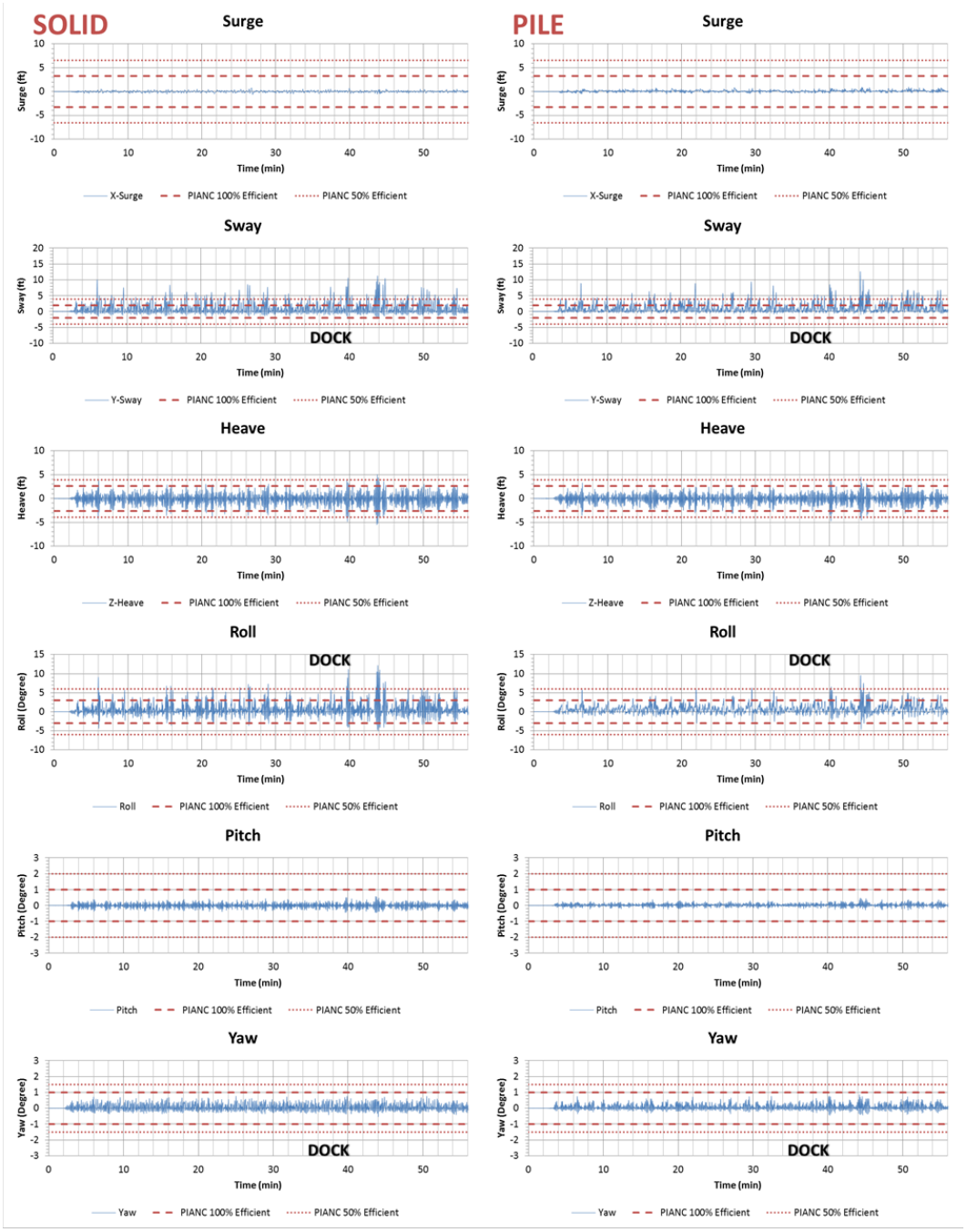

Test08	X-Surge	Y-Sway	Z-Heave	Roll	Pitch	Yaw	Test08p	X-Surge	Y-Sway	Z-Heave	Roll	Pitch	Yaw
Maximum	0.74	11.28	5.07	12.21	0.57	0.77	Maximum	0.96	12.66	4.54	9.60	0.48	0.88
Minimum	-0.62	-2.11	-5.53	-5.09	-0.46	-0.54	Minimum	-0.50	-1.05	-4.75	-4.72	-0.29	-0.45
Significant	0.39	5.45	4.26	5.65	0.52	0.75	Significant	0.50	4.58	3.42	4.14	0.35	0.59
Total Num	627	488	503	586	594	480	Total Num	673	366	561	323	574	677
Upper %	0.00%	18.85%	0.61%	3.92%	0.00%	0.00%	Upper%	0.00%	16.12%	0.27%	1.55%	0.00%	0.00%
Lower%	0.00%	0.00%	0.82%	0.00%	0.00%	0.00%	Lower%	0.00%	0.00%	0.82%	0.00%	0.00%	0.00%

Appendix Figure 8. Motion comparison of test 08 Hs=1.13m, Tp=7.99s, Dir=143˚

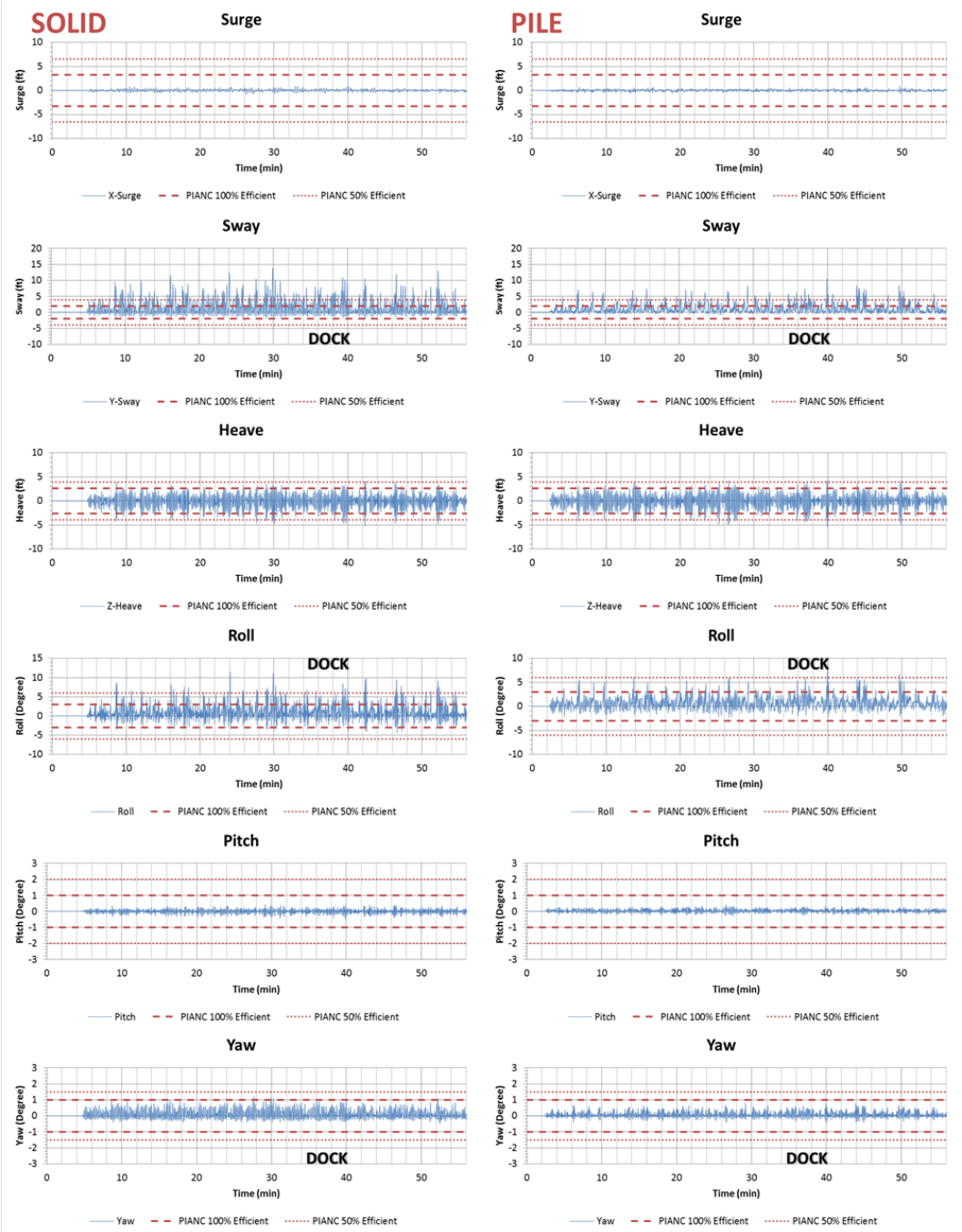

Test09	X-Surge	Y-Sway	Z-Heave	Roll	Pitch	Yaw	Test09p	X-Surge	Y-Sway	Z-Heave	Roll	Pitch	Yaw
Maximum	0.89	13.98	4.19	11.59	0.43	1.23	Maximum	0.89	10.55	4.52	7.86	0.39	0.80
Minimum	-0.84	-2.06	-5.27	-4.40	-0.49	-0.51	Minimum	-0.65	-0.79	-5.42	-2.37	-0.29	-0.46
Significant	0.39	6.29	4.16	4.71	0.37	0.68	Significant	0.44	3.13	4.97	3.49	0.30	0.57
Total Num	867	646	738	966	857	1025	Total Num	748	591	516	615	853	736
Upper %	0.00%	21.83%	0.15%	4.45%	0.00%	0.00%	Upper%	0.00%	8.29%	0.85%	0.65%	0.00%	0.00%
Lower%	0.00%	0.00%	2.17%	0.00%	0.00%	0.00%	Lower%	0.00%	0.00%	3.05%	0.00%	0.00%	0.00%

Appendix Figure 9. Motion comparison of test 09 Hs=1.85m, Tp=9.97s, Dir=143°

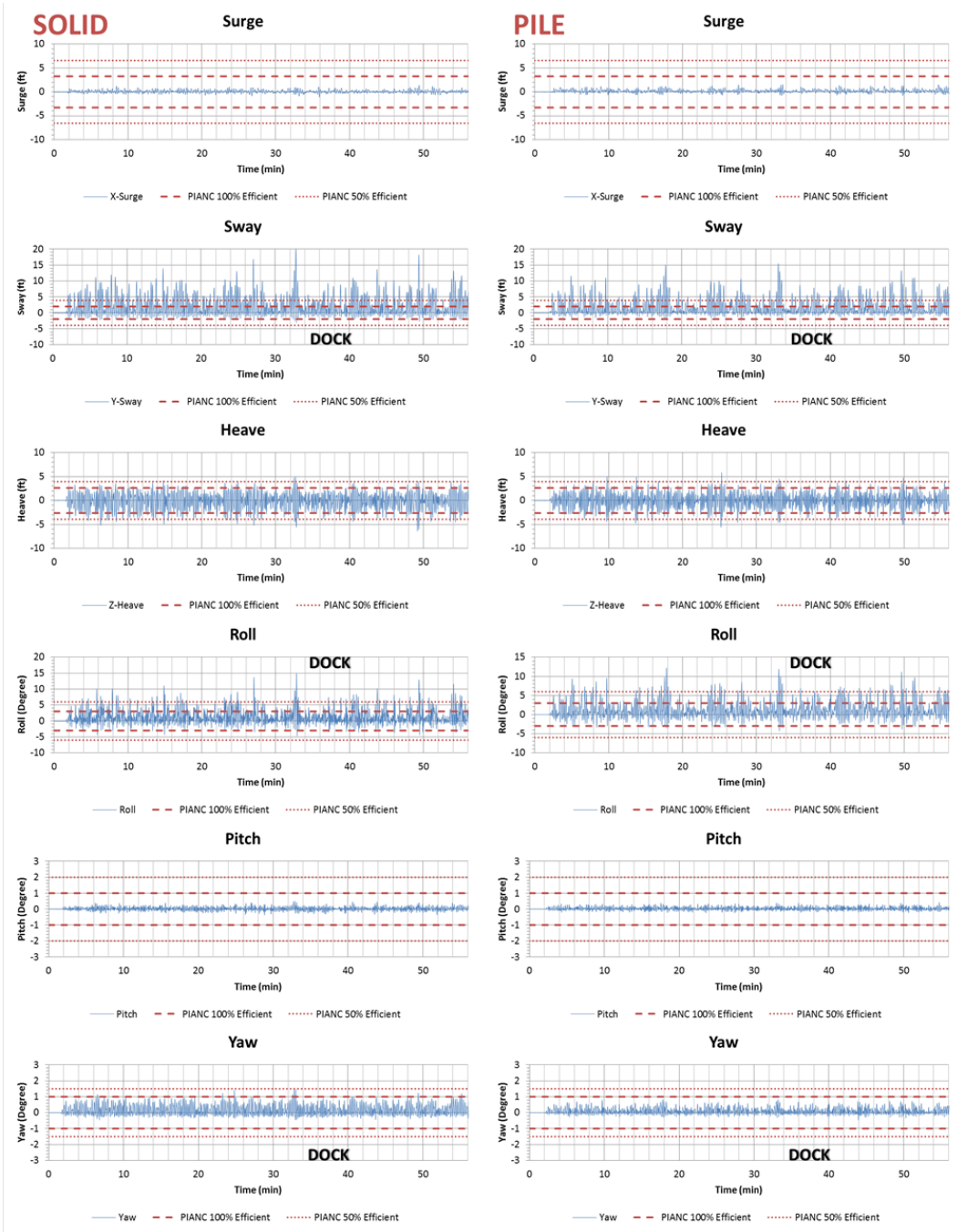

Test10	X-Surge	Y-Sway	Z-Heave	Roll	Pitch	Yaw
Maximum	1.39	20.29	4.94	15.01	0.51	1.55
Minimum	-1.09	-3.09	-6.42	-4.75	-0.37	-0.46
Significant	0.86	9.67	6.04	6.76	0.37	1.02
Total Num	434	390	347	613	648	481
Upper %	0.00%	41.54%	1.03%	9.95%	0.00%	0.21%
Lower%	0.00%	0.00%	6.15%	0.00%	0.00%	0.00%

Test10p	X-Surge	Y-Sway	Z-Heave	Roll	Pitch	Yaw
Maximum	1.56	15.46	5.87	12.23	0.43	0.84
Minimum	-0.79	-2.00	-5.61	-4.30	-0.25	-0.46
Significant	0.88	6.51	5.14	7.60	0.32	0.53
Total Num	511	527	465	376	703	754
Upper%	0.00%	22.96%	1.52%	13.56%	0.00%	0.00%
Lower%	0.00%	0.00%	2.28%	0.00%	0.00%	0.00%

Appendix Figure 10. Motion comparison of test 10 Hs=1.85m, Tp=14s, Dir=143˚

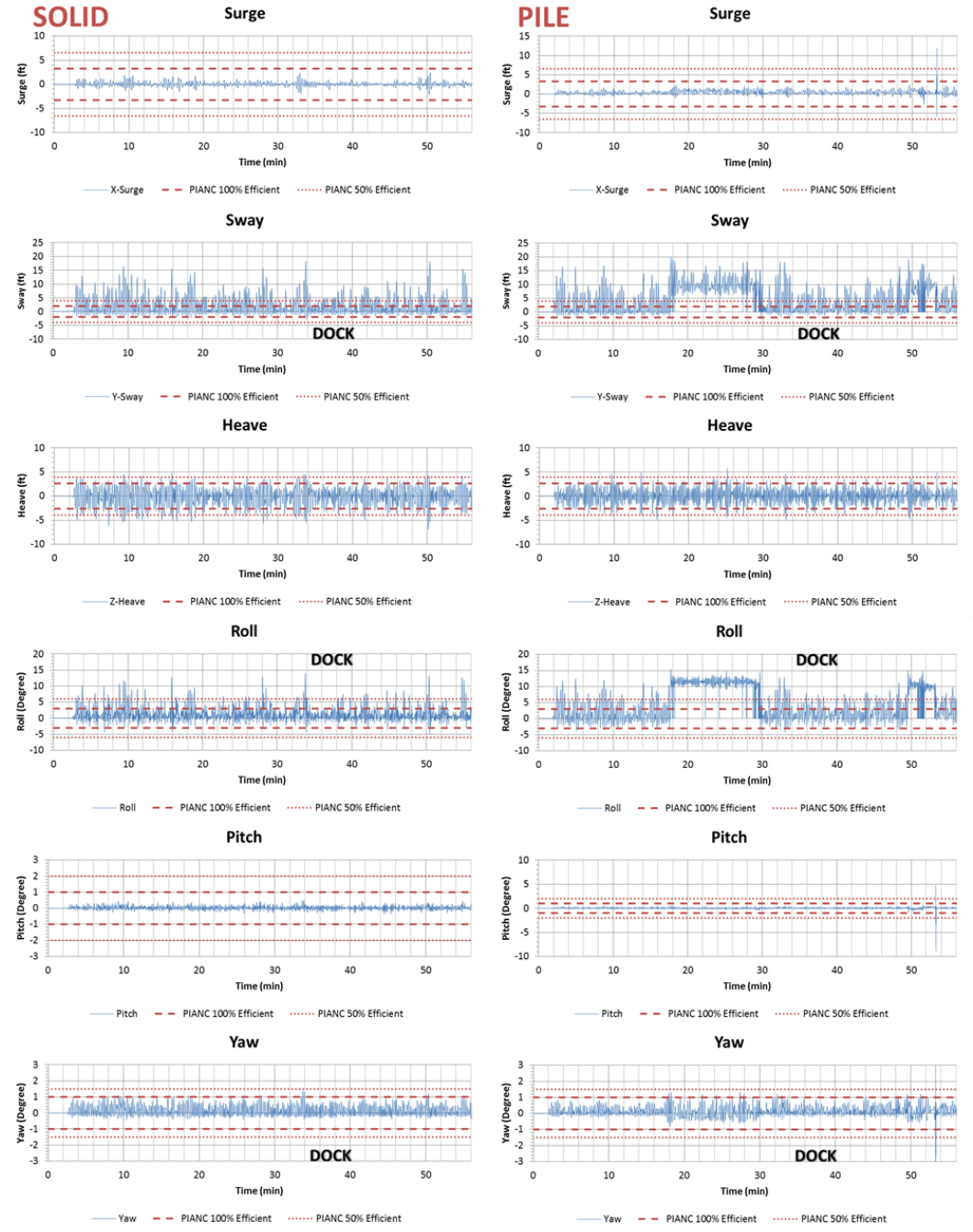

Test11	X-Surge	Y-Sway	Z-Heave	Roll	Pitch	Yaw
Maximum	2.54	18.36	4.83	14.17	0.51	1.38
Minimum	-2.13	-2.97	-6.99	-4.90	-0.37	-0.44
Significant	1.69	6.82	6.30	7.67	0.41	0.98
Total Num	235	708	389	407	398	458
Upper %	0.00%	20.90%	1.41%	13.02%	0.00%	0.00%
Lower%	0.00%	0.00%	5.93%	0.00%	0.00%	0.00%

Test11p	X-Surge	Y-Sway	Z-Heave	Roll	Pitch	Yaw
Maximum	11.62	19.96	5.77	15.49	4.55	3.83
Minimum	-5.75	-2.42	-4.96	-4.70	-8.69	-6.50
Significant	1.61	12.35	4.77	11.09	0.43	1.08
Total Num	549	500	502	548	808	495
Upper%	0.18%	55.00%	1.20%	36.68%	0.12%	0.20%
Lower%	0.00%	0.00%	2.00%	0.00%	0.62%	1.01%

Appendix Figure 11. Motion comparison of test 11 Hs=1.85m, Tp=15.98s, Dir=143°

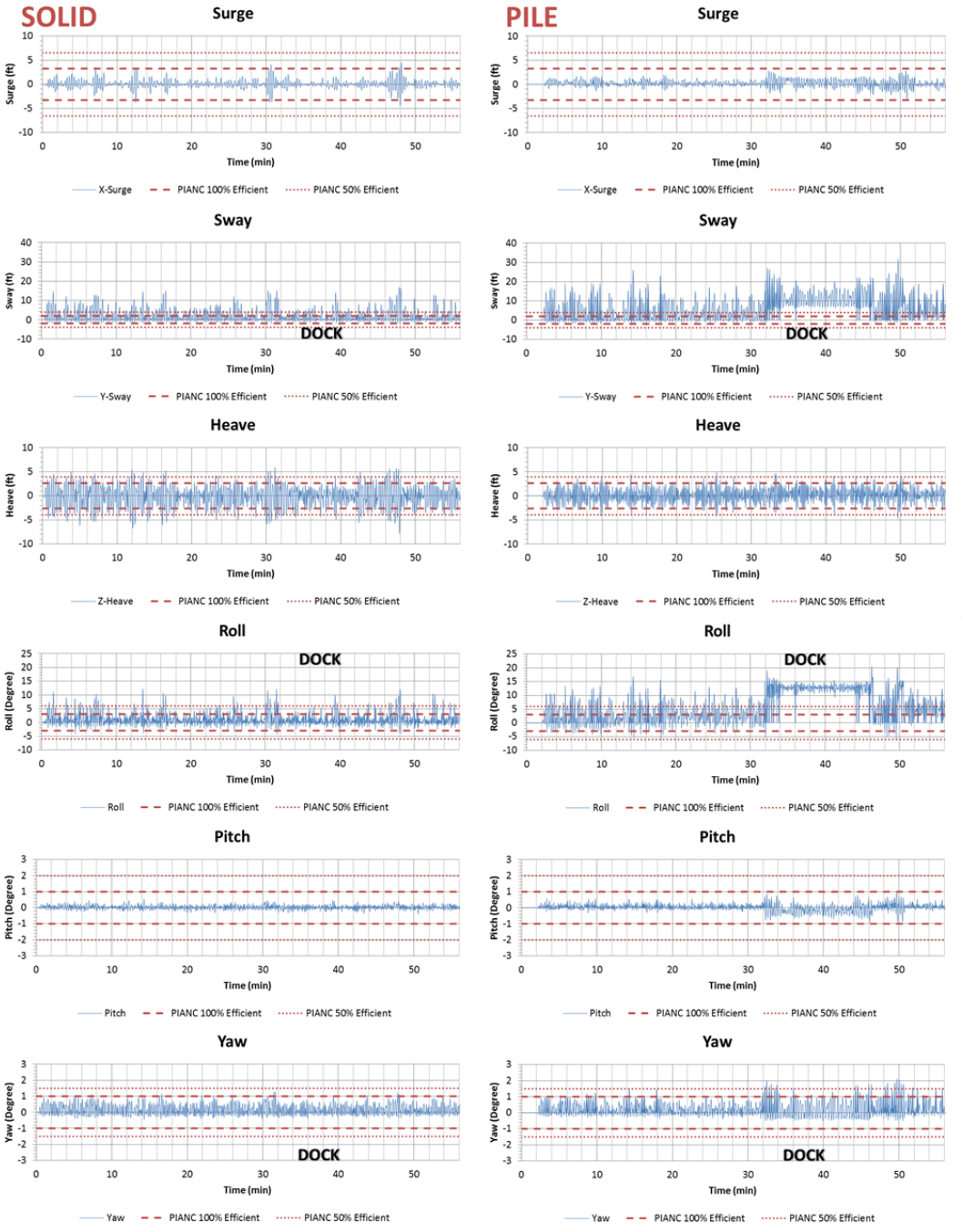

Test12	X-Surge	Y-Sway	Z-Heave	Roll	Pitch	Yaw	Test12p	X-Surge	Y-Sway	Z-Heave	Roll	Pitch	Yaw
Maximum	4.58	16.91	5.91	12.23	0.54	1.30	Maximum	2.86	31.66	4.95	20.55	0.91	2.13
Minimum	-4.45	-2.51	-7.87	-4.44	-0.40	-0.46	Minimum	-3.17	-2.17	-4.80	-6.38	-0.92	-0.51
Significant	2.31	17.65	5.02	10.60	0.63	1.03	Significant	2.88	9.68	7.96	7.53	0.42	1.27
Total Num	283	397	371	618	423	300	Total Num	226	345	246	379	353	601
Upper %	0.00%	38.84%	8.12%	11.87%	0.00%	0.00%	Upper%	0.00%	54.41%	1.76%	25.73%	0.00%	4.99%
Lower%	0.00%	0.00%	13.62%	0.00%	0.00%	0.00%	Lower%	0.00%	0.00%	1.01%	0.32%	0.00%	0.00%

Appendix Figure 12. Motion comparison of test 12 Hs=1.85m, Tp=18.03s, Dir=143°

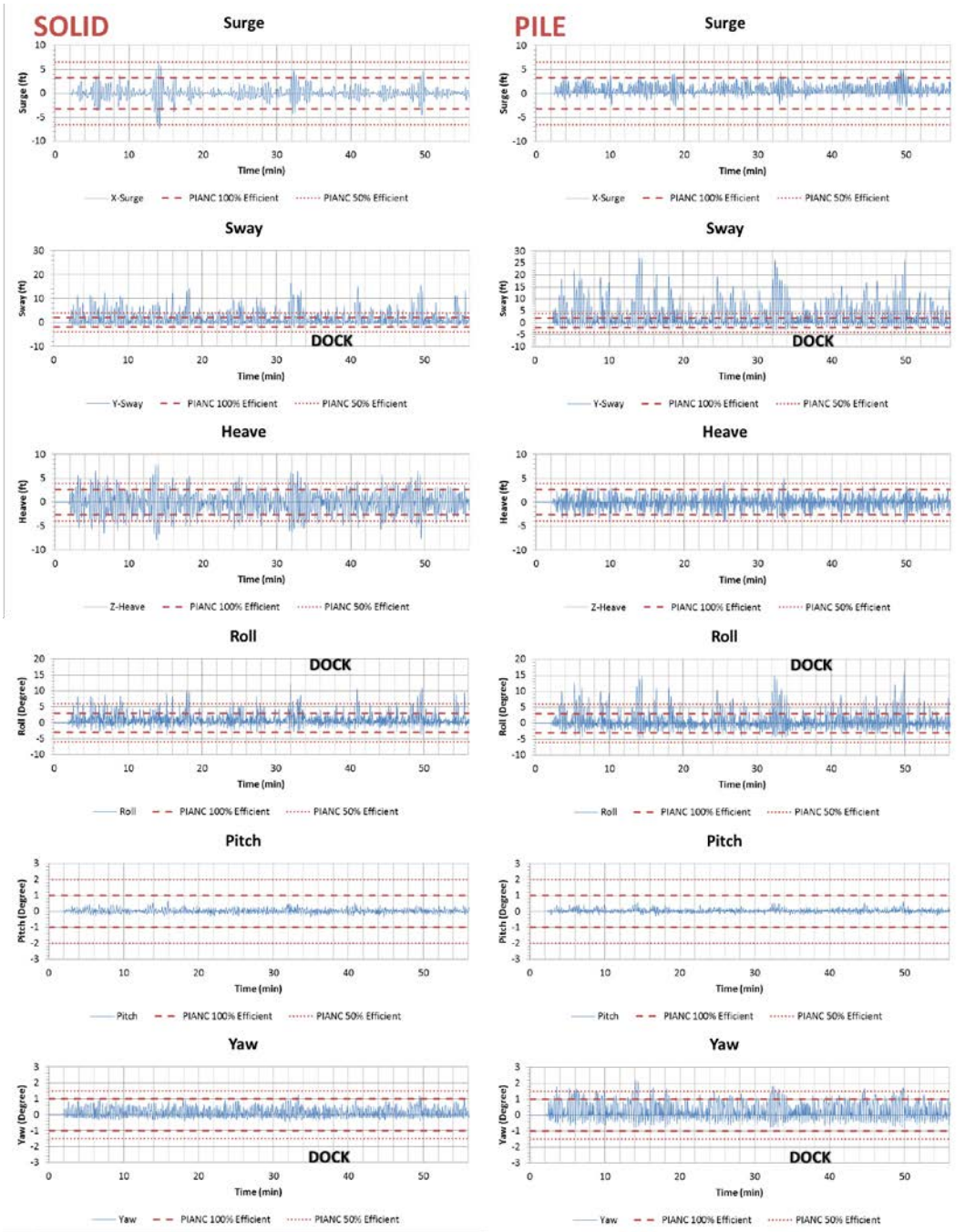

Test13	X-Surge	Y-Sway	Z-Heave	Roll	Pitch	Yaw
Maximum	6.47	16.48	7.89	12.23	0.65	1.27
Minimum	-7.34	-2.42	-7.88	-3.87	-0.39	-0.46
Significant	4.09	6.75	7.05	5.11	0.44	0.94
Total Num	219	563	425	625	417	357
Upper %	0.00%	20.07%	7.46%	4.79%	0.00%	0.00%
Lower%	45.66%	0.00%	10.12%	0.00%	0.00%	0.00%

Test13p	X-Surge	Y-Sway	Z-Heave	Roll	Pitch	Yaw
Maximum	5.02	27.23	4.91	15.98	0.61	2.22
Minimum	-2.85	-3.59	-4.73	-6.64	-0.31	-0.84
Significant	2.79	7.51	3.75	5.78	0.29	1.01
Total Num	692	922	633	823	765	837
Upper%	0.00%	21.37%	0.43%	5.83%	0.00%	2.27%
Lower%	0.00%	0.00%	0.65%	0.12%	0.00%	0.00%

Appendix Figure 13. Motion comparison of test 13 Hs=1.85m, Tp=20.01s, Dir=143˚

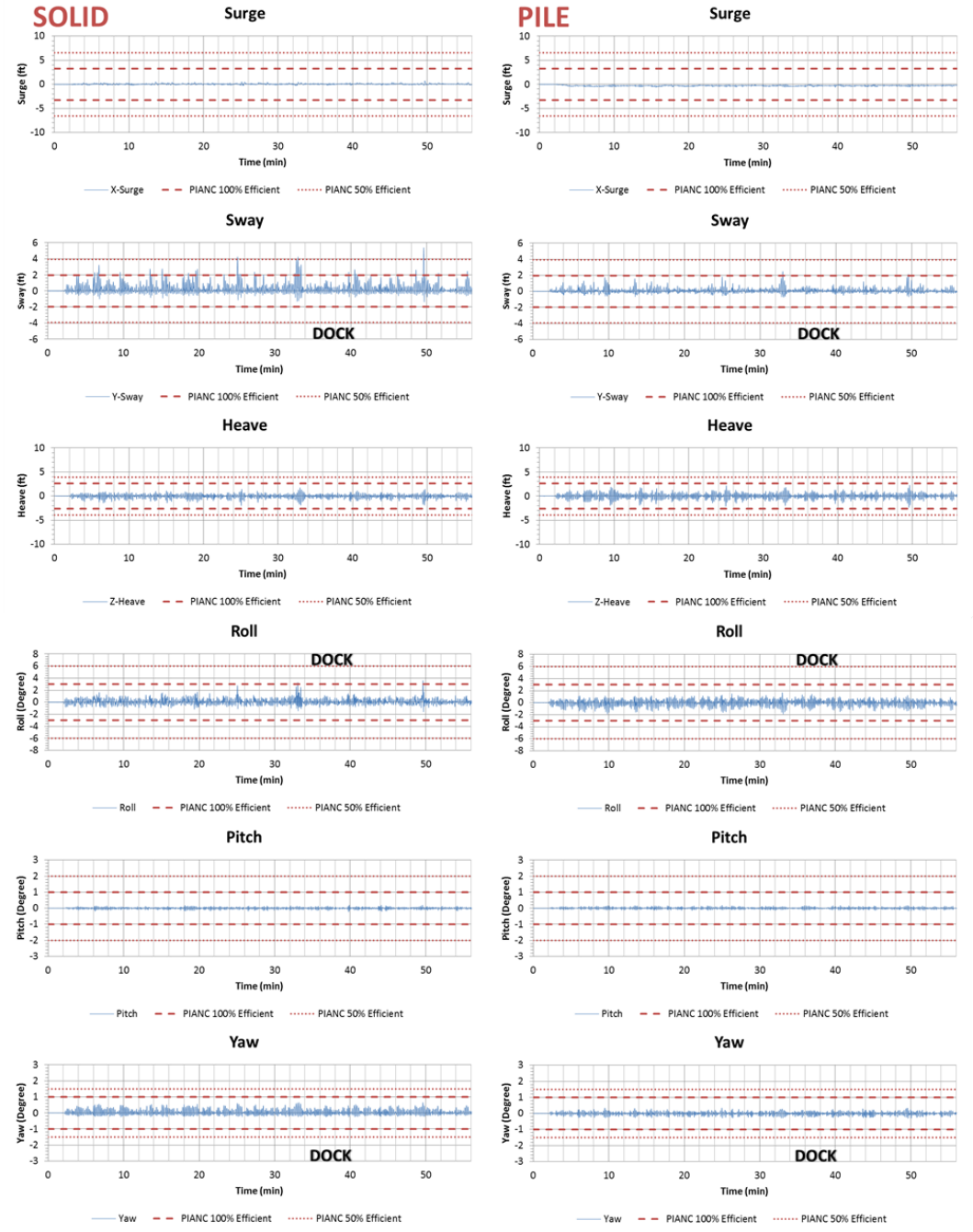

Test14b	X-Surge	Y-Sway	Z-Heave	Roll	Pitch	Yaw
Maximum	0.72	5.39	1.75	3.61	0.20	0.66
Minimum	-0.26	-1.39	-2.01	-1.64	-0.22	-0.25
Significant	0.28	1.42	1.43	1.35	0.16	0.51
Total Num	645	783	493	760	778	611
Upper %	0.00%	0.00%	0.00%	0.00%	0.00%	0.00%
Lower%	0.00%	0.00%	0.00%	0.00%	0.00%	0.00%

Test14p	X-Surge	Y-Sway	Z-Heave	Roll	Pitch	Yaw
Maximum	0.09	2.50	2.29	1.70	0.19	0.35
Minimum	-0.63	-0.76	-2.42	-1.92	-0.16	-0.31
Significant	0.05	0.72	2.01	1.80	0.19	0.36
Total Num	314	753	397	469	546	542
Upper%	0.00%	0.00%	0.00%	0.00%	0.00%	0.00%
Lower%	0.00%	0.00%	0.00%	0.00%	0.00%	0.00%

Appendix Figure 14. Motion comparison of test 14 Hs=0.6m, Tp=12.02s, Dir=143°

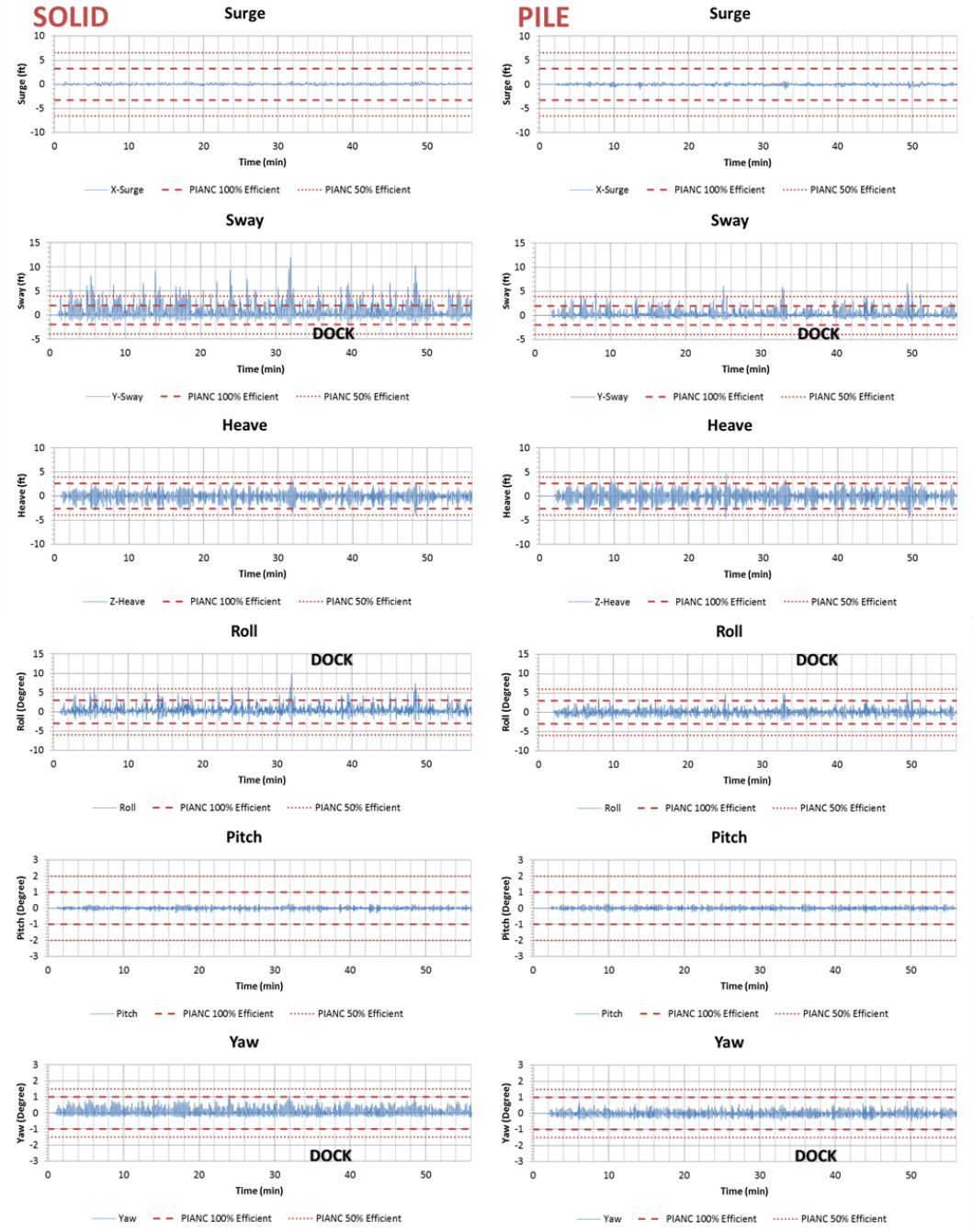

Test15	X-Surge	Y-Sway	Z-Heave	Roll	Pitch	Yaw
Maximum	0.76	12.06	3.75	9.76	0.32	1.10
Minimum	-0.46	-2.11	-4.02	-3.90	-0.33	-0.36
Significant	0.48	5.40	3.56	3.91	0.33	0.89
Total Num	467	420	380	522	496	378
Upper %	0.00%	17.14%	0.00%	1.53%	0.00%	0.00%
Lower%	0.00%	0.00%	0.48%	0.00%	0.00%	0.00%

Test15p	X-Surge	Y-Sway	Z-Heave	Roll	Pitch	Yaw
Maximum	0.82	6.78	4.70	5.36	0.33	0.83
Minimum	-1.06	-1.30	-4.69	-2.34	-0.28	-0.48
Significant	0.59	2.45	4.56	2.67	0.35	580.00
Total Num	587	695	338	588	528	0.6504
Upper%	0.00%	2.01%	0.29%	0.00%	0.00%	0.00%
Lower%	0.00%	0.00%	0.43%	0.00%	0.00%	0.00%

Appendix Figure 15. Motion comparison of test 15 Hs=1.2m, Tp=12.02s, Dir=143°

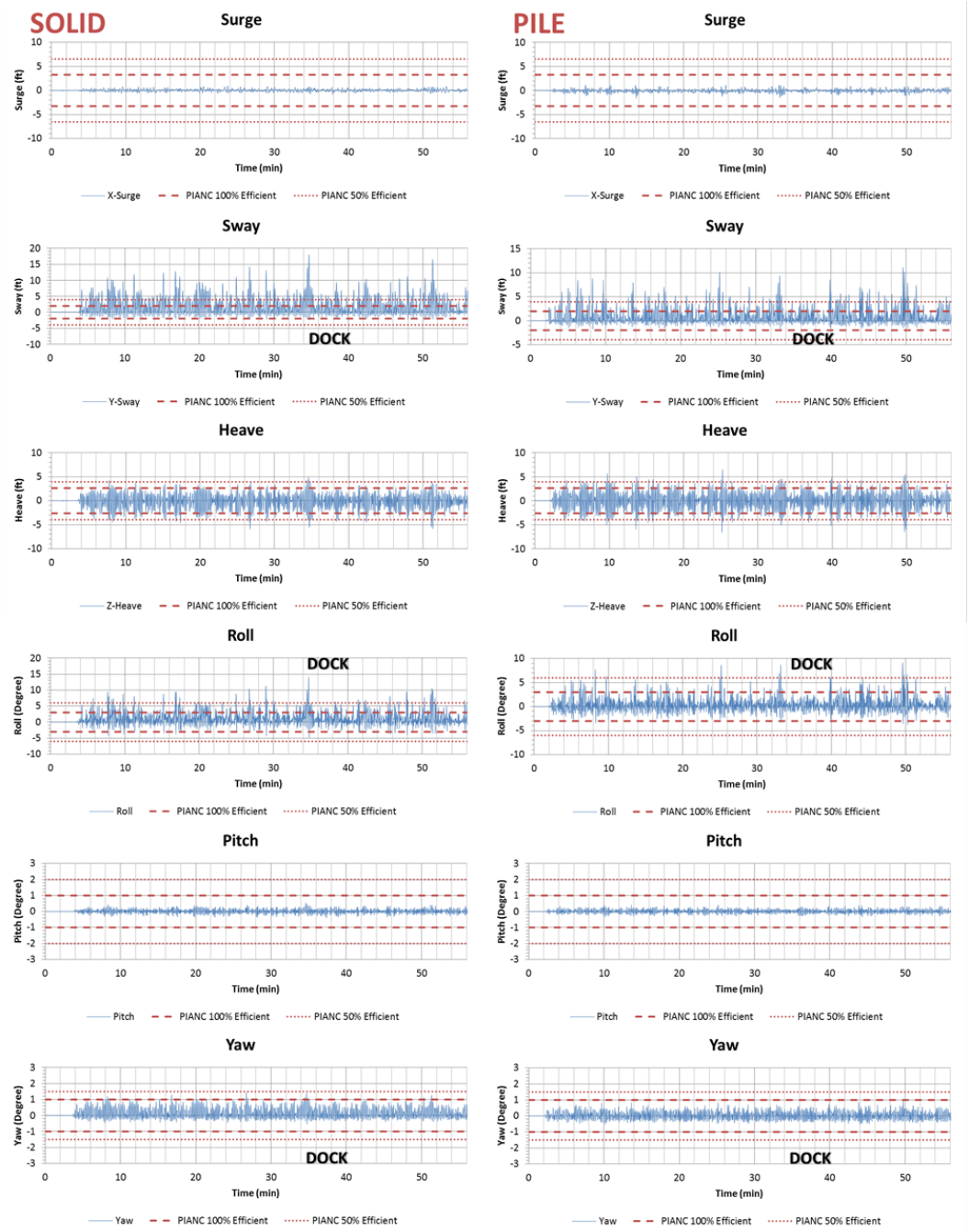

Test16	X-Surge	Y-Sway	Z-Heave	Roll	Pitch	Yaw
Maximum	0.93	18.06	4.91	14.19	0.55	1.45
Minimum	-0.79	-2.41	-5.91	-4.87	-0.40	-0.53
Significant	0.66	8.38	4.45	7.76	0.35	0.97
Total Num	486	446	686	391	924	622
Upper %	0.00%	35.65%	0.90%	10.74%	0.00%	0.00%
Lower%	0.00%	0.00%	3.59%	0.00%	0.00%	0.00%

Test16p	X-Surge	Y-Sway	Z-Heave	Roll	Pitch	Yaw
Maximum	1.12	11.10	6.51	9.15	0.42	0.94
Minimum	-1.69	-1.77	-6.63	-3.76	-0.33	-0.52
Significant	0.85	5.49	6.27	4.55	0.40	0.85
Total Num	591	493	428	577	518	467
Upper%	0.00%	19.47%	5.27%	1.73%	0.00%	0.00%
Lower%	0.00%	0.00%	4.26%	0.00%	0.00%	0.00%

Appendix Figure 16. Motion comparison of test 16 Hs=2.45m, Tp=12.02s, Dir=143˚

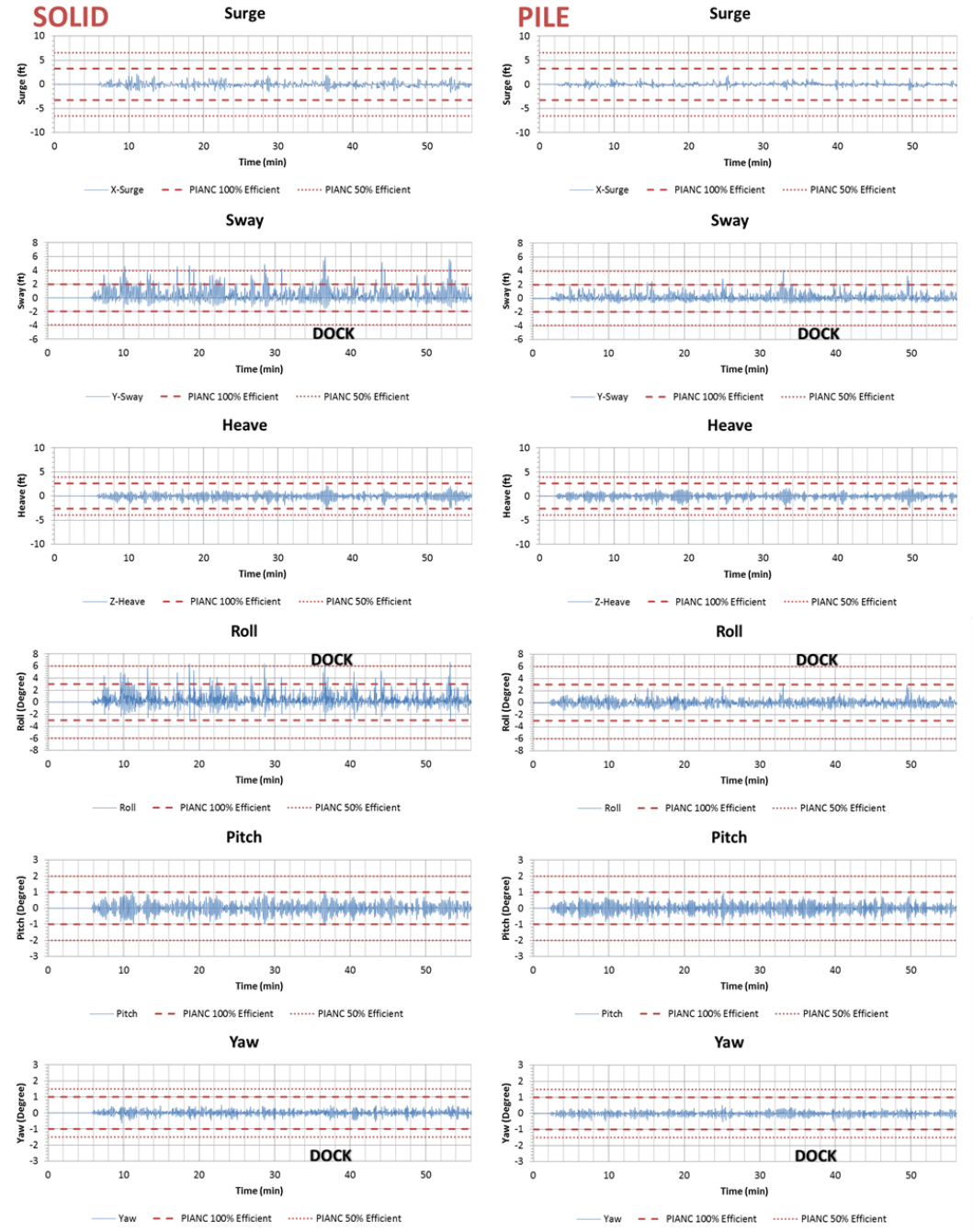

Test17	X-Surge	Y-Sway	Z-Heave	Roll	Pitch	Yaw
Maximum	2.19	5.91	2.26	6.70	1.06	0.51
Minimum	-1.78	-1.58	-2.79	-3.25	-1.09	-0.64
Significant	0.82	1.43	1.40	2.29	0.56	0.36
Total Num	741	1180	815	1014	1154	1061
Upper %	0.00%	1.02%	0.00%	0.39%	0.00%	0.00%
Lower%	0.00%	0.00%	0.00%	0.00%	0.00%	0.00%

Test17p	X-Surge	Y-Sway	Z-Heave	Roll	Pitch	Yaw
Maximum	1.90	4.14	1.73	3.20	0.95	0.53
Minimum	-1.31	-0.83	-2.48	-1.55	-1.12	-0.55
Significant	1.01	1.67	2.09	1.92	1.03	0.54
Total Num	306	412	327	383	392	335
Upper%	0.00%	0.24%	0.00%	0.00%	0.00%	0.00%
Lower%	0.00%	0.00%	0.00%	0.00%	0.00%	0.00%

Appendix Figure 17. Motion comparison of test 17 Hs=1.85m, Tp=12.02s, Dir=113°

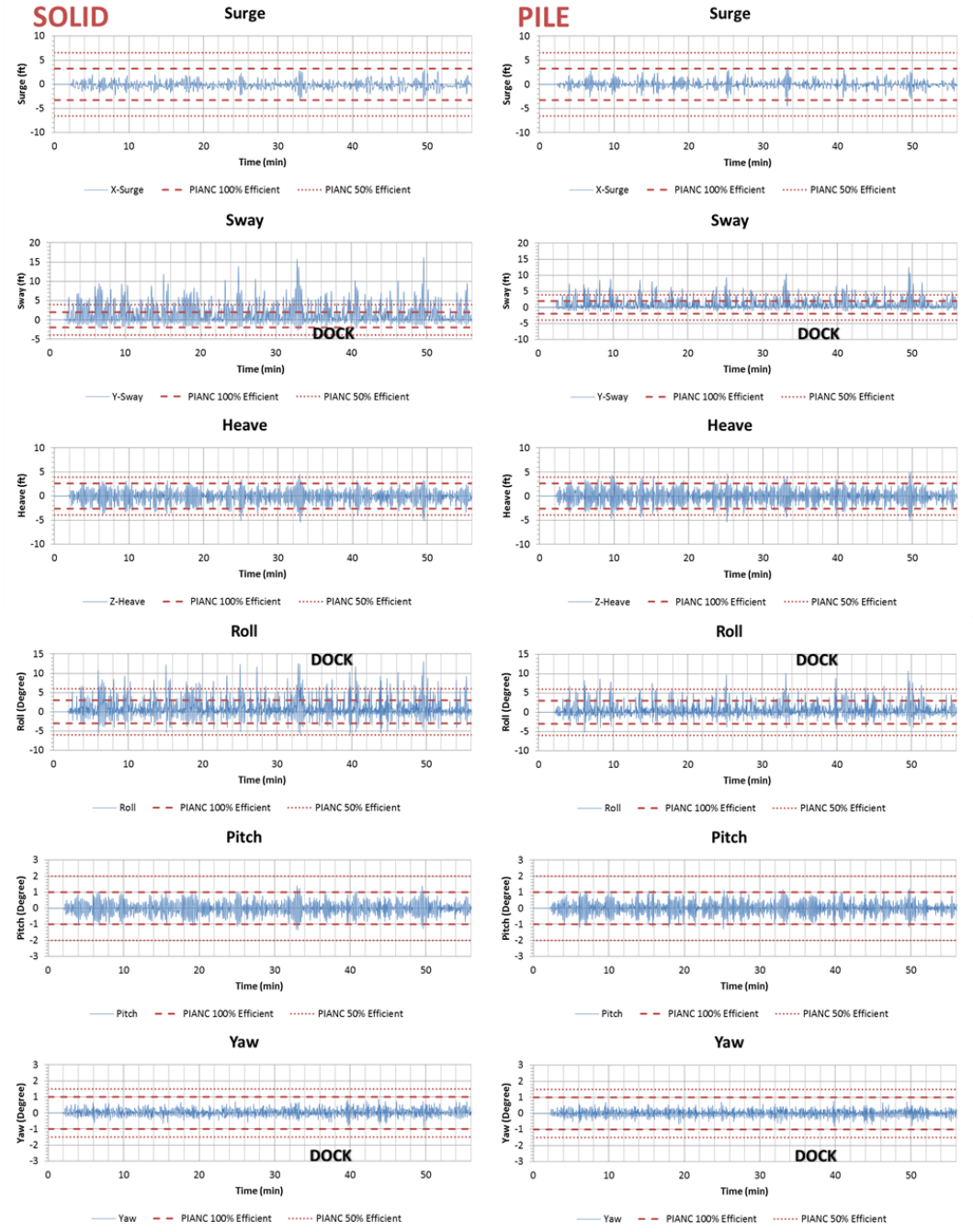

Test18b	X-Surge	Y-Sway	Z-Heave	Roll	Pitch	Yaw
Maximum	3.16	16.24	4.58	13.05	1.42	0.88
Minimum	-3.50	-2.74	-5.41	-5.93	-1.35	-0.90
Significant	2.45	7.42	4.47	8.68	1.33	0.76
Total Num	323	455	421	494	490	496
Upper %	0.00%	29.67%	0.22%	13.16%	0.00%	0.00%
Lower%	0.00%	0.00%	1.10%	0.00%	0.00%	0.00%

Test18p	X-Surge	Y-Sway	Z-Heave	Roll	Pitch	Yaw
Maximum	3.75	12.55	4.87	10.77	1.22	0.78
Minimum	-4.64	-1.65	-5.44	-5.22	-1.29	-0.82
Significant	2.09	4.72	4.81	5.93	1.10	0.68
Total Num	536	570	447	462	728	602
Upper%	0.00%	14.74%	1.23%	4.11%	0.00%	0.00%
Lower%	0.00%	0.00%	1.58%	0.00%	0.00%	0.00%

Appendix Figure 18. Motion comparison of test 18 Hs=1.85m, Tp=12.02s, Dir=128°

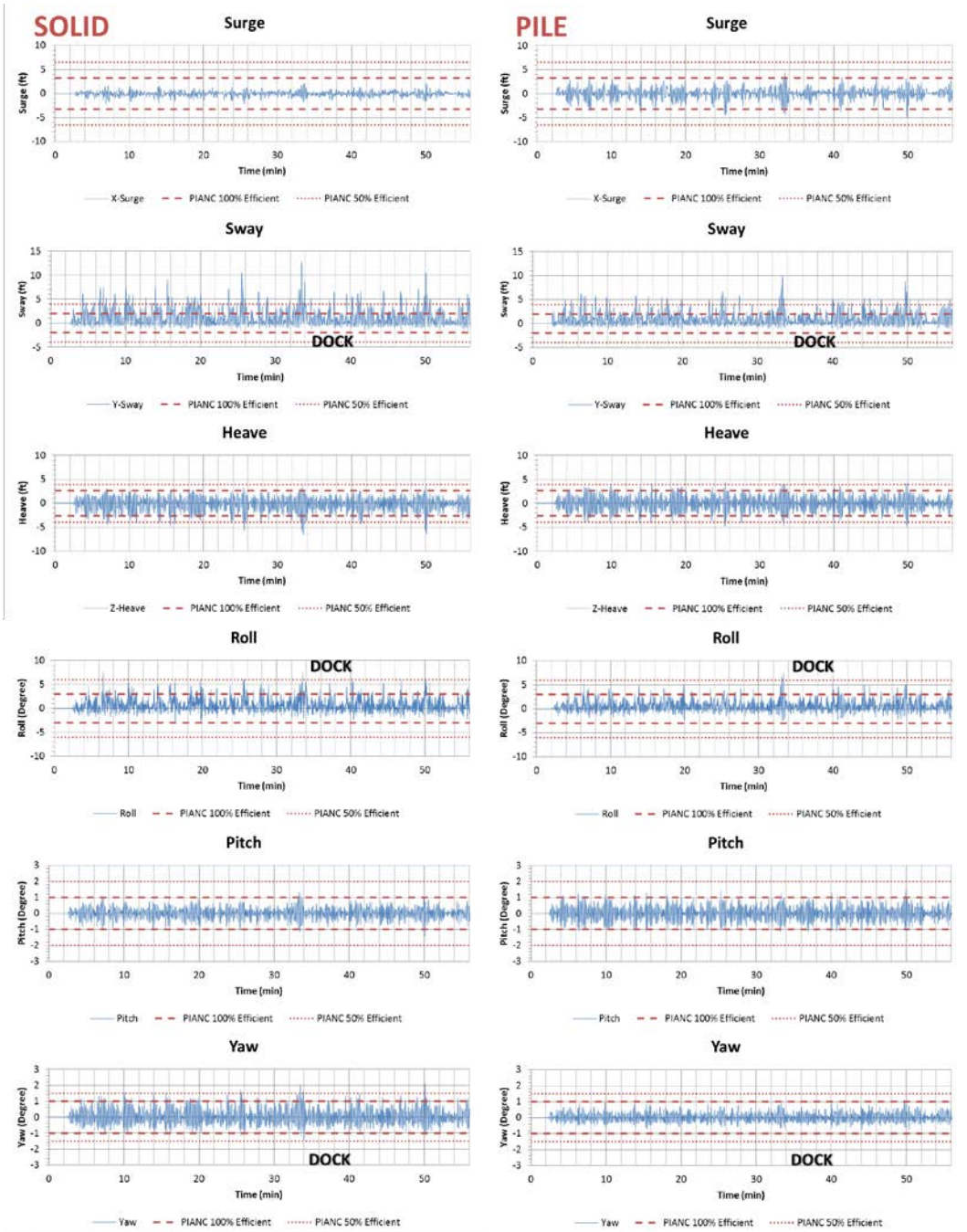

Test19	X-Surge	Y-Sway	Z-Heave	Roll	Pitch	Yaw
Maximum	2.16	12.77	3.80	7.62	1.35	2.14
Minimum	-2.29	-1.71	-6.59	-3.09	-1.43	-1.46
Significant	1.32	3.71	4.28	3.29	1.18	1.31
Total Num	676	779	613	884	440	782
Upper %	0.00%	8.60%	0.00%	0.57%	0.00%	1.02%
Lower%	0.00%	0.00%	1.93%	0.00%	0.00%	0.00%

Test19p	X-Surge	Y-Sway	Z-Heave	Roll	Pitch	Yaw
Maximum	4.40	9.90	4.52	7.59	1.45	1.10
Minimum	-5.11	-1.37	-4.84	-2.51	-1.17	-0.74
Significant	2.95	3.57	4.91	3.39	1.48	0.90
Total Num	573	604	452	632	473	554
Upper%	0.00%	7.45%	0.99%	0.32%	0.00%	0.00%
Lower%	0.00%	0.00%	1.16%	0.00%	0.00%	0.00%

Appendix Figure 19. Motion comparison of test 19 Hs=1.85m, Tp=12.02s, Dir=158°

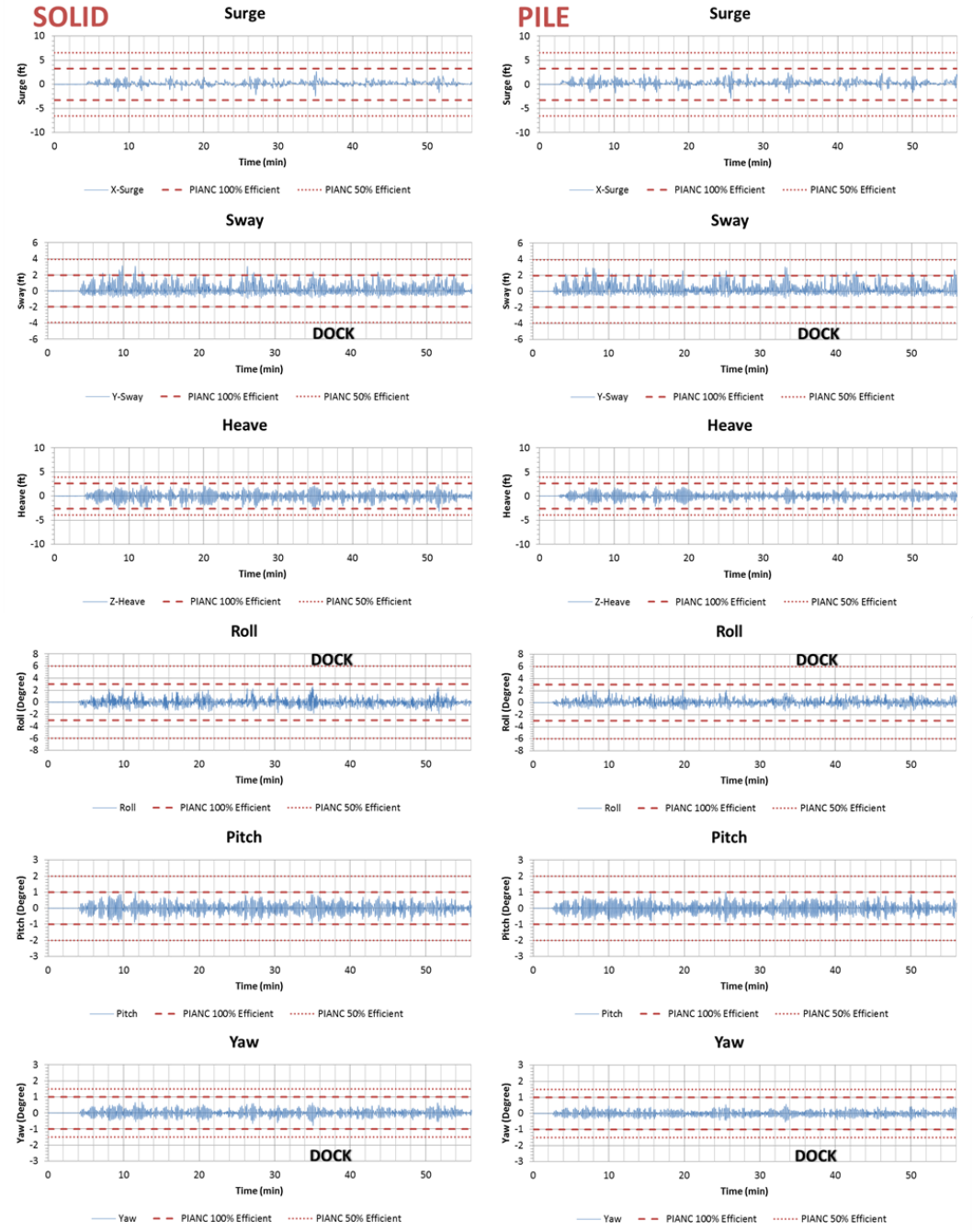

Test20	X-Surge	Y-Sway	Z-Heave	Roll	Pitch	Yaw
Maximum	2.74	3.17	2.48	2.63	0.98	0.69
Minimum	-2.51	-0.98	-3.23	-1.93	-1.07	-0.80
Significant	1.01	1.61	2.25	1.33	0.74	0.60
Total Num	563	743	708	1180	877	631
Upper %	0.00%	0.00%	0.00%	0.00%	0.00%	0.00%
Lower%	0.00%	0.00%	0.00%	0.00%	0.00%	0.00%

Test20p	X-Surge	Y-Sway	Z-Heave	Roll	Pitch	Yaw
Maximum	2.74	3.07	2.04	2.24	1.00	0.58
Minimum	-2.95	-0.90	-2.30	-1.42	-0.87	-0.55
Significant	1.63	1.77	2.20	1.61	1.06	0.60
Total Num	457	606	407	556	438	341
Upper%	0.00%	0.00%	0.00%	0.00%	0.00%	0.00%
Lower%	0.00%	0.00%	0.00%	0.00%	0.00%	0.00%

Appendix Figure 20. Motion comparison of test 20 Hs=1.85m, Tp=12.02s, Dir=173˚

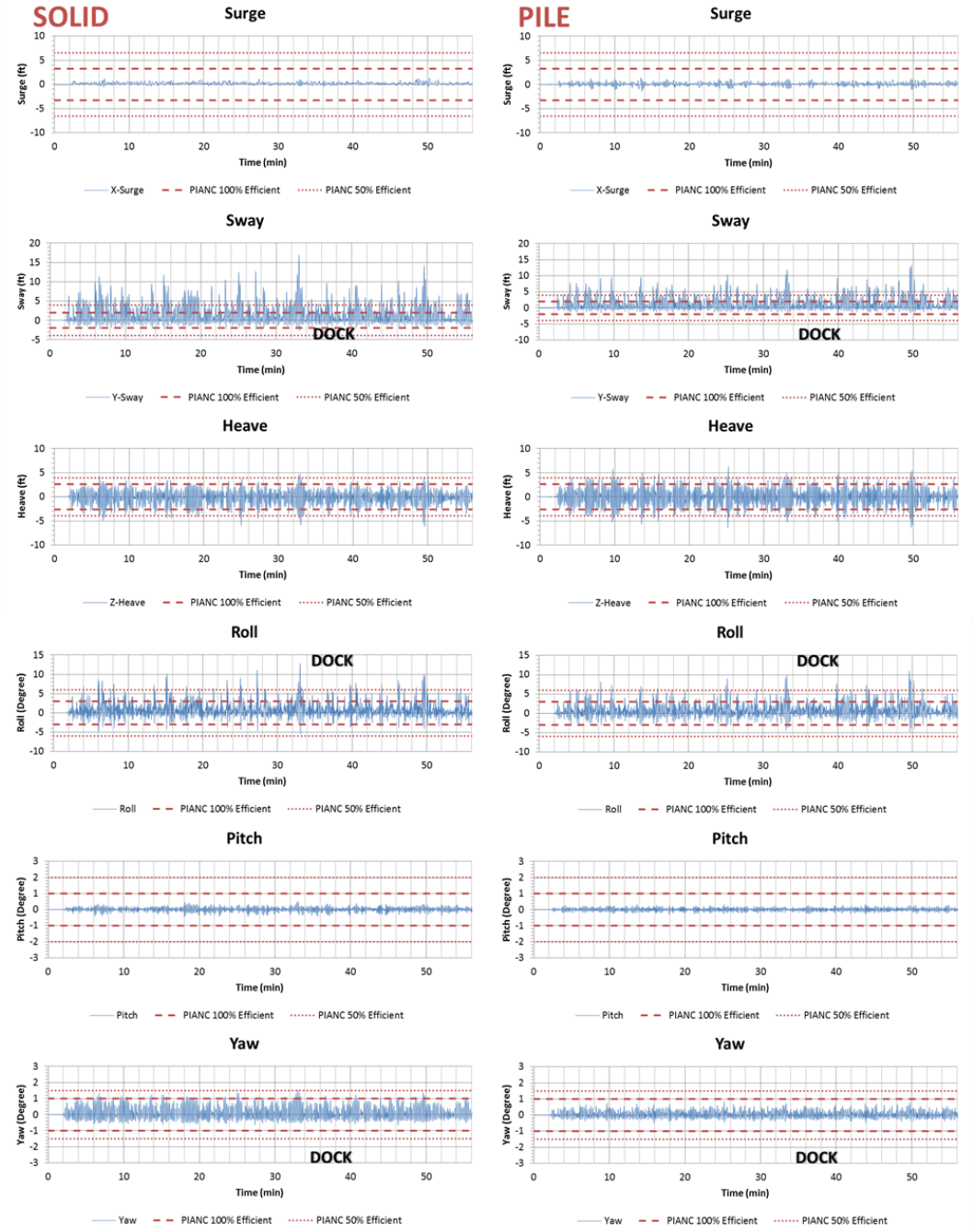

Test21	X-Surge	Y-Sway	Z-Heave	Roll	Pitch	Yaw
Maximum	1.29	16.88	4.75	12.82	0.52	1.57
Minimum	-0.59	-2.78	-6.16	-5.53	-0.49	-0.66
Significant	0.66	6.37	5.50	5.36	0.43	1.27
Total Num	416	662	347	744	602	560
Upper %	0.00%	20.69%	0.60%	4.97%	0.00%	0.18%
Lower%	0.00%	0.00%	2.27%	0.00%	0.00%	0.00%

Test21p	X-Surge	Y-Sway	Z-Heave	Roll	Pitch	Yaw
Maximum	1.37	13.25	6.32	10.97	0.34	0.85
Minimum	-1.47	-1.79	-6.48	-4.80	-0.30	-0.51
Significant	0.98	5.64	6.56	6.01	0.35	0.74
Total Num	538	557	378	481	466	459
Upper%	0.00%	19.93%	4.49%	4.78%	0.00%	0.00%
Lower%	0.00%	0.00%	3.59%	0.00%	0.00%	0.00%

Appendix Figure 21. Motion comparison of test 21 Hs=1.85m, Tp=12.02s, Dir=143°

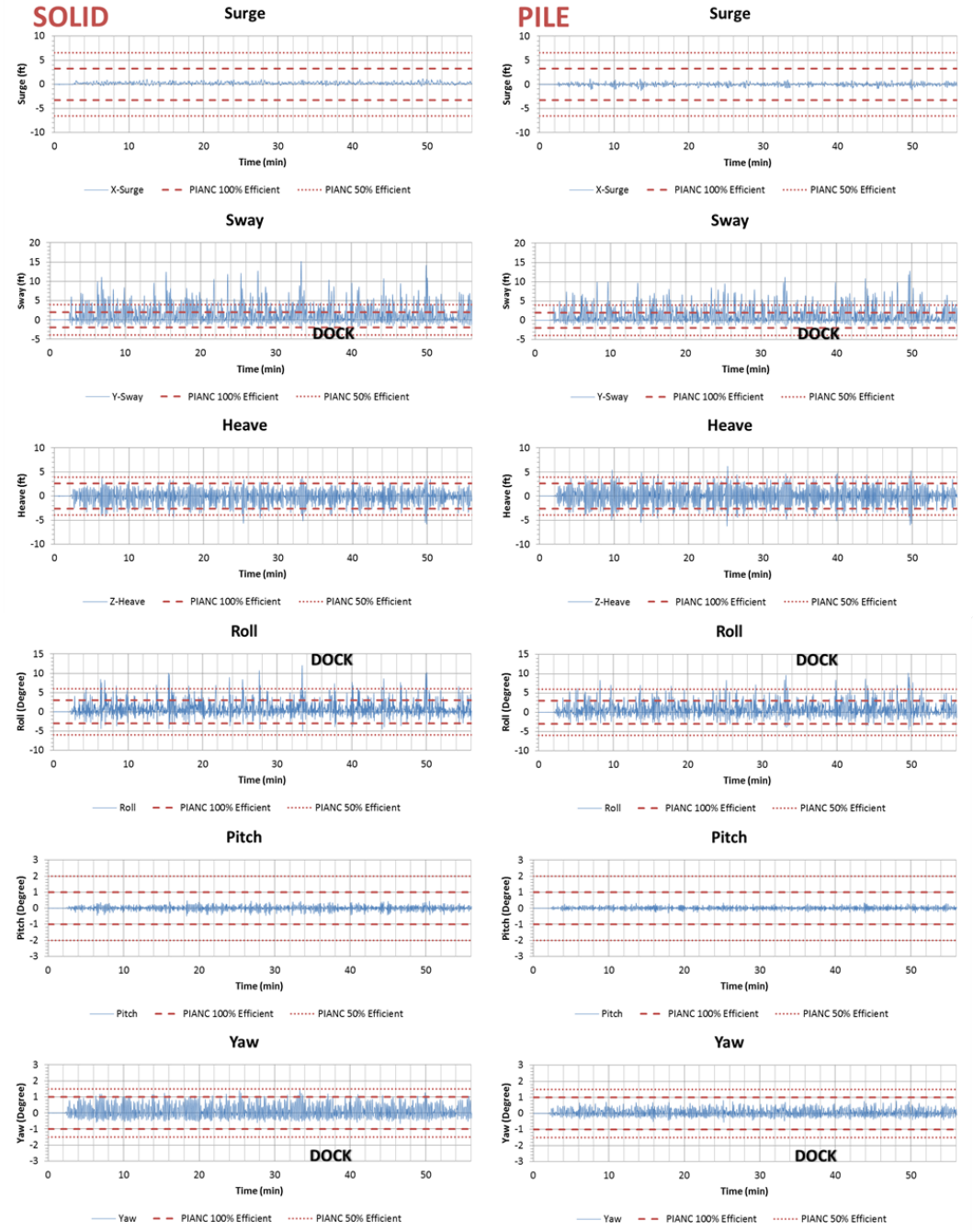

Test22	X-Surge	Y-Sway	Z-Heave	Roll	Pitch	Yaw
Maximum	1.15	15.21	4.05	12.05	0.48	1.45
Minimum	-0.52	-2.72	-5.85	-5.13	-0.49	-0.67
Significant	0.66	6.37	5.50	5.36	0.43	1.28
Total Num	416	662	347	744	602	495
Upper %	0.00%	24.68%	0.36%	4.21%	0.00%	0.00%
Lower%	0.00%	0.00%	2.16%	0.00%	0.00%	0.00%

Test22p	X-Surge	Y-Sway	Z-Heave	Roll	Pitch	Yaw
Maximum	1.16	12.81	6.21	10.22	0.35	0.82
Minimum	-1.34	-1.87	-6.28	-4.60	-0.31	-0.56
Significant	0.98	5.64	6.56	6.01	0.35	0.75
Total Num	538	557	378	481	466	469
Upper%	0.00%	17.54%	2.53%	3.65%	0.00%	0.00%
Lower%	0.00%	0.00%	3.16%	0.00%	0.00%	0.00%

Appendix Figure 22. Motion comparison of test 22 Hs=1.85m, Tp=12.02s, Dir=143°

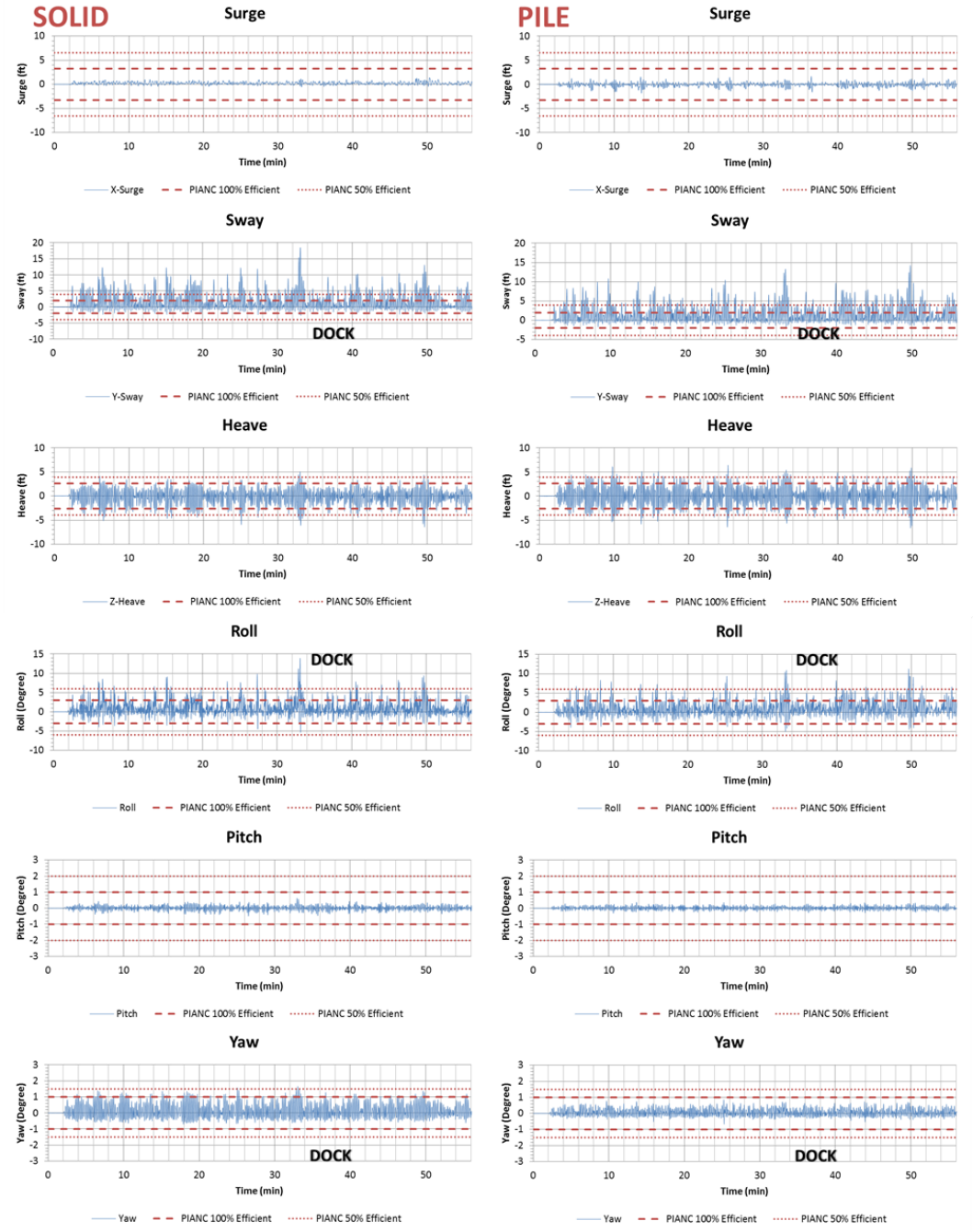

Test23	X-Surge	Y-Sway	Z-Heave	Roll	Pitch	Yaw
Maximum	1.37	18.50	5.06	13.92	0.63	1.66
Minimum	-0.57	-2.67	-6.45	-5.42	-0.49	-0.71
Significant	0.96	6.62	5.77	5.49	0.45	1.56
Total Num	207	641	309	632	545	316
Upper %	0.00%	22.46%	0.62%	3.96%	0.00%	0.63%
Lower%	0.00%	0.00%	2.81%	0.00%	0.00%	0.00%

Test23p	X-Surge	Y-Sway	Z-Heave	Roll	Pitch	Yaw
Maximum	1.67	14.25	6.45	11.28	0.38	0.85
Minimum	-1.84	-1.87	-6.65	-5.06	-0.31	-0.67
Significant	1.19	5.89	6.58	5.62	0.34	0.75
Total Num	494	573	440	570	507	439
Upper%	0.00%	21.12%	7.50%	4.56%	0.00%	0.00%
Lower%	0.00%	0.00%	4.71%	0.00%	0.00%	0.00%

Appendix Figure 23. Motion comparison of test 23 Hs=1.85m, Tp=12.02s, Dir=143˚

Test 24
No ship present, no motion data.

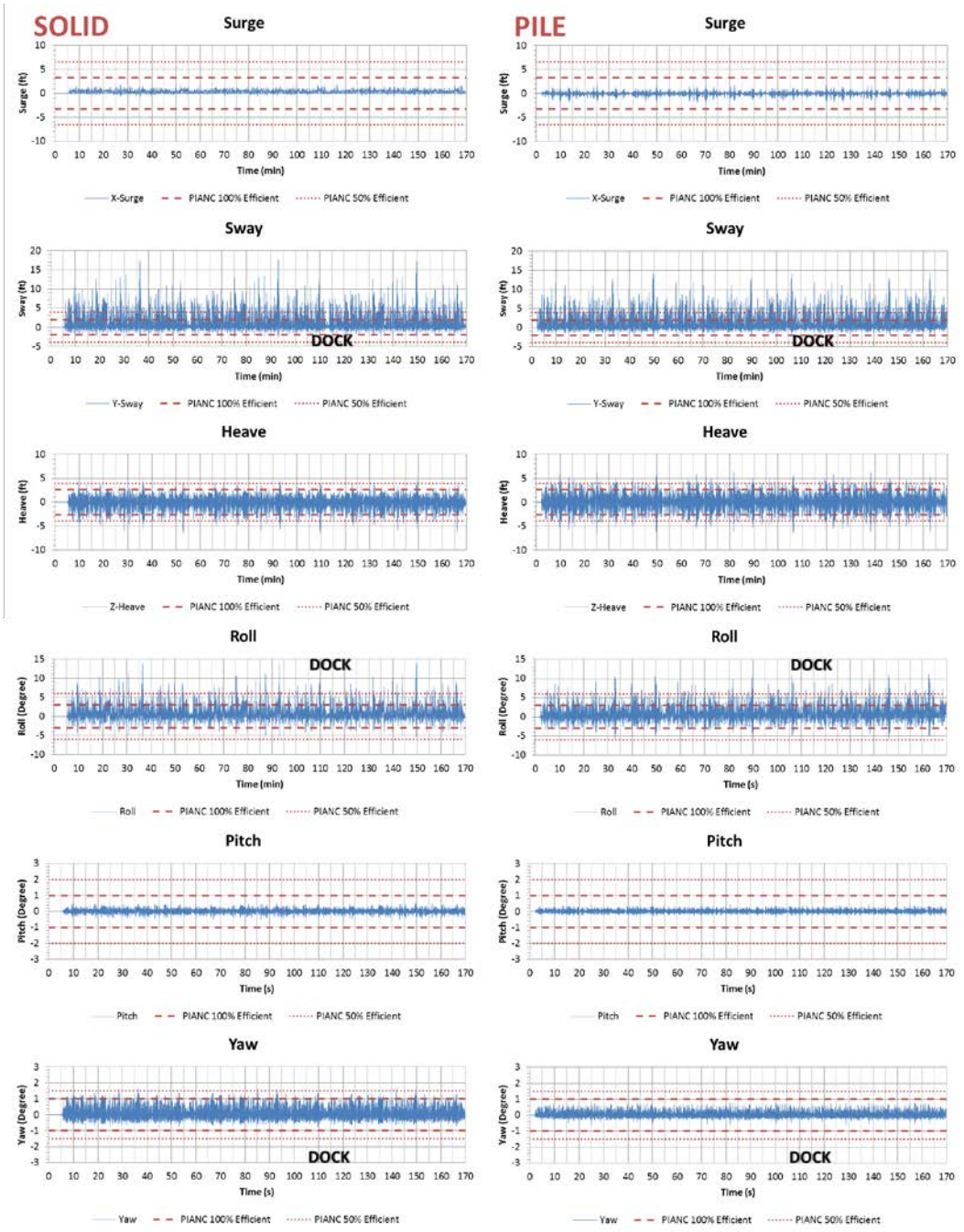

Test25	X-Surge	Y-Sway	Z-Heave	Roll	Pitch	Yaw	Test25p	X-Surge	Y-Sway	Z-Heave	Roll	Pitch	Yaw
Maximum	1.89	17.73	4.67	13.78	0.62	1.64	Maximum	1.73	14.33	6.39	11.19	0.42	0.85
Minimum	-0.60	-2.59	-6.41	-5.48	-0.53	-0.76	Minimum	-1.92	-1.91	-6.47	-5.70	-0.33	-0.62
Significant	0.82	6.86	4.91	5.97	0.44	1.29	Significant	1.42	7.54	6.79	7.57	0.40	0.76
Total Num	1091	1727	1514	1744	2186	1925	Total Num	1055	1198	1080	1086	1236	1133
Upper %	0.00%	25.30%	0.58%	6.36%	0.00%	0.31%	Upper%	0.00%	35.39%	7.60%	8.93%	0.00%	0.00%
Lower%	0.00%	0.00%	2.90%	0.00%	0.00%	0.00%	Lower%	0.00%	0.00%	5.68%	0.00%	0.00%	0.00%

Appendix Figure 24. Motion comparison of test 25 Hs=1.85m, Tp=12.02s, Dir=143˚

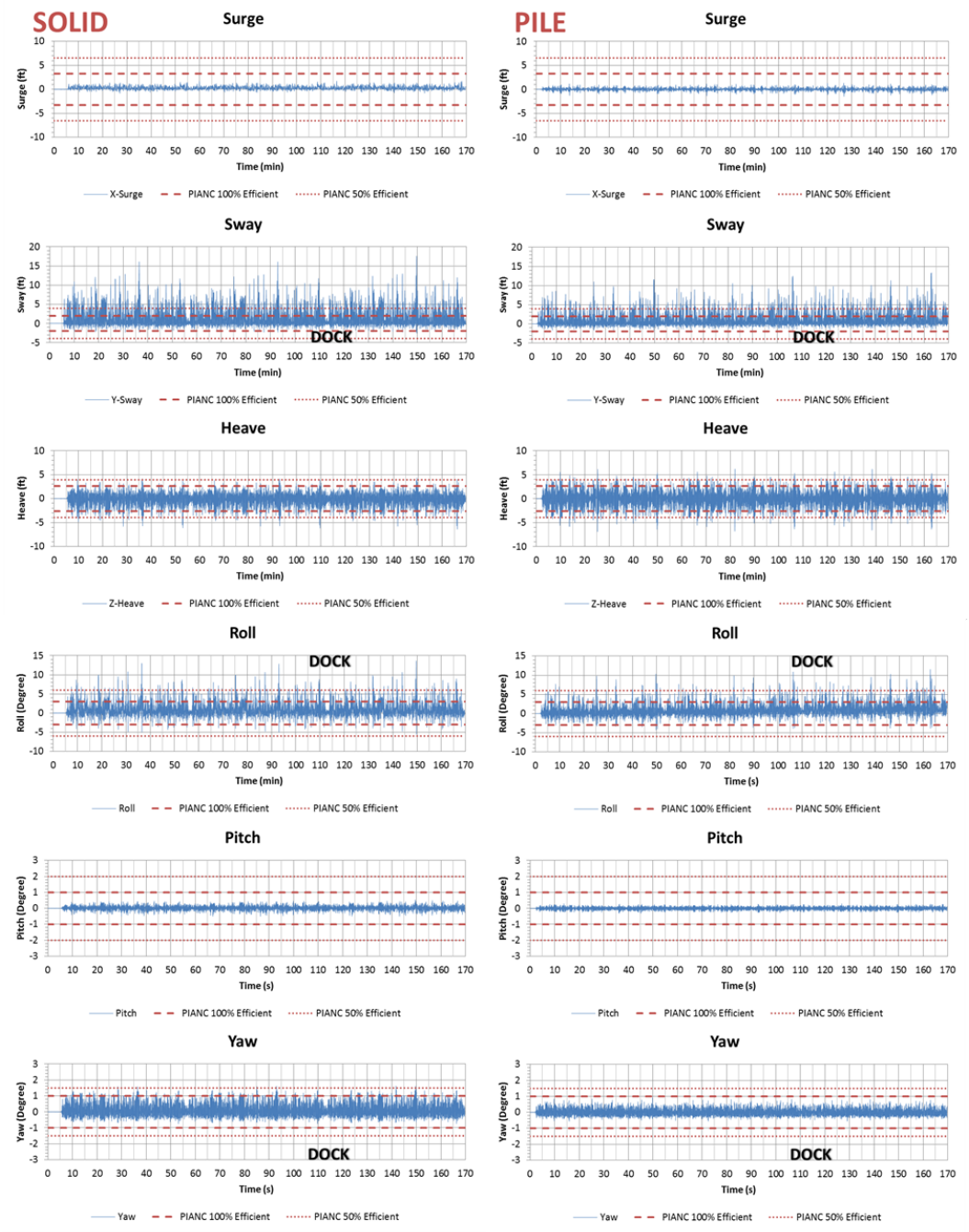

Test26	X-Surge	Y-Sway	Z-Heave	Roll	Pitch	Yaw
Maximum	0.97	7.15	2.66	7.36	0.33	0.31
Minimum	-1.73	-1.73	-3.16	-2.38	-0.24	-0.22
Significant	1.10	3.73	2.39	2.70	0.20	0.31
Total Num	686	590	703	885	875	583
Upper %	0.00%	6.10%	0.00%	0.45%	0.00%	0.00%
Lower%	0.00%	0.00%	0.00%	0.00%	0.00%	0.00%

Test26p	X-Surge	Y-Sway	Z-Heave	Roll	Pitch	Yaw
Maximum	0.45	5.63	2.90	5.48	0.33	0.33
Minimum	-0.71	-0.80	-3.51	-1.34	-0.29	-0.26
Significant	0.54	2.09	3.45	2.38	0.34	0.31
Total Num	792	715	489	478	454	591
Upper%	0.00%	1.12%	0.00%	0.00%	0.00%	0.00%
Lower%	0.00%	0.00%	0.00%	0.00%	0.00%	0.00%

Appendix Figure 25. Motion comparison of test 26 Hs=1.85m, Tp=12.02s, Dir=143˚

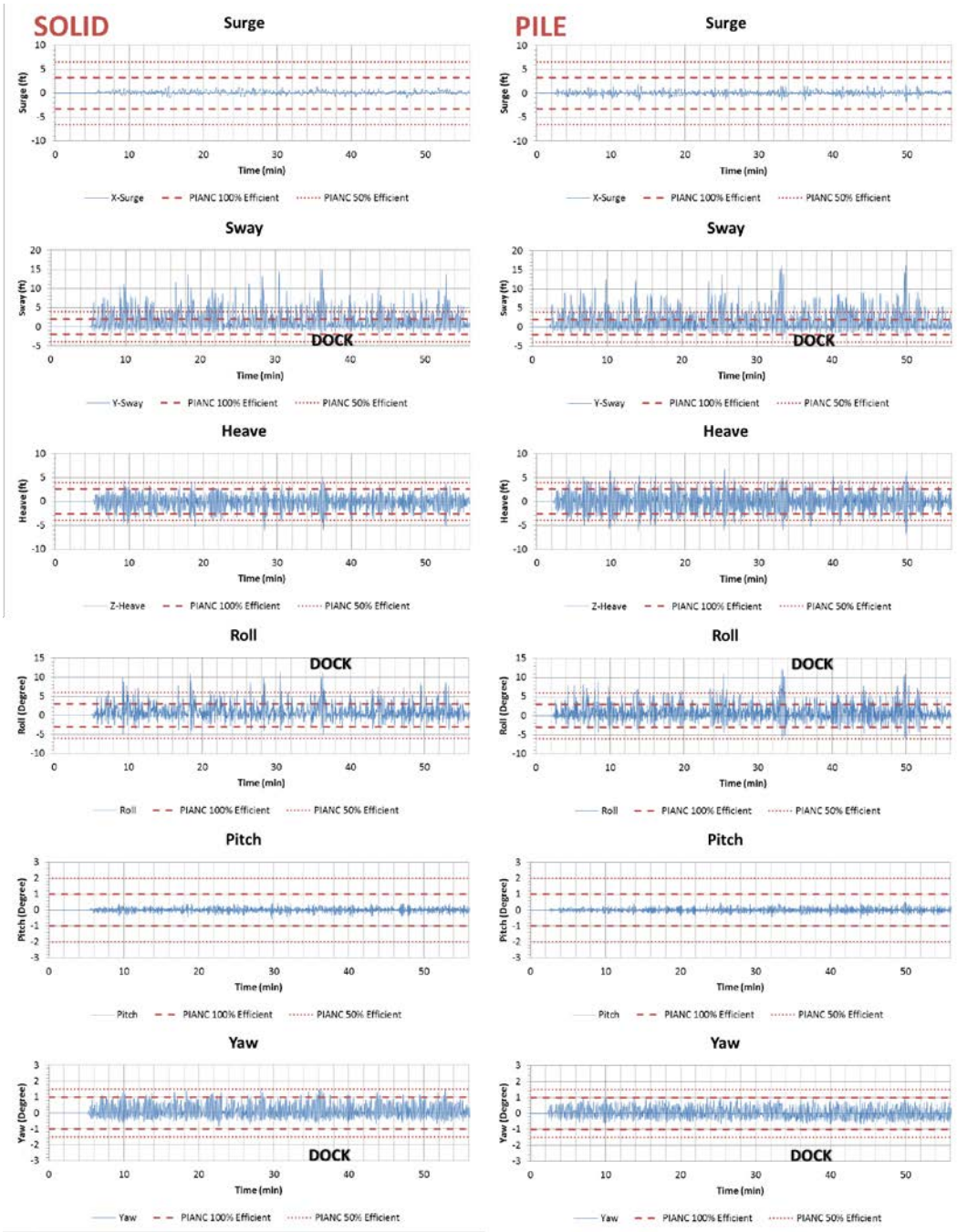

Test27	X-Surge	Y-Sway	Z-Heave	Roll	Pitch	Yaw
Maximum	1.56	15.00	5.21	11.38	0.45	1.59
Minimum	-1.00	-2.35	-5.98	-5.05	-0.58	-0.83
Significant	0.66	3.38	3.66	3.06	0.36	1.20
Total Num	525	1267	878	1295	963	708
Upper %	0.00%	10.58%	0.32%	2.47%	0.00%	0.42%
Lower%	0.00%	0.00%	1.34%	0.00%	0.00%	0.00%

Test27p	X-Surge	Y-Sway	Z-Heave	Roll	Pitch	Yaw
Maximum	2.05	16.31	6.77	12.32	0.55	1.06
Minimum	-1.91	-3.26	-6.86	-6.18	-0.52	-0.69
Significant	1.19	7.67	7.13	8.09	0.48	1.15
Total Num	524	491	410	394	495	379
Upper%	0.00%	28.51%	9.37%	10.15%	0.00%	0.00%
Lower%	0.00%	0.00%	8.35%	0.25%	0.00%	0.00%

Appendix Figure 26. Motion comparison of test 27 Hs=1.85m, Tp=12.02s, Dir=143˚

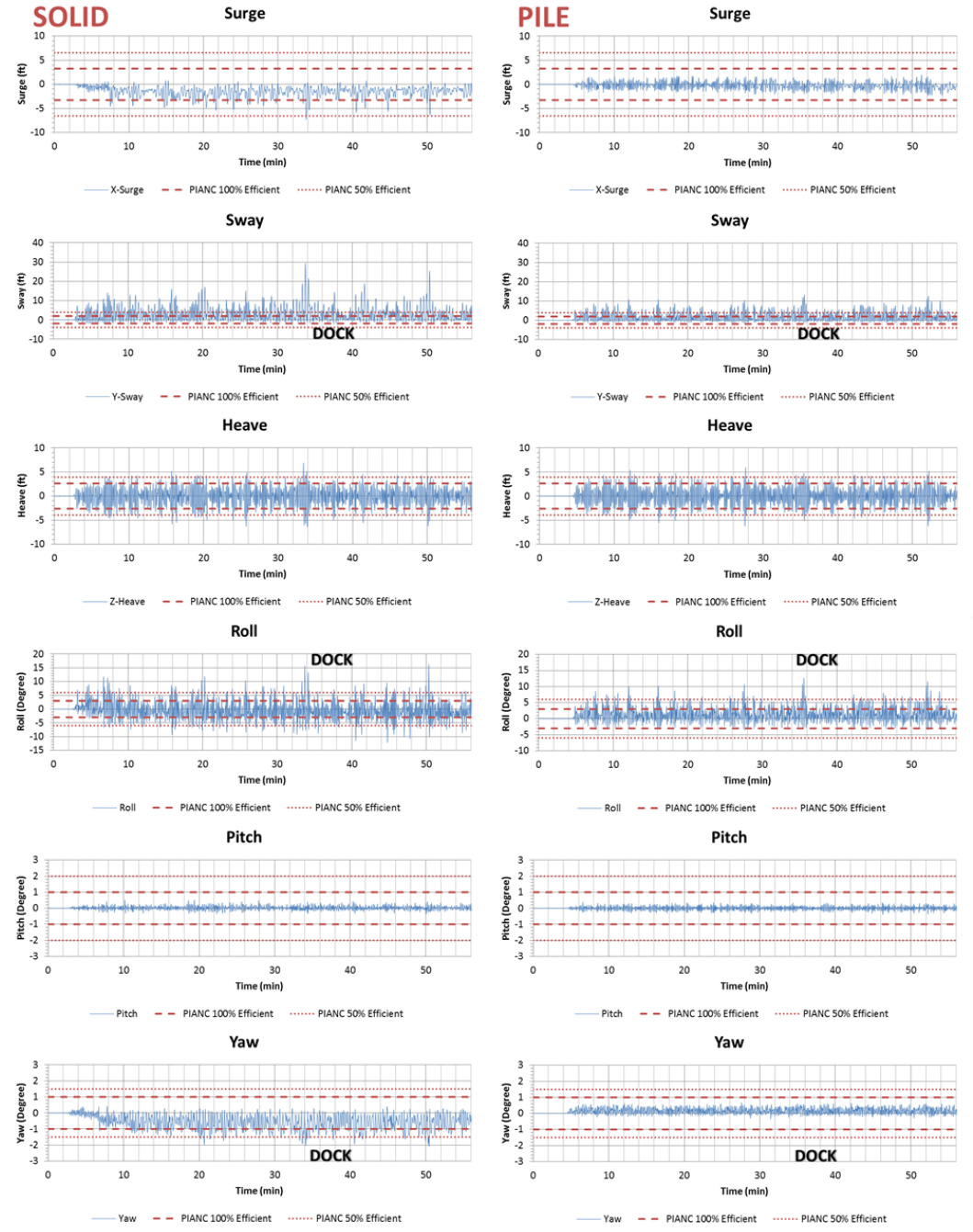

Test28	X-Surge	Y-Sway	Z-Heave	Roll	Pitch	Yaw
Maximum	0.82	29.36	6.91	16.20	0.53	0.41
Minimum	-7.35	-2.39	-6.42	-12.22	-0.35	-2.09
Significant	1.11	11.95	6.71	12.66	0.39	1.44
Total Num	357	260	345	338	541	237
Upper %	0.00%	60.80%	9.23%	18.05%	0.00%	0.00%
Lower%	0.28%	0.00%	13.85%	19.53%	0.00%	7.17%

Test28p	X-Surge	Y-Sway	Z-Heave	Roll	Pitch	Yaw
Maximum	1.97	13.31	5.94	12.66	0.38	0.70
Minimum	-2.41	-1.93	-6.27	-3.60	-0.40	-0.35
Significant	1.27	5.78	6.81	4.93	0.32	0.61
Total Num	1024	677	303	929	890	382
Upper%	0.00%	20.83%	3.99%	5.17%	0.00%	0.00%
Lower%	0.00%	0.00%	3.10%	0.00%	0.00%	0.00%

Appendix Figure 27. Motion comparison of test 28 Hs=1.85m, Tp=12.02s, Dir=143˚

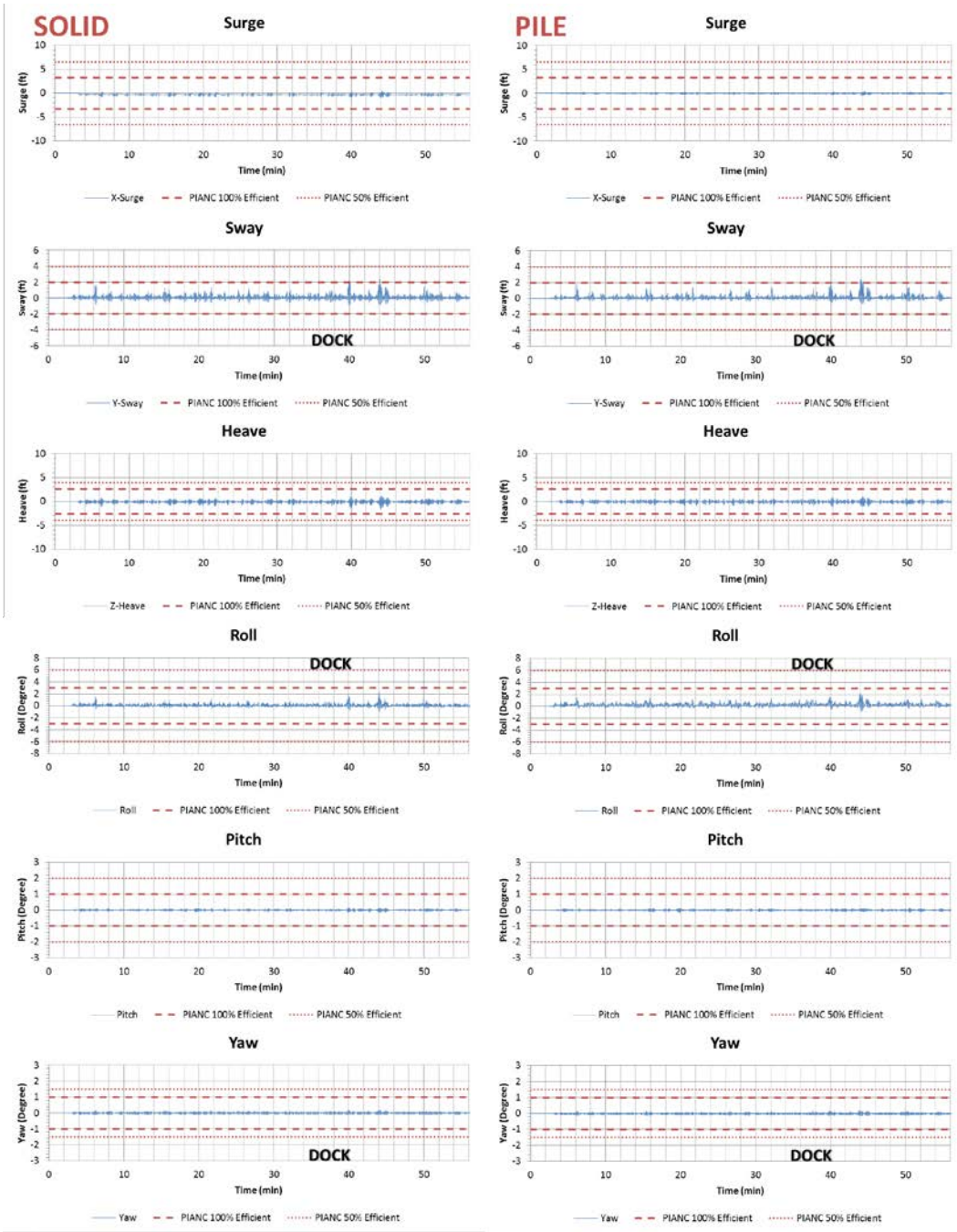

Test29	X-Surge	Y-Sway	Z-Heave	Roll	Pitch	Yaw
Maximum	0.49	2.44	1.22	2.18	0.16	0.18
Minimum	-0.94	-0.91	-1.58	-0.97	-0.16	-0.13
Significant	0.36	0.80	0.96	0.60	0.14	0.18
Total Num	274	879	578	978	619	756
Upper %	0.00%	0.00%	0.00%	0.00%	0.00%	0.00%
Lower%	0.00%	0.00%	0.00%	0.00%	0.00%	0.00%

Test29p	X-Surge	Y-Sway	Z-Heave	Roll	Pitch	Yaw
Maximum	0.44	2.40	1.01	2.30	0.15	0.19
Minimum	-0.52	-0.68	-1.18	-0.88	-0.18	-0.16
Significant	0.25	0.72	0.87	0.89	0.14	0.17
Total Num	1136	749	626	533	693	740
Upper%	0.00%	0.00%	0.00%	0.00%	0.00%	0.00%
Lower%	0.00%	0.00%	0.00%	0.00%	0.00%	0.00%

Appendix Figure 28. Motion comparison of test 29 Hs=0.6m, Tp=7.99s, Dir=143˚

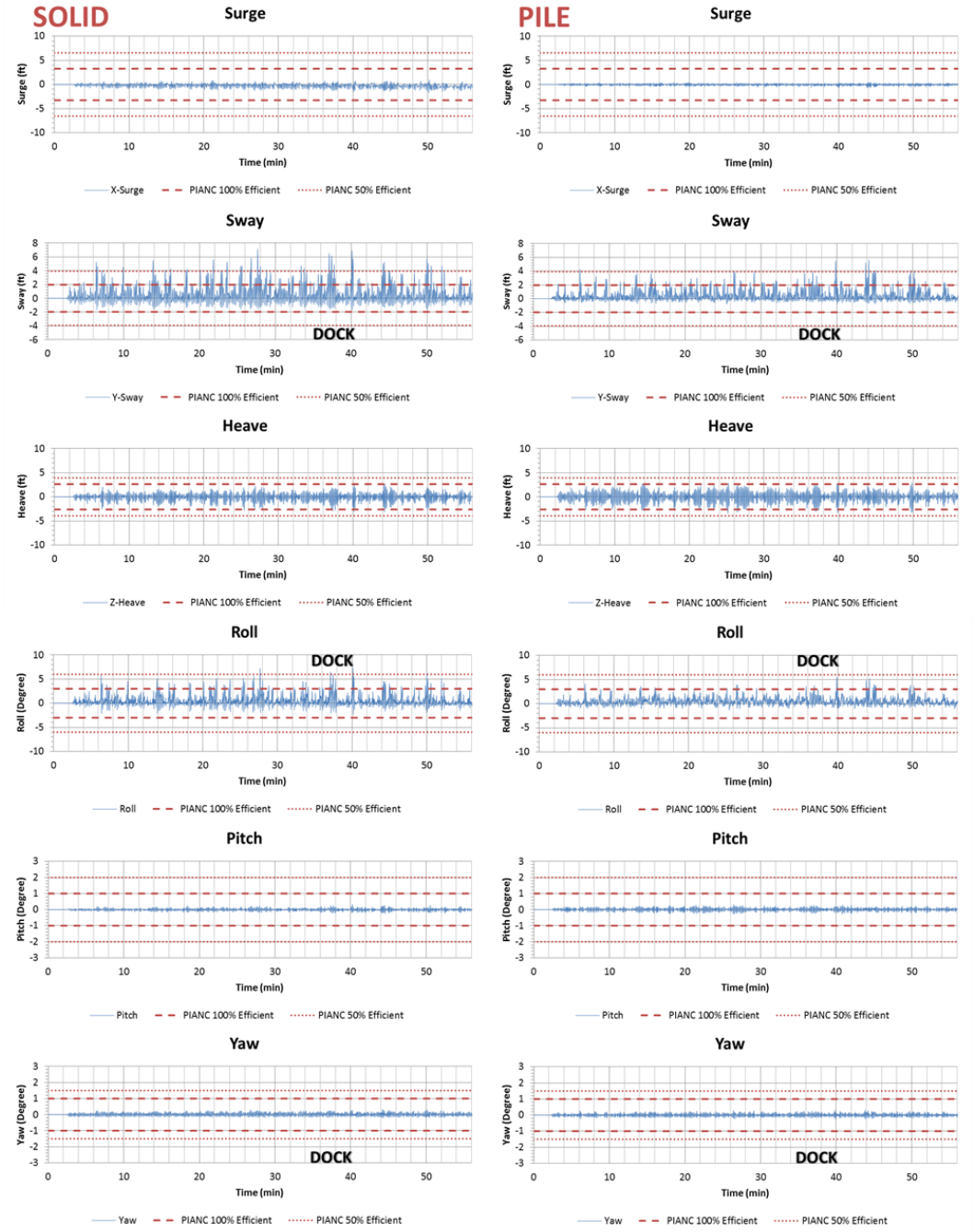

Test30	X-Surge	Y-Sway	Z-Heave	Roll	Pitch	Yaw
Maximum	0.97	7.15	2.66	7.36	0.33	0.31
Minimum	-1.73	-1.73	-3.16	-2.38	-0.24	-0.22
Significant	1.10	3.73	2.39	2.70	0.20	0.31
Total Num	686	590	703	885	875	583
Upper %	0.00%	6.10%	0.00%	0.45%	0.00%	0.00%
Lower%	0.00%	0.00%	0.00%	0.00%	0.00%	0.00%

Test30p	X-Surge	Y-Sway	Z-Heave	Roll	Pitch	Yaw
Maximum	0.45	5.63	2.90	5.48	0.33	0.33
Minimum	-0.71	-0.80	-3.51	-1.34	-0.29	-0.26
Significant	0.54	2.09	3.45	2.38	0.34	0.31
Total Num	792	715	489	478	454	591
Upper%	0.00%	1.12%	0.00%	0.00%	0.00%	0.00%
Lower%	0.00%	0.00%	0.00%	0.00%	0.00%	0.00%

Appendix Figure 29. Motion comparison of test 30 Hs=1.2m, Tp=9.97s, Dir=143˚

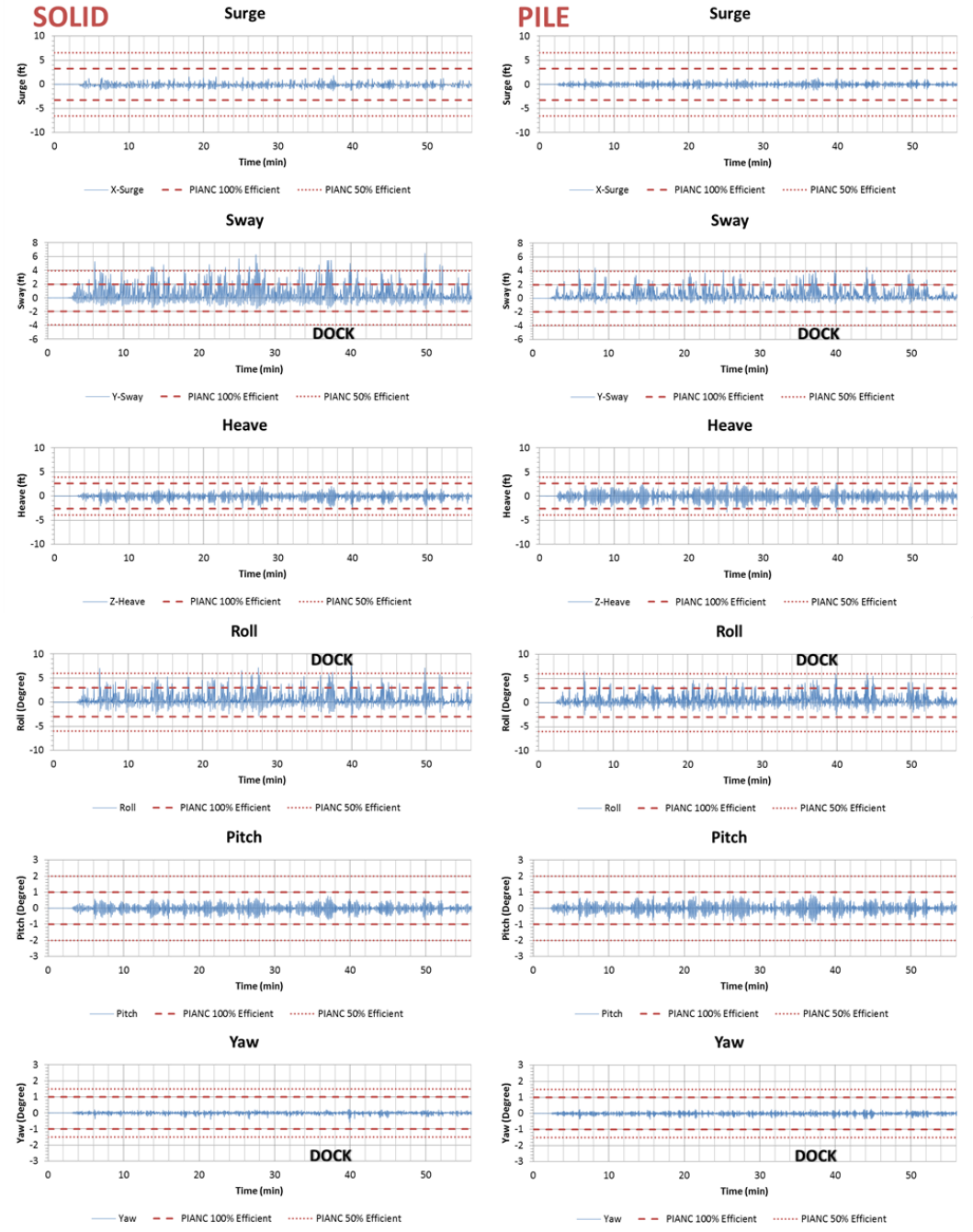

Test31	X-Surge	Y-Sway	Z-Heave	Roll	Pitch	Yaw
Maximum	1.86	6.50	2.07	7.84	0.78	0.25
Minimum	-1.42	-1.65	-2.57	-3.08	-0.73	-0.59
Significant	1.15	2.86	2.33	4.05	0.20	0.24
Total Num	797	845	405	645	614	899
Upper %	0.00%	3.67%	0.00%	1.09%	0.00%	0.00%
Lower%	0.00%	0.00%	0.00%	0.00%	0.00%	0.00%

Test31p	X-Surge	Y-Sway	Z-Heave	Roll	Pitch	Yaw
Maximum	1.38	4.50	2.95	6.52	0.87	0.29
Minimum	-1.28	-0.92	-3.40	-2.61	-0.91	-0.37
Significant	1.33	1.98	3.30	3.90	1.01	0.35
Total Num	563	676	442	519	426	554
Upper%	0.00%	0.89%	0.00%	0.58%	0.00%	0.00%
Lower%	0.00%	0.00%	0.00%	0.00%	0.00%	0.00%

Appendix Figure 30. Motion comparison of test 31 Hs=1.2m, Tp=9.97s, Dir=128°

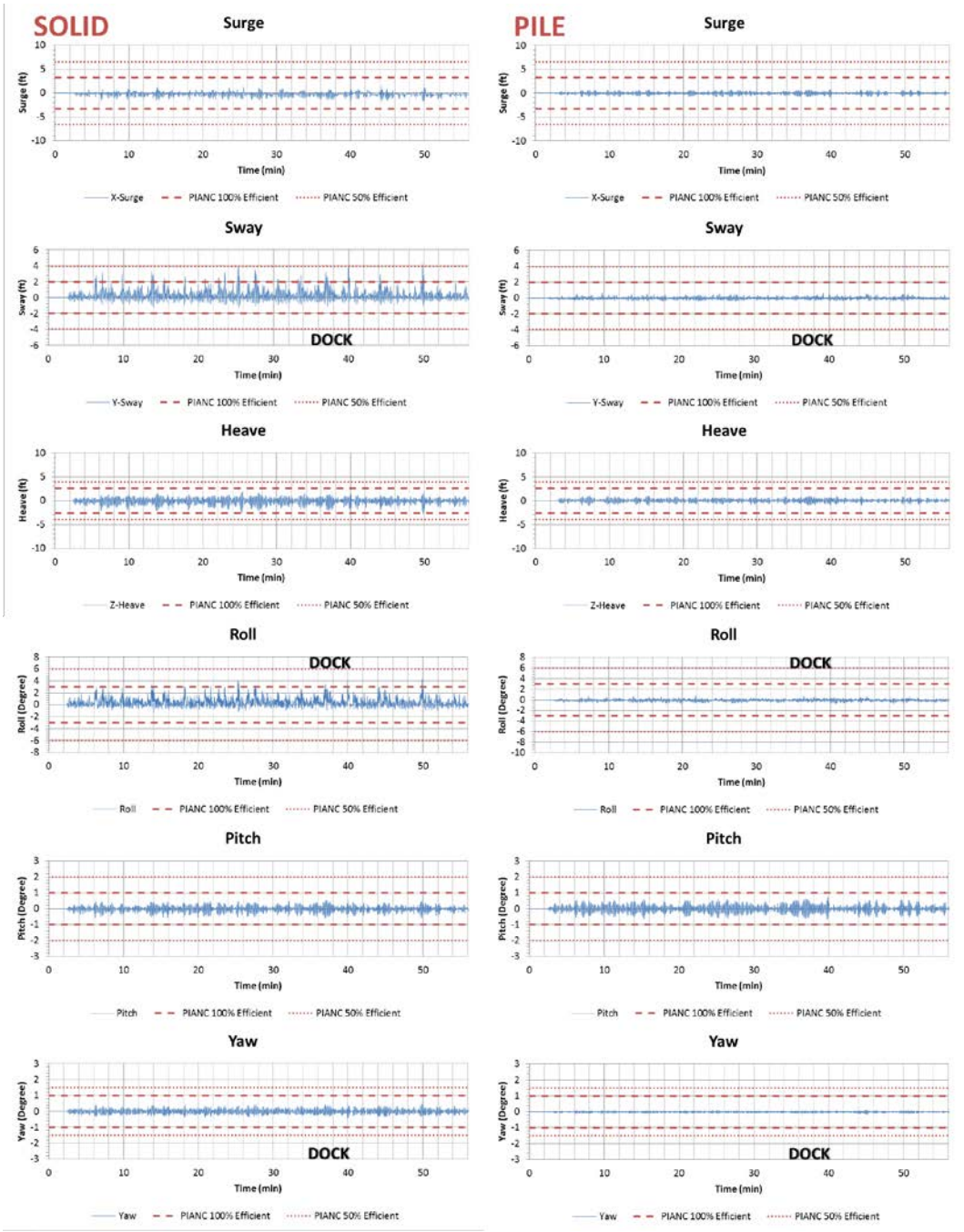

Test32	X-Surge	Y-Sway	Z-Heave	Roll	Pitch	Yaw	Test32p	X-Surge	Y-Sway	Z-Heave	Roll	Pitch	Yaw
Maximum	1.54	4.32	1.90	4.35	0.54	0.50	Maximum	0.77	0.68	1.12	0.83	0.73	0.12
Minimum	-1.96	-1.31	-2.78	-1.32	-0.61	-0.43	Minimum	-0.97	-0.44	-1.11	-0.78	-0.68	-0.17
Significant	1.24	1.88	2.23	1.87	0.55	0.49	Significant	0.97	0.43	1.19	0.67	0.83	0.15
Total Num	575	642	504	798	738	514	Total Num	488	919	468	661	433	590
Upper %	0.00%	0.12%	0.00%	0.00%	0.00%	0.00%	Upper%	0.00%	0.00%	0.00%	0.00%	0.00%	0.00%
Lower%	0.00%	0.00%	0.00%	0.00%	0.00%	0.00%	Lower%	0.00%	0.00%	0.00%	0.00%	0.00%	0.00%

Appendix Figure 31. Motion comparison of test 32 Hs=1.2m, Tp=9.97s, Dir=158˚

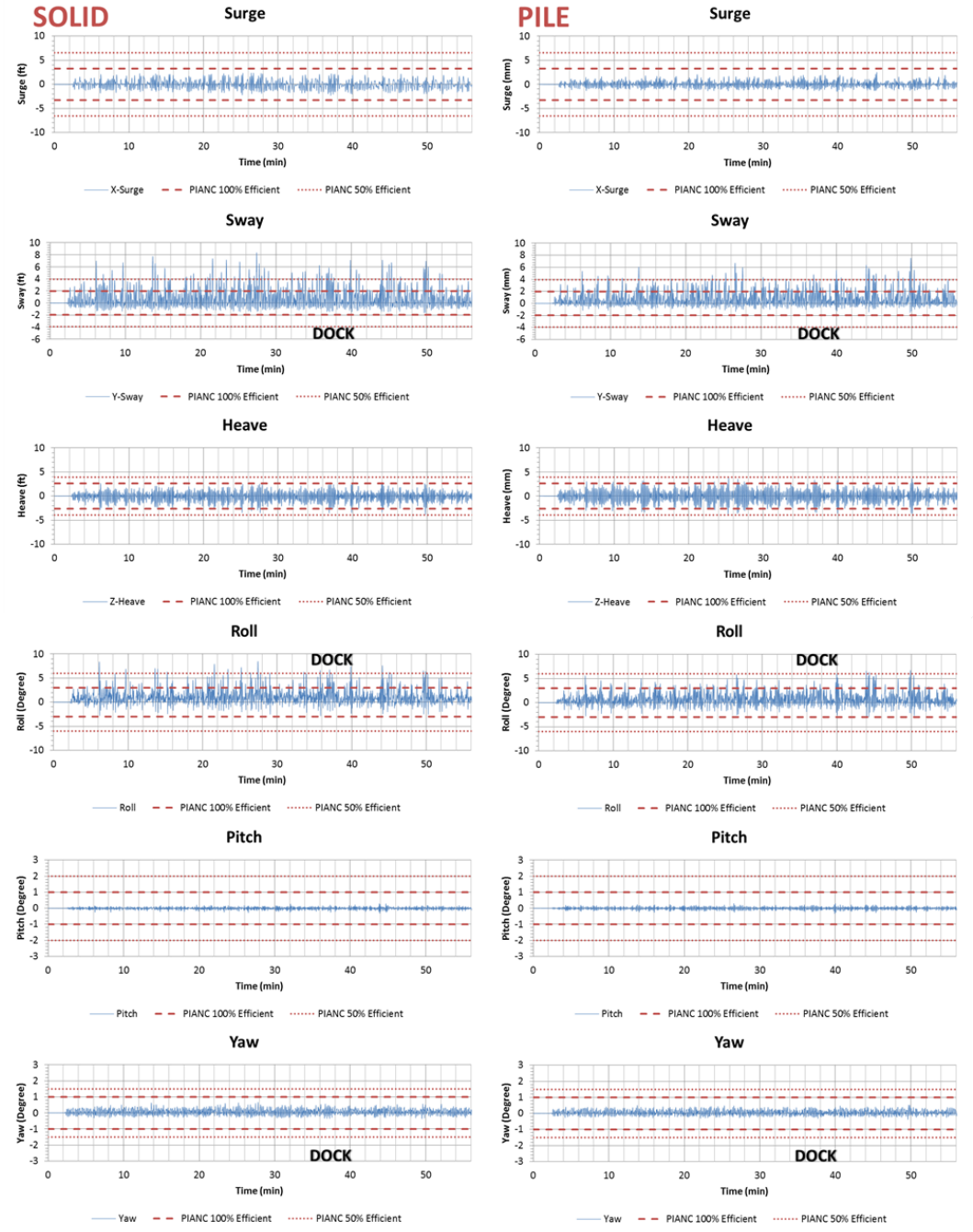

Test33	X-Surge	Y-Sway	Z-Heave	Roll	Pitch	Yaw
Maximum	2.38	8.37	2.73	8.49	0.30	0.67
Minimum	-2.34	-1.66	-3.85	-2.86	-0.32	-0.36
Significant	2.85	5.07	3.42	5.10	0.26	0.64
Total Num	348	400	473	466	510	361
Upper %	0.00%	14.75%	0.00%	4.29%	0.00%	0.00%
Lower%	0.00%	0.00%	0.00%	0.00%	0.00%	0.00%

Test33p	X-Surge	Y-Sway	Z-Heave	Roll	Pitch	Yaw
Maximum	2.53	7.54	3.79	6.72	0.31	0.53
Minimum	-1.52	-1.55	-3.88	-3.16	-0.34	-0.39
Significant	1.82	2.91	4.13	3.60	0.25	0.46
Total Num	664	847	483	776	802	759
Upper%	0.00%	4.13%	0.00%	0.39%	0.00%	0.00%
Lower%	0.00%	0.00%	0.00%	0.00%	0.00%	0.00%

Appendix Figure 32. Motion comparison of test 33 Hs=1.2m, Tp=9.97s, Dir=143˚

Test 34

No motion data

Test 35

No motion data

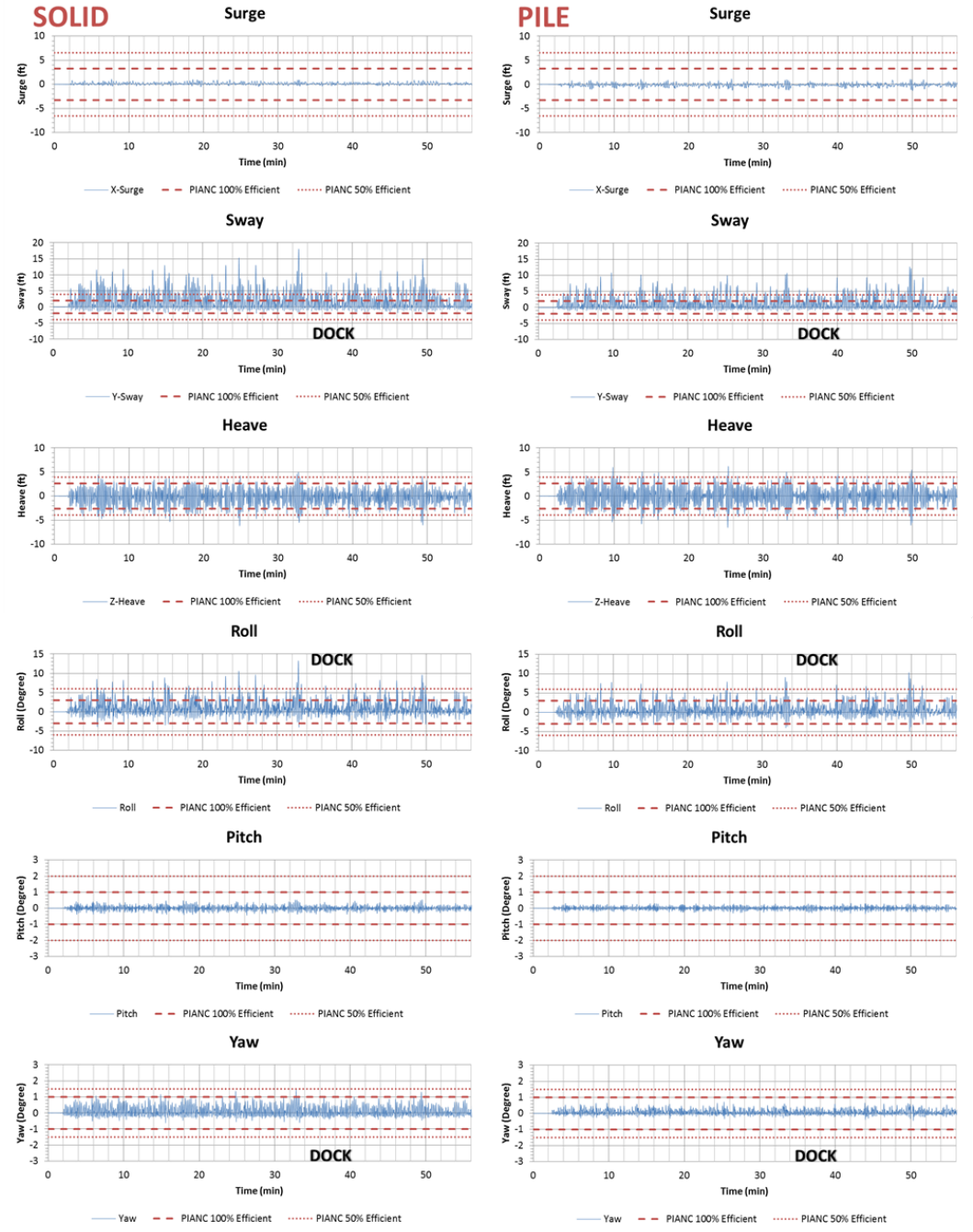

Test36	X-Surge	Y-Sway	Z-Heave	Roll	Pitch	Yaw
Maximum	1.06	18.05	4.97	13.25	0.54	1.48
Minimum	-0.54	-2.04	-6.19	-4.02	-0.44	-0.62
Significant	0.62	7.58	5.50	5.34	0.44	0.93
Total Num	473	560	445	674	689	617
Upper %	0.00%	30.18%	1.07%	5.00%	0.00%	0.00%
Lower%	0.00%	0.00%	4.46%	0.00%	0.00%	0.00%

Test36p	X-Surge	Y-Sway	Z-Heave	Roll	Pitch	Yaw
Maximum	1.13	12.67	6.18	10.35	0.32	0.72
Minimum	-1.30	-1.44	-6.56	-4.98	-0.35	-0.45
Significant	0.82	5.04	5.85	5.39	0.31	0.45
Total Num	579	656	510	486	772	824
Upper%	0.00%	17.07%	4.12%	2.88%	0.00%	0.00%
Lower%	0.00%	0.00%	3.05%	0.00%	0.00%	0.00%

Appendix Figure 33. Motion comparison of test 36 Hs=1.85m, Tp=12.02s, Dir=173˚

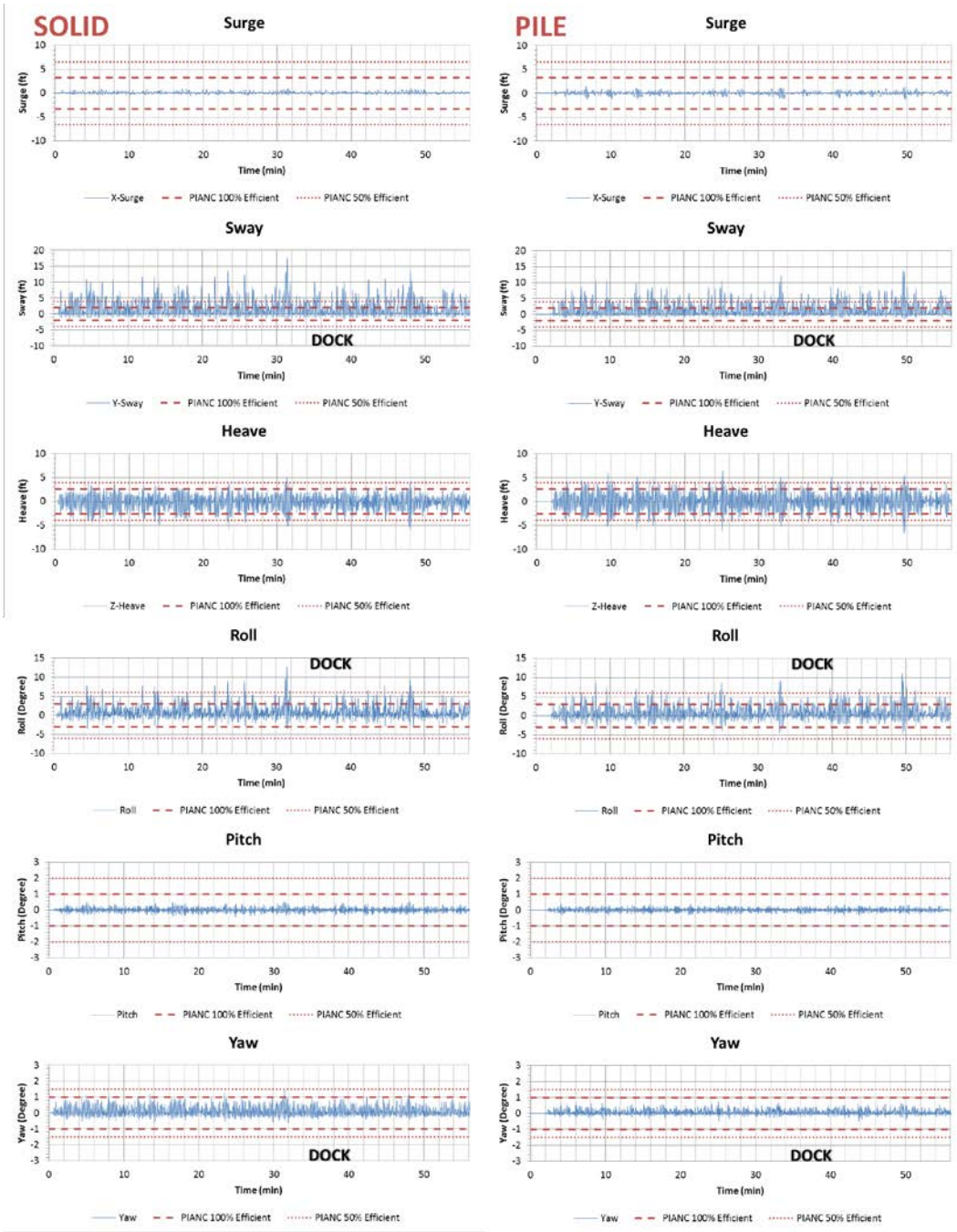

Test37	X-Surge	Y-Sway	Z-Heave	Roll	Pitch	Yaw
Maximum	0.99	17.64	4.99	12.81	0.54	1.48
Minimum	-0.63	-2.03	-5.99	-3.66	-0.46	-0.61
Significant	0.71	7.65	5.31	5.50	0.47	1.00
Total Num	392	471	376	502	536	446
Upper %	0.00%	36.09%	0.85%	4.18%	0.00%	0.00%
Lower%	0.00%	0.00%	3.18%	0.00%	0.00%	0.00%

Test37p	X-Surge	Y-Sway	Z-Heave	Roll	Pitch	Yaw
Maximum	1.44	13.88	6.38	11.15	0.38	0.74
Minimum	-1.38	-1.46	-6.57	-4.76	-0.33	-0.47
Significant	0.99	6.06	6.21	4.77	0.38	0.48
Total Num	487	525	463	690	609	785
Upper%	0.00%	24.57%	4.95%	2.61%	0.00%	0.00%
Lower%	0.00%	0.00%	4.57%	0.00%	0.00%	0.00%

Appendix Figure 34. Motion comparison of test 37 Hs=1.85m, Tp=12.02s, Dir=143˚

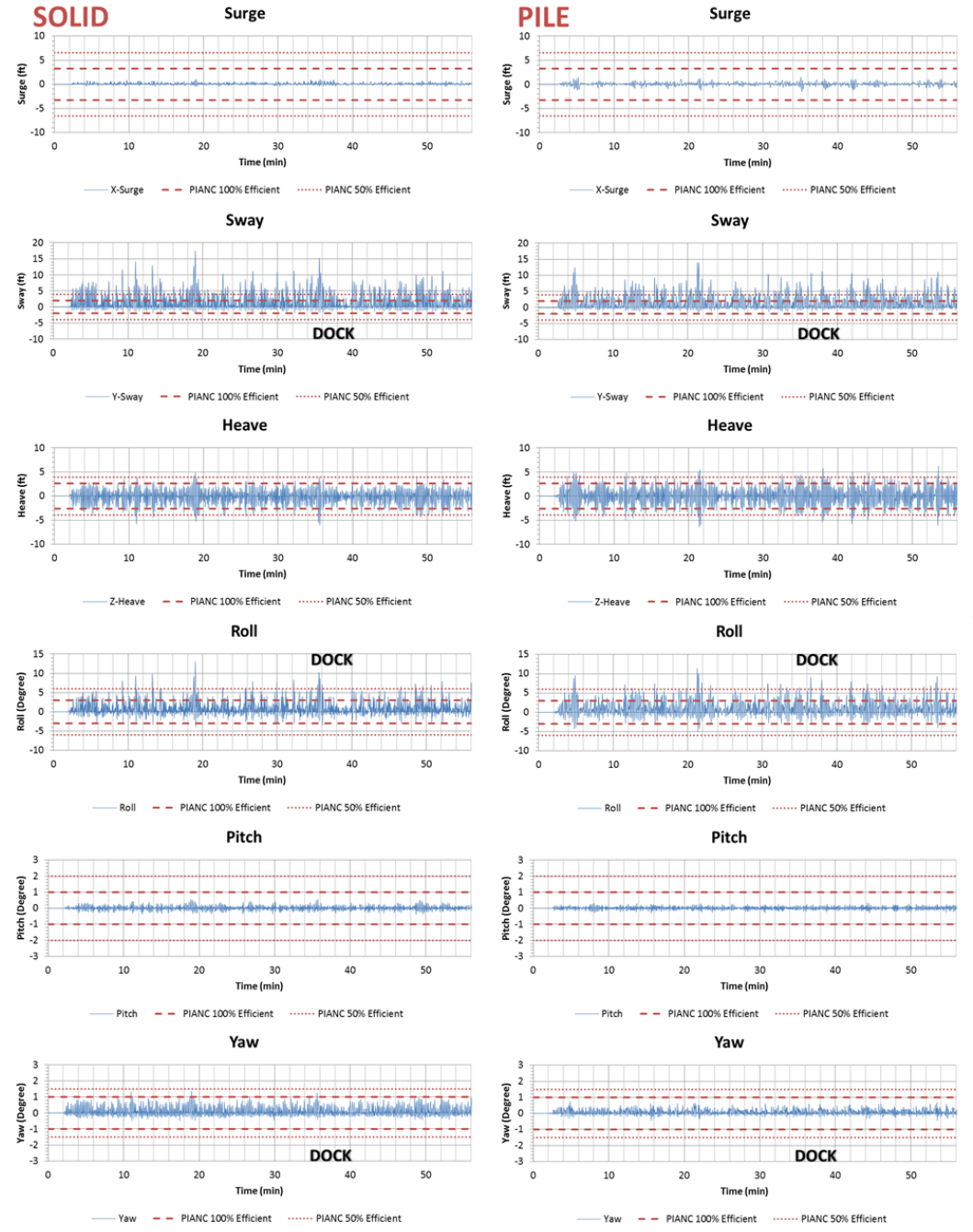

Test38	X-Surge	Y-Sway	Z-Heave	Roll	Pitch	Yaw
Maximum	1.04	17.48	4.88	13.02	0.57	1.38
Minimum	-0.46	-2.09	-6.01	-4.00	-0.40	-0.51
Significant	0.49	4.94	3.43	3.61	0.30	0.62
Total Num	1387	1606	1069	1753	1367	1204
Upper %	0.00%	18.80%	0.25%	1.43%	0.00%	0.00%
Lower%	0.00%	0.00%	0.93%	0.00%	0.00%	0.00%

Test38p	X-Surge	Y-Sway	Z-Heave	Roll	Pitch	Yaw
Maximum	1.54	14.04	6.25	11.43	0.36	0.75
Minimum	-1.59	-1.66	-6.49	-5.05	-0.31	-0.46
Significant	1.12	7.45	6.65	6.92	0.34	0.56
Total Num	356	343	362	373	423	483
Upper%	0.00%	38.48%	8.75%	7.24%	0.00%	0.00%
Lower%	0.00%	0.00%	6.71%	0.00%	0.00%	0.00%

Appendix Figure 35. Motion comparison of test 38 Hs=1.85m, Tp=12.02s, Dir=143˚

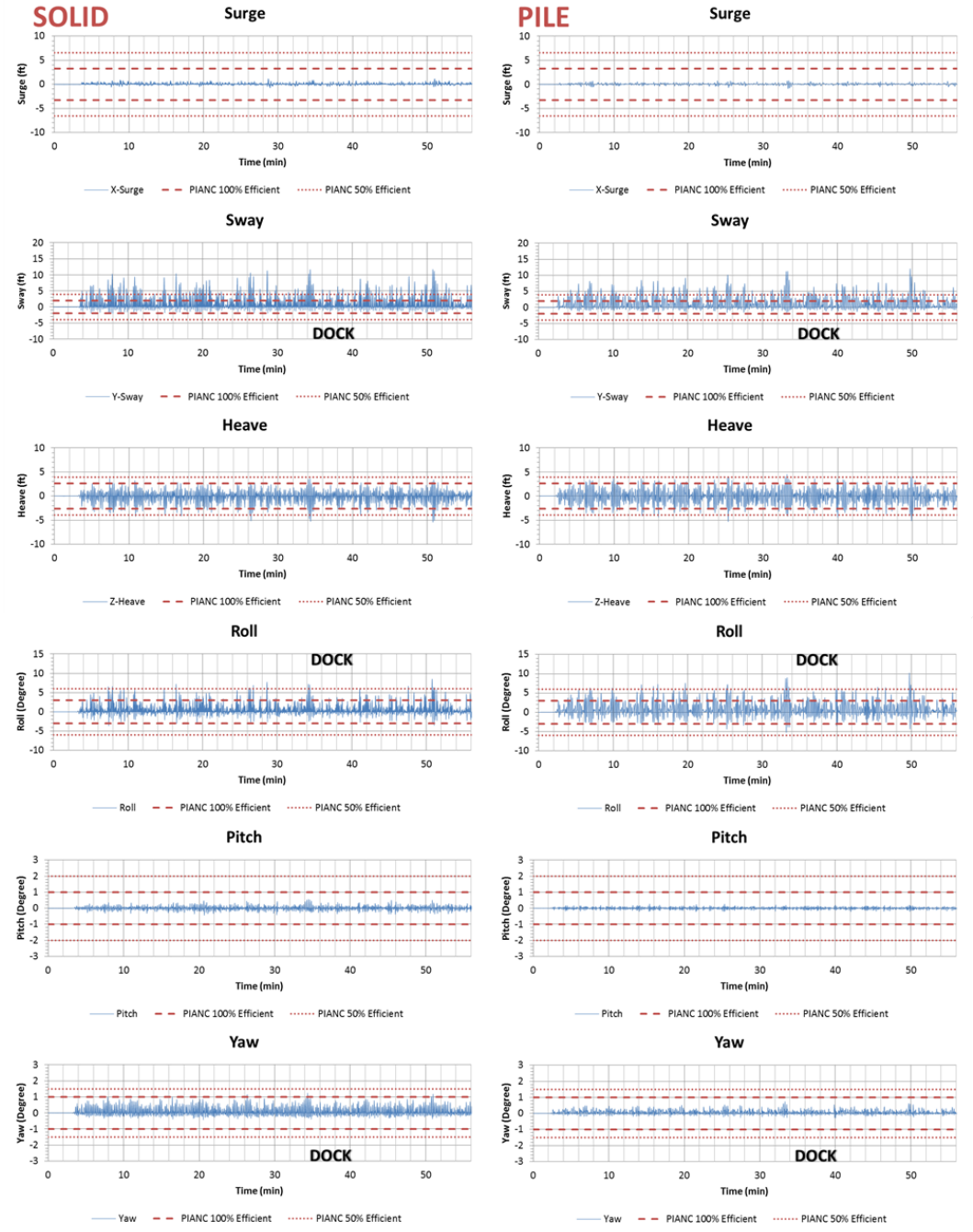

Test39	X-Surge	Y-Sway	Z-Heave	Roll	Pitch	Yaw
Maximum	1.17	11.71	3.68	8.51	0.56	1.24
Minimum	-0.78	-2.07	-5.44	-3.66	-0.44	-0.43
Significant	0.49	5.03	2.31	3.43	0.25	0.58
Total Num	3295	3785	2028	3159	2485	2943
Upper %	0.00%	22.54%	0.00%	1.20%	0.00%	0.00%
Lower%	0.00%	0.00%	0.21%	0.00%	0.00%	0.00%

Test39p	X-Surge	Y-Sway	Z-Heave	Roll	Pitch	Yaw
Maximum	0.79	12.06	4.52	10.23	0.27	0.74
Minimum	-0.92	-1.65	-5.32	-5.35	-0.22	-0.28
Significant	0.47	6.14	5.17	7.03	0.20	0.33
Total Num	552	396	360	325	765	950
Upper%	0.00%	25.51%	1.26%	4.92%	0.00%	0.00%
Lower%	0.00%	0.00%	2.02%	0.00%	0.00%	0.00%

Appendix Figure 36. Motion comparison of test 39 Hs=1.85m, Tp=12.02s, Dir=143˚